1-31-1991

Novel way of sub-carrier coherent detection and clock recovery in fiber-optic communications

Narayan Gehlot
New Jersey Institute of Technology

Copyright Warning & Restrictions

The copyright law of the United States (Title 17, United States Code) governs the making of photocopies or other reproductions of copyrighted material.

Under certain conditions specified in the law, libraries and archives are authorized to furnish a photocopy or other reproduction. One of these specified conditions is that the photocopy or reproduction is not to be "used for any purpose other than private study, scholarship, or research." If a, user makes a request for, or later uses, a photocopy or reproduction for purposes in excess of "fair use" that user may be liable for copyright infringement,

This institution reserves the right to refuse to accept a copying order if, in its judgment, fulfillment of the order would involve violation of copyright law.

Please Note: The author retains the copyright while the New Jersey Institute of Technology reserves the right to distribute this thesis or dissertation

Printing note: If you do not wish to print this page, then select "Pages from: first page # to: last page #" on the print dialog screen

ABSTRACT

NOVEL WAY OF SUB-CARRIER COHERENT DETECTION AND CLOCK RECOVERY IN FIBER-OPTIC COMMUNICATIONS

January 1991

Narayan Gehlot

B.E.(Hons) EEE & M.Sc.(Hons) Physics, Birla Institute of Technology & Science, Pilani, India.
M.S.(Electrical Engineering), New Jersey Institute of Technology, Newark, NJ, USA.

We experimentally demonstrate a novel concept for recovery of a Sub-Carrier and Timing Clock in fiber-optic communication systems using a Wavelength Division Multiplexing technique. The idea is to send a low radio frequency (RF) as a reference pilot from the transmitter to the receiver on a separate laser using the principle of Wavelength Division Multiplexing (WDM). This low frequency signal is taken to be a subharmonic of the subcarrier used to carry information and intensity modulate another laser. Such approach will be expected to generate at the receiver a local oscillator in high coherence with the subcarrier.

We show that transmission of Coherent microwave signal on two different wavelengths will remain sufficiently coherent up to 100 Km or more, and experimentally demonstrate this fact for 36 Km fiber.

We believe that this concept could be very useful for subcarrier systems operating beyond 1 GHz and upto 20 GHz, where in other approaches subcarrier and timing clock recovery will be limited due to laser chirp and residual fiber dispersion. The WDM proposed approach can provide a subcarrier for coherent detection and timing clock at the receiver up to 100 Km with minimum optical power penalty. With subcarrier frequency of 20 GHz, and repeater span of 100 Km, extraction of subcarrier and timing clock by other methods will be too expensive, complicated or will require very high optical power penalty. Thus the concept proposed here will make sub-carrier based systems more attractive for transmission of analog and digital information, simple and cost-effective as compared to other very high speed time division multiplexed systems.

THESIS

NOVEL WAY OF SUB-CARRIER COHERENT DETECTION AND CLOCK RECOVERY IN FIBER-OPTIC COMMUNICATIONS

by

Narayan Gehlot

139-86-4994

Electrical Engineering, New Jersey Institute of Technology, Newark, NJ, USA

Under the Guidance of

Prof.(Dr.) Yeheskel Bar-Ness

EE Department, NJIT, Newark, NJ, USA

(201) 596-3520

&

Dr. Thomas Banwell

Applied Research, *Bell Communications Research, Inc., Morristown, NJ, USA*

(201) 829-5117

Submitted to the Graduate Faculty of New Jersey Institute of Technology
In partial fulfillment of the requirements for the degree of

MASTER OF SCIENCE
OF
ELECTRICAL ENGINEERING

January 1991

THESIS

NOVEL WAY OF SUB-CARRIER COHERENT DETECTION AND CLOCK RECOVERY IN FIBER-OPTIC COMMUNICATIONS

Narayan Gehlot
139-86-4994
Electrical Engineering, New Jersey Institute of Technology, Newark, NJ, USA

Approved as to style and content by:

Prof (Dr.) Yeheskel Bar-Ness, Chairperson of Committee

Dr. Thomas Banwell, Member

Dr. Haim Grebel, Member

VITA

Name	:	NARAYAN GEHLOT
Mailing Address	:	
Permanent Address	:	
Date of Birth	:	
Place of Birth	:	

Education

01/1991 to 01/1991	:	M.S. Electrical Engineering New Jersey Institute of Technology, Newark, New Jersey, USA
01/1980 to 06/1986	:	B.E.(Honors) EEE and M.Sc.(Honors) Physics Birla Institute of Technology & Science, Pilani, India

Work Experience

01/1990 to 12/1990	:	Bell Communications Research, Morristown, NJ, USA
07/1989 to 08/1989	:	Bell Communications Research, Morristown, NJ, USA
08/1986 to 12/1988	:	Indian Institute of Technology, Madras, India

this thesis is dedicated to :

Almighty Shri **Harikaka Gosawi**

Prof (Dr) Yeheskel Bar-Ness

Dr Thomas Banwell

Dr. Gabor Kiss

Dr. Haim Grebel

Sadhana Gehlot

Everybody, who created an opportunity for me to be at Bellcore, those who helped me understand concepts and to all those who trusted me with their expensive equipment:

David Burpee

William Anderson
Felix Kapron
Howard Lemberg
William Stephens
Joyce Kilmer
Sunil Joshi

Ronald Menendez
Stuart Wagner
Charles Lo
Henri Tohme
Koon Loh
Beecher Adams
Orville Cockings
Ariel Dori
Anatoly Frenkel
Robert Kanen
Wayne Jones
Alan Chambers
Charles Bricker

TABLE OF CONTENTS

Introduction

Fiber-optics as a telecommunication media with almost unlimited bandwidth [several GHz × Km], immunity to electromagnetic interferences, low attenuation and hence higher repeater spacing and with many other desirable qualities is by now well known [1, 2, 3]. With the advent of fiber to the home and fiber to the curb network topologies a common person will enjoy fiber-optics based services very soon [4, 5]. With more and more demand for different services on fiber based systems in densely populated areas there is an ever increasing demand for high bandwidth systems. There have been a few laboratory results with systems operating about 4 to 20 GHz rate [6, 7] and some have reportedly been field tested at a 2.5 GHz rate. Most of these systems are digital systems, where a laser is turned ON for transmitting a **1** and turned OFF for transmitting a **0**. Beyond 2.5 GHz rates there is a limitation due to available electronics and therefore digital schemes are less popular.

Homodyne or Coherent Detection

It is necessary to shift the frequency of a baseband signal in many cases for various reasons. The baseband signal modulates a high frequency carrier at the transmitter. The modulated carrier is sent over a communication channel to the receiver.

At the receiver a local oscillator provides a carrier for information recovery from the incoming modulated signal. If the frequency of the local oscillator is synchronized to that of the incoming carrier, they are said be coherent with each other. The extraction of information by mixing of local and incoming coherent carriers is called Homodyne detection. Any loss of synchronization between incoming and local carrier will result in loss of information. On occasions information could be lost completely. The advantages of homodyne technique are

1. Improved signal to noise to ratio (SNR),

2. Selection of one particular channel out of many, and more details can be found in communication literature.

In Optical Homodyne detection the information is regularly transmitted either on the frequency or phase of an optical lightwave. At the receiver a lightwave of identical optical frequency (wavelength) is mixed with the incoming light and an optical homodyne detection recovers information. In optical frequency shift keying (FSK) the optical frequency (wavelength) of a laser is changed by applying different current proportional to information. In optical phase shift keying, the phase of a lightwave is changed according to the information to be transmitted. For optical homodyne detection at the receiver it is crucial that the phase of incoming light be synchronized all the time to the phase of local laser light, or else information will be lost. This is very difficult because lasers have inherent phase noise, which is a random process and is difficult to track. Optical phase lock loops are being studied for this purpose. Optical Homodyne detection is being persued in different laboratories [8, 9, 10].

Apart from direct digital transmission of data on a laser and Optical Homodyne detection schemes there is yet another way of using fiber-optics channel in todays opto-electronic technology. It is known as Sub-Carrier fiber-optics communication system.

In a Sub-Carrier fiber-optics system, a high frequency RF wave is first modulated with the digital or analog signal. This modulated RF Sub-Carrier in turn modulates a laser by varying the power of the light accordingly and thus converting the electrical signal to optical so that can be transmitted through fiber-optics media [11, 12, 13, 14].

Sub-carrier fiber-optic systems have a very high potential for using high bandwidth offered by fiber-optic media. Sub-Carrier systems have an advantage over time division multiplexed (TDM) system using fiber-optic technology in that services carried by different Sub-Carriers are independent of each other. Hence, it is possible to send analog video on one RF Sub-Carrier while transmitting another digital signal on other Sub-Carrier on same laser.

In order to perform coherent detection of Sub-carrier at the receiver, there is a need for a local reference Carrier synchronized with the incoming Sub-Carrier both in phase and frequency. There are various schemes which can be used to generate a synchronized carrier at the receiver [15], such as

a. Self-synchronization, where the timing or Sub-Carrier is extracted from the incoming signal.
b. Transmitting a separate synchronizing signal (pilot carrier)

Each approach has it's own merits and limitations. Scheme (a) could require sophisticated and expensive technology at the receiver and (b) would require compensation for system degradations.

The RF Sub-Carrier can be recovered in two ways for scheme (a) as shown in figure I.1. The first scheme is called Squaring Loop Carrier Recovery and second is called Costas Loop Carrier Recovery. The non-linearity of the squaring device will degrade signal to ratio for the first method.

Recovery of Subcarrier depend on the modulation technique and type of modulating signal. Modulating signal can be digital or analog. If it is analog it, may be sent on a carrier by single sideband (SSB) modulation or double sideband-suppressed carrier (DSB-SC) modulation or other analog modulation technique. If signal is digital then it is customary in lightwave to use binary phase shift keying (BPSK) or higher M-ary PSK. Other digital modulating techniques may also be used.

As stated previously satisfactory synchronization between the local and the subcarrier is crucial. To see this, let the subcarrier be $\cos \omega_c t$, with angular frequency ω_c and phase 0, which is amplitude modulated by an analog information m(t), using DSB-SC technique. An ideal local oscillator at the receiver should be $\cos \omega_c t$. In fact multiplying the incoming modulated subcarrier $m(t)\cos \omega_c t$ by the local oscillator output, we get;

$$m(t) \cos \omega_c t \times \cos \omega_c t = m(t)/2 + \cos 2\omega_c t \qquad (I.1)$$

and after the low pass filter (LPF) we get back the information m(t)/2. If the local subcarrier oscillator has an error of $\Delta\omega$ in frequency and δ in it's phase, the output of the coherent detection is then given by

$$m(t) \cos \omega_c t \times \cos[(\omega_c + \Delta\omega)t + \delta] = [m(t)/2] \{\cos[(\Delta\omega)t + \delta] + \cos[(2\omega_c + \Delta\omega)t + \delta]\} \quad (I.2)$$

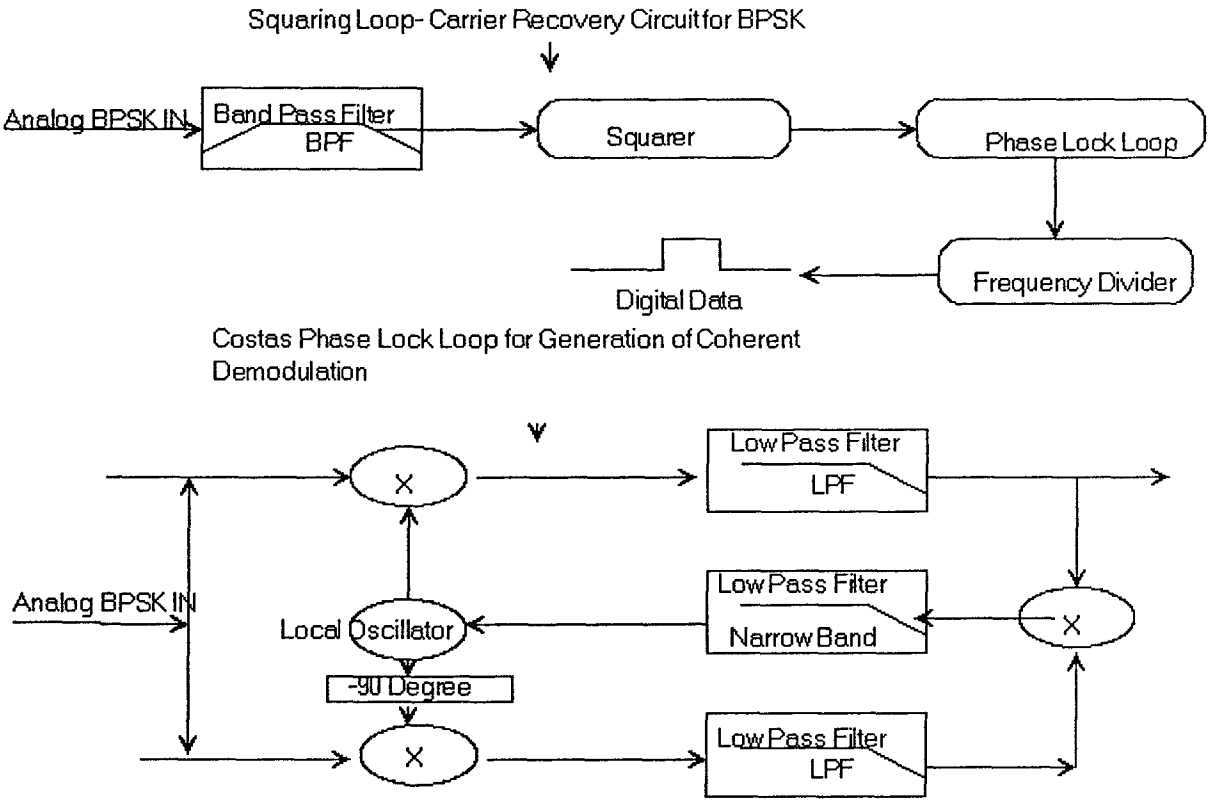

Figure I.1 Squaring loop-carrier recovery and Costas phase lock loop circuit for coherent demodulation

The second term will be filtered by the LPF as it has twice the subcarrier frequency. The remaining term passed by the filter contains the message;

$$e_d(t) = [m(t)/2] \cos[(\Delta\omega)t + \delta] \quad (I.3)$$

If $\Delta\omega = \delta = 0$, we have again exact replica of the signal m(t). If $\Delta\omega = 0$ but $\delta \neq 0$ then equation (I.3) is reduced to

$$e_0(t) = [m(t)/2] \cos \delta \quad (I.4)$$

In the above equation if δ is constant, the output is maximum when $\delta = 0$ and minimum when $\delta = \pm \pi/2$. Thus the phase error in the local subcarrier causes the attenuation of the output signal (reduction in SNR) without distortion. Unfortunately, the phase error δ is not constant, may vary randomly with time. This may occur, for example, because of variation in the propagation path. This causes the gain factor $\cos \delta$ to vary causing information distortion unless it is very small to be neglected or it is tracked by similar change of the local oscillator phase. Such tracking can be obtained by phase lock loop.

If $\Delta\omega \neq 0$, and $\delta = 0$, then equation (I.3) becomes

$$e_0(t) = [m(t)/2] \cos(\Delta\omega)t \quad (I.5)$$

In this case the output is not merely an attenuated replica of the signal m(t) but is rather distorted. Since $\Delta\omega$ is small, the shifted spectrum of signal pass through the filter. Such a "beating" effect is rather serious type of distortion.

Usually quartz crystal are used for stable oscillator source, which can be cut for very close frequency at the transmitter and receiver but never with $\Delta\omega = 0$ for a very long time of operation. Particularly for very high carrier frequency, where output frequencies are harmonic of a quartz crystal frequency performance is inadequate. Therefore it is impossible to perform coherent detection with an adequate synchronization of the local oscillator. Otherwise a pilot should be transmitted from transmitter to the receiver. Notice that, if SSB is used to transmit signal to conserve bandwidth squaring techniques and costas loop cannot be used [15].

Similarly, for digital signal modulation on subcarrier, amplitude variations due phase error of local subcarrier may result in higher bit error rate (BER). If digital information transmitted via amplitude shift keying (ASK) on a subcarrier then it may be demodulated coherently or non-coherently (envelop detection) at the receiver. The non-coherent detection of ASK is close to the performance of the

coherent detection when the noise is small. The difference in coherent and non-coherent detection is pronounced when noise is large.

Digital data, modulating the phase of the subcarrier to generate PSK at the transmitter, and it's coherent detection at receiver is shown in figure I.2. PSK sent on a subcarrier cannot be demodulated by envelop detection. Squarer or Costas loop shown in figure I.1, will give subcarrier with a sign ambiguity when used to generate a carrier from PSK. Hence, carrier extracted from PSK by these two methods cannot be used for coherent demodulation. Non-availability of a suitable local subcarrier at the receiver in PSK is overcome by encoding the data by differential code before modulation as shown in figure I.3, and is called DPSK.

If $\cos \omega_c t$ is the subcarrier, and p'(t) the baseband pulse, then the subcarrier pulse can be represented by;

$$p(t) = [\sqrt{2}]\, p'(t) \times \cos \omega_c t \qquad (I.6)$$

If E_p is the energy in the received pulse and N/2 is the baseband noise power spectral density, the energy SNR, designated by, ρ is [16]

$$\rho^2 = 2E_p / N, \qquad (I.7)$$

then the probability of error, P_e, is found to be given by

$$P_e = Q(\rho) \qquad (I.8)$$

where Q is the error function [15]. Probability of error will increase as the SNR decreases or as the phase and frequency of local oscillator goes out of synchronization.

There is always a need to conserve bandwidth and develop systems with high bandwidth efficiency. Table I.1, lists the bandwidth efficiency for different modulation techniques.

There is always a need to conserve bandwidth and develop systems with high bandwidth efficiency. Table I.1, lists the bandwidth efficiency for different modulation techniques.

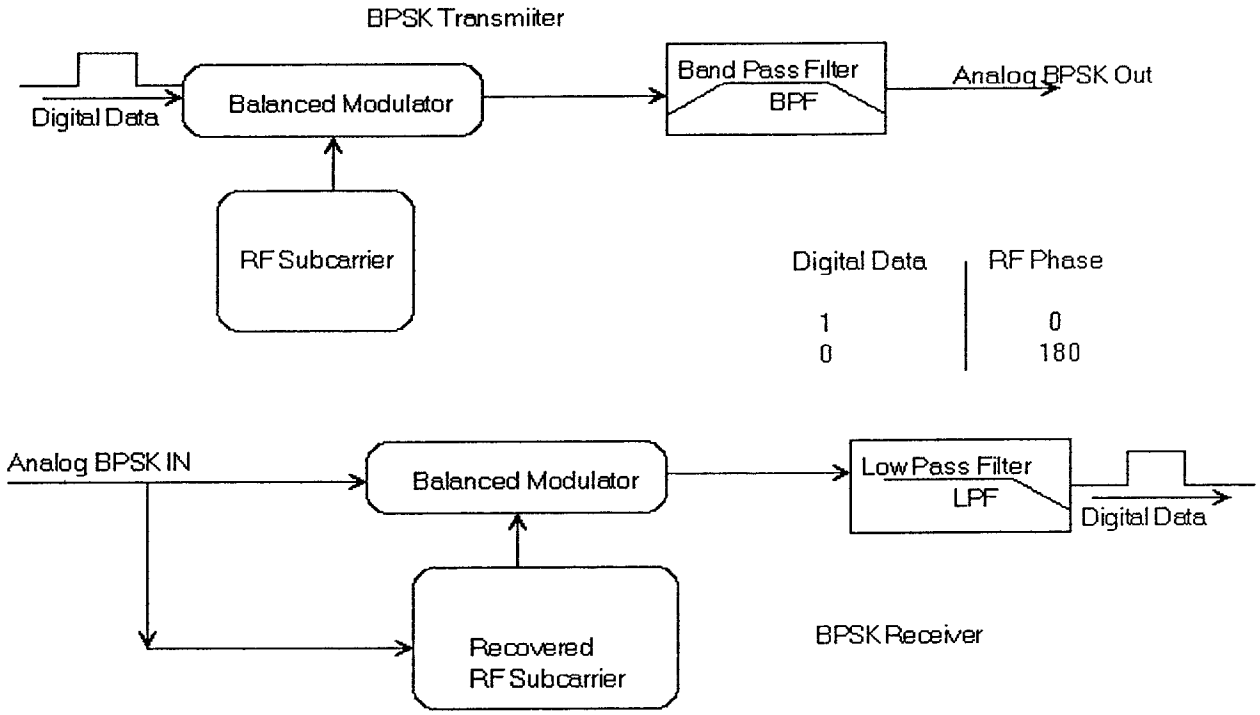

Figure I.2 BPSK transmitter and receiver

If instead of BPSK we use QPSK, or any higher order M-ary PSK the differential phase approach becomes complicated [17] and there is a tighter limit on the stability of local subcarrier. Table I.2, shows how the carrier to noise or energy to noise per bit ratio changes when instead of BPSK, we use QPSK, 8PSK or 16PSK for a BER of 10^{-9}. Inadequate coherency of the local oscillator will make the situation even worst. Transmitting a pilot can guarantee the availability of local subcarrier for coherent detection, nevertheless there are some questions to be addressed in this case.

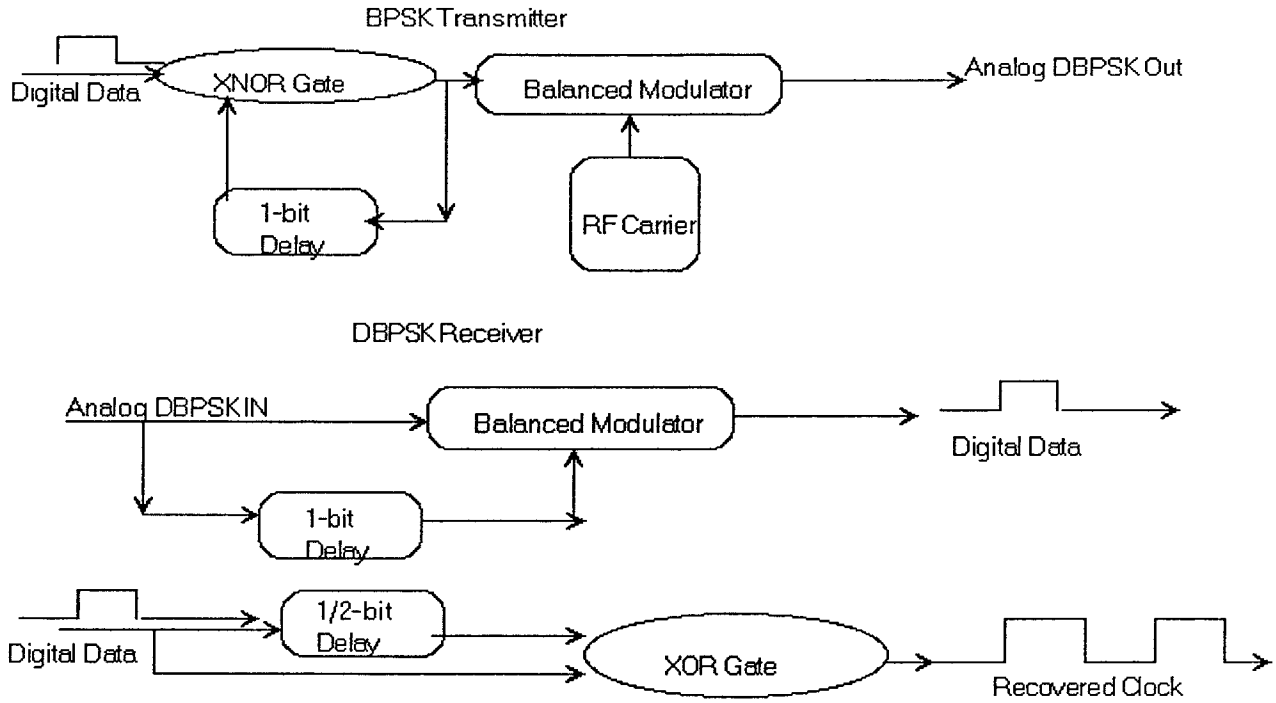

Figure I.3 DBPSK transmitter, receiver and clock recovery circuits

Table I.1

Modulation	Encoding	Bandwidth	Baud	Bandwidth Efficiency
FSK	single bit	$\geq F_b$ = Bit Rate/2	F_b	≤ 1
BPSK	single bit	F_b	F_b	1
QPSK	Dibit	$F_b/2$	$F_b/2$	2
8PSK	Tribit	$F_b/3$	$F_b/3$	3
16QPSK	Quadbit	$F_b/4$	$F_b/4$	4
256QPSK	Octabit	$F_b/8$	$F_b/8$	8

Other issue for consideration when digital communication is persued is that of timing clock recovery. Example of such timing clock recovery schematic for BPSK is shown in Figure I.3c. The disadvantage of clock recovery by this scheme is that digital data should contain a substantial number of transitions (1/0 sequence) for the recovered clock to be maintained. Manchester coding is often used to overcome this problem. But Manchester coding doubles the bandwidth of data. Another scheme known as data scrambling at the transmitting end and descrambling at the receiver is widely used to reduce clock recovery jitter [16,17]. We would need clock and fast digital chips as information rate goes up for scrambling. As the rate of data is pushed up the digital technology does not exist or even if it exist it is too expensive !

Table I.2

Modulation Technique	Carrier to Noise ratio C/N(dB)	E_b/N_0 ratio (dB)
BPSK	13.6	10.6
QPSK	13.6	10.6
8PSK	18.8	14
16PSK	24.3	18.3

PROPOSED CONCEPT:

The idea of this Thesis is to transport a low frequency RF as a reference pilot from the transmitter to the receiver on a separate laser using the principle of Wavelength Division Multiplexing. This pilot is taken to be the subcarrier frequency divided by an integer (N).

At the receiver end, the pilot is extracted from one of the two wavelengths, then frequency multiplied by an integer (N) to obtain a local oscillator which is coherent to the subcarrier modulating the other wavelength and which carries the information.

Wavelength Division Multiplexing of the pilot and the information carrying subcarrier has its advantages. Nevertheless the question remain is whether such an arrangement will cause, due to a different dispersion of the two wavelengths, degradation in coherency that will effect performance and increase the probability of error.

Figure I.4 shows block diagram of this concept.

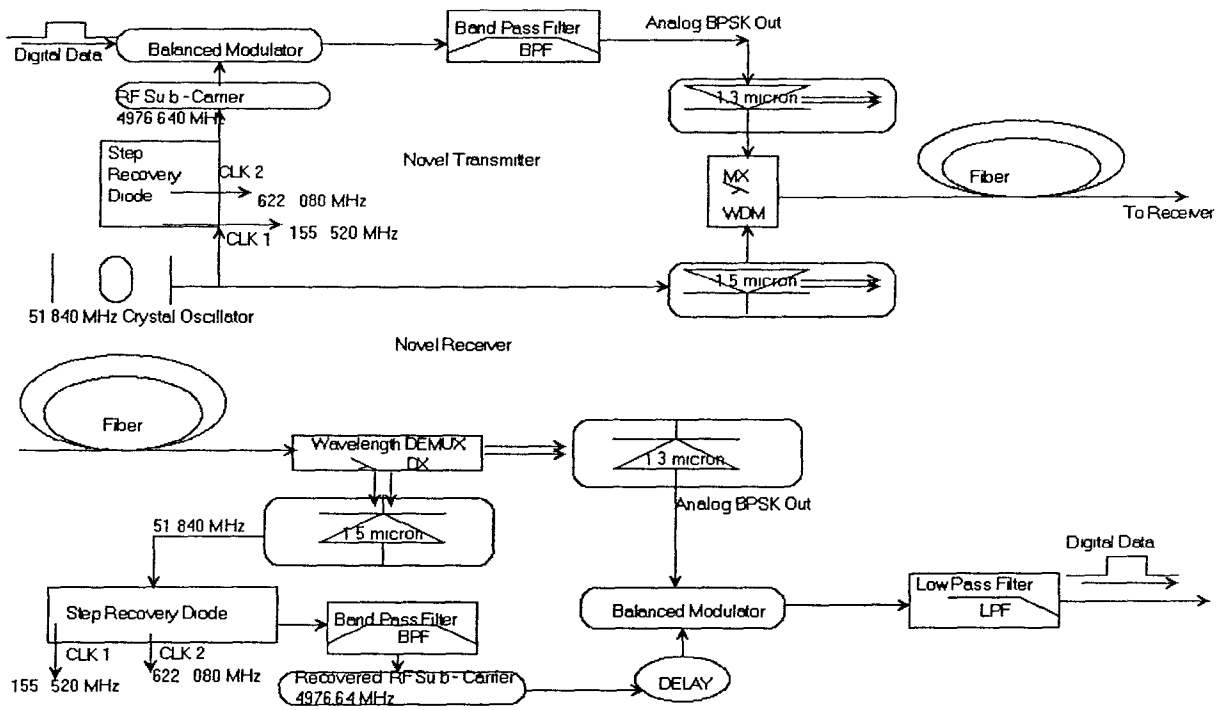

Figure I.4 Transmitter and receiver as per our concept

At the transmitter end a stable crystal oscillator of 51.840 MHz frequency serves as a pilot to modulate a laser at 1533 nm laser. With this judicious choice of 51.840 MHz frequency we can generate the subcarrier frequency of 4976.64 MHz (= 96 × 51.840) as well as other harmonics of 51.840 MHz which

might be used as data clock (example 155.520 MHz, 522.080 MHz). A step recovery diode can be used to generate these and other frequencies.

The availability of 51.840 MHz pilot at the receiver after propagation through fiber on a different laser light and it's coherency with subcarrier frequencies (send on different laser lights) at the receiver is the subject of investigation in this thesis.

Apparently an approach similar to our concept was reported in [18] , it differs from our concept in two aspects; it uses one wavelength for direct modulation of the laser with digital data and transmit a digital clock (clock frequency $\geq$ data rate) on a second wavelength.

Transmitting a high frequency digital clock on the second wavelength rather than sinusoidal pilot result in the following limiting factors:

1. Availability and cost of electronics at frequencies higher than 2.5 GHz.
2. Dispersion of non-sinusoidal clock in fiber due to it's electrical harmonic contents as compared to 51.87 MHz single tone,
3. Bandwidth of such clock will restrict it's application in a dense WDM, specially at higher rates of a 5 GHz or more,
4. Very high laser chirp frequency for non-sinusoidal clock with residual dispersion of fiber will limit the transmission distance.

These and other questions related to the coherency of subcarrier and its effect on data transmission using the concept proposed here are to be discussed in the next chapters.

Albert Einstein:

The formulation of a problem is often more essential than it's solutions, which may be merely a matter of mathematical expressions or experimental verifications.....

Chapter 1

Wave Propagation in Fiber-optic Communication System

For transmitting signals on a fiber it is essential to convert them to optical frequencies using laser sources. Normally laser diodes can be directly driven by the electrical signals. In Subcarrier fiberoptic system information, analog or digital, modulates a RF microwave frequency (say 4976 640 MHz) called subcarrier. The electrical current generated by modulating subcarrier with information drives the laser diode. Thus it is a two stage modulation before information is coupled to a fiberoptic media for transmission. Driving laser diode with signal current is called intensity modulation At the transmitter a laser diode converts electrical subcarrier and information to optical form and a reverse process is carried out in a photodetector at the receiver. Due to electrical to optical (E/O) conversion at transmitter, propagation of lightwave in fiberoptic media and optical to electrical (O/E) conversion at the receiver, subcarrier and information will interact with different noise processes. **In this chapter we will formulate the problem to be investigated with the aid of different noise processes in a subcarrier fiberoptic system.**

1.1 Intensity Modulation of Laser

Intensity Modulation (IM) is similar to Amplitude Modulation (AM) in principle but differs from it in one important aspect. The average power of the transmitted wave , rather than it's amplitude, varies in proportion to the modulating signal [3].

If we designate our RF carrier bearing the information as

$$A \cos(\omega_{rf} t + \theta(t)) \qquad (1.1)$$

where $\theta(t) = 0$ or π ; will be Binary Phase Shift Keying (BPSK) modulation, then the intensity of the lightwave will be given by

$$P_O(t) = P_C[\,1 + mA\cos(\omega_{rf}t + \theta(t))\,] \text{ watts} \qquad (1.2)$$

where P_C is average laser optical power.

The spectrum of an intensity-modulated wave can be found by taking the Fourier Transform (FT) of the electric field (Ec) phasor. The optical power P_C is proportional to the square of the amplitude of E_C;

$$E(t) = E_c \surd[\,1 + mA\cos(\omega_{rf}t + \theta(t))\,], \qquad (1.3)$$

where E(t) is the signal that modulates the lightwave carrier amplitude so that intensity will vary in proportion to the signal. It is obvious from above equations that E(t) is not sinusoidal. Nevertheless it is periodic, and can be expanded in an infinite power series. Then the Fourier transform of E(t) can be obtained from this series;

$$\surd[\,1 + mA\cos(\omega_{rf}t + \theta(t))\,] =$$

$$1 + [mA\cos(\omega_{rf}t + \theta(t))]/2 - [mA\cos(\omega_{rf}t + \theta(t))]^2/2\times4 + 3\times[mA\cos(\omega_{rf}t + \theta(t))]^3/2\times4\times6$$

$$+\text{other terms} \qquad (1.4)$$

The above equation suggests that IM spectrum has infinite bandwidth. If the depth of modulation (m) is small then only a few terms are to be considered and bandwidth approaches that of an AM modulation. The following example demonstrate this fact.

Let A = 1, modulation index be m = 0.8 (80%) and if we are using a light source with optical frequency Ω_l then the equation for the modulated wave, in it's simplest form,

$$e_t(t) = E_c\{\surd[\,1 + 0.8\cos(\omega_{rf}t + \theta(t))]\}\cos(\Omega_l t),$$

$$= E_c \Sigma a_n \cos(\Omega_l t \pm n\omega_{rf}t + n\theta(t)) \qquad (1.5)$$

where we assumed that the laser is pure sinusoidal with no phase noise. Simple trignometric expansions would give the following equation

$$e_t(t) = E_c\,[0.96+0.432\cos(\omega_{rf}t + \theta(t))-0.04\cos2(\omega_{rf}t + \theta(t))+0.008\cos3(\omega_{rf}t + \theta(t))]\times\cos(\Omega_l t)$$

$$= 0.96\,E_c\cos(\Omega_l t) + 0.216\,E_c\,[\cos(\Omega_l t-\omega_{rf}t-\theta(t)) + \cos(\Omega_l t+\omega_{rf}t+\theta(t))]$$

$$- 0.02\,E_c\,[\cos(\Omega_l t-2\omega_{rf}t-2\theta(t)) + \cos(\Omega_l t+2\omega_{rf}t+2\theta(t))] +\ldots\ldots\ldots\ldots \quad (1.6)$$

The remaining terms are small and hence can be neglected. However, if we omit the higher order terms, say by band limiting, for example, it will represent distortion in RF wave [2, 3]. Obviously a square wave has many more frequency terms than a single tone sine wave. Therefore, for the same bandwidth a square wave would suffer more distortion than a single tone sinewave.

Intensity Noise

Intensity modulation of laser produces intensity noise. Detail discussion on this topic is beyond the scope of this work. Interested authors are refereed to [1, 3, 18, 19, 20]. Laser Intensity fluctuations are an inherent device characteristics, given the quantum nature of the transitions. These fluctuations give rise to Intensity Noise. Intensity noise (IN) peaks at threshold and decreases as the injection current level increases. The excess noise attributed primarily to spontaneous emission depends on laser structural parameters. Relation between the intensity modulation of the output light wave and the modulation frequency (f) of the driving current is as follows

$$M(f) = [\,1 - (f / f_0)^2 + j\,(2\alpha)\,f / f_0^2\,]^{-1} \quad (1.7)$$

where, f_0 is due to resonance between electron and hole populations, α is the damping constant (α is related to, f_d, the damping frequency),

Using equation (1.7) we obtain the spectrum of the laser intensity noise

$$IN(f) = [f_0^2/a] \times [1+b^2f^2] \div |[f_0^2 - f^2 + j\, f\, f_d]|^2 = [f_0^2/a] \times [1+b^2f^2] \div \{[f_0^2 - f^2]^2 + [f\, f_d]^2\} \quad (1.8)$$

where a and b depend on Langevin noise source [18,21]

Equation (1.8) suggest that modulating a laser with high frequency will increase intensity noise and hence our concept has an advantage in that transmitting a pilot of 51.840 MHz will have less intensity noise resulting in more repeater distance as compared to transmitting a digital clock of same frequency in a WDM scheme.

Effect of reflections on Intensity Noise

It is important to note that in any practical system there will be optical fiber discontinuities and there will always be reflected light. Reflection power could vary from -25 dB to -65 dB. The factors governing these variations are the type of connection used - fusion splice, mechanical splice or connectors and environment temperatures. In air gap connectors there is a discontinuity in refractive index of fiber which will vary with temperature and in length for individual connection. This forms like an air cavity and light gets reflected and oscillate in the air gap. In mechanical splices there is an index matching gel which varies it's refractive index with temperature and therefore the amount of reflected light energy. It is worst under temperature extremes and is a serious concern in analog transmission systems. Reflections will aggravate IN(f) noise by several dB and could lead to system failures if not properly accounted for or minimized. There will be two types of reflections - far end and near end. They will become critical in full duplex systems. Details can be found in [19].

Laser Chirp Noise

Chirp imposes ultimate channel density limitations in a WDM and subcarrier frequency division multiplexed systems. The chirp broadens the power spectrum of a modulated single - longitudinal mode laser introduces limitations in the bit-rate distance product, due to residual dispersion in optical fibers. The important determining characteristics is the modulated power spectrum of laser. A spread

in this spectrum due to chirp translates to a spread in the transit time through the fiber, resulting in distortion of the optical pulse. This pulse broadening results in inter-symbol interference in long-haul high speed optical communication link. The peak chirp increases linearly with the Intensity Modulation index. For a laser operating at 1300 nm, biased at $1.8I_{th}$ (I_{th} is laser threshold current) and being modulated by electrical frequency of 700 MHz, figure 1.1 illustrate the chirp frequency for sinusoid, square and pseudo random binary sequence.

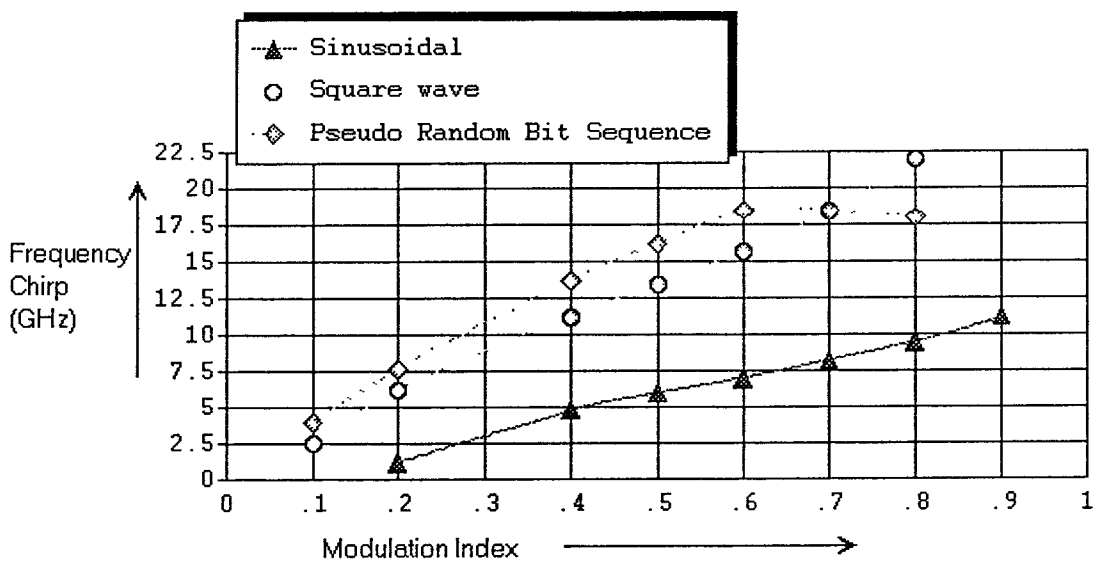

Figure 1.1 Chirp frequency for sinusoid, square and pseudo random binary sequence

This clearly indicates that a modulation of a laser with a sinewave with 0.8 modulation depth has far less chirp frequency as compared to a digital square wave clock. As the frequency of data and subcarrier modulation is increased chirp frequency will be in the bandwidth of the signal and will be a serious problem as pointed out in introduction due to "beating" effect. Recovery of carrier from signal will be limited and chirp combined with dispersion will limit the transmission distance. Hence transmission of a low frequency pilot as per our concept will provide a desirable carrier at the receiver and could result in longer repeater span for subcarrier systems.

Laser Phase Noise

Neglecting optical intensity fluctuations, the electric field of the laser can be described by a wave with constant envelope:

$$E(t) = E_0 \exp [-j(\Omega_{1.3} t + \Phi_{1.3}(t))] \qquad (1.9)$$

where E_0 is the amplitude, Ω_l is the central optical angular frequency of laser, and $\Phi_l(t)$ is the laser phase noise. We can treat $\Phi_l(t)$ as a Gaussian random process [24].

If we are to transmit the coherent pilot on a different wavelength, say 1533 nanometer (nm) we will have a similar expression

$$E(t) = E_0 \exp [-j(\Omega_{1.5} t + \Phi_{1.5}(t))] \qquad (1.10)$$

From equation (1.8) and (1.9), it is clear that two lasers will have independent random phase noise. Hence, they will contribute different noise to the sucarrier and pilot due to their linewidth and fiber dispersion.

In optical Homodyne detection laser phase noise is a problem and lots of work is being done in its investigation. Laser phase noise is the limiting factor for Optical PSK coherent detection and because of it's random characteristics can damage information totally.

How can this affect the performance of a subcarrier intensity modulation system ? As the frequency of signal or subcarrier is increased to several GHz, the laser phase noise bandwidth will be close to signal bandwidth and hence it will interact with the subcarrier and impose optical power penalty or reduce repeater span [24, 25], see also equation I.4, of the introduction.

1.2 Wave Propagation in fiber using Intensity Modulation

Subcarrier modulated with signal on one laser and pilot on another laser are to be sent on fiber using optical Wavelength Division Multiplexing (WDM) device. To examine the effect of fiber on such combined lightwave signal we review some characteristics of fiber:

Let Ω be angular frequency of optical wave, β it's wave propagation constant; V_p phase velocity

$$V_p = \Omega/\beta \qquad (1.11)$$

and group velocity

$$V_g = d\Omega/d\beta \qquad (1.12)$$

Any signal or disturbance superimposed onto a wave propagates not at the phase velocity V_p, but at the group velocity V_g, justification for this assertion can be found in most texts on wave propagation. In non-dispersive medium the phase velocity is independent of the wave frequency, and the group velocity and phase velocity are same i e. $V_p = V_g$. But in dispersive media such as fiber, where by definition the phase velocity is a function of frequency, and $V_p \neq V_g$ We can write by using (1.11)

$$dV_p / d\Omega = [\beta - \Omega \, d\beta/d\Omega] / \beta^2$$

$$= [1 - V_p \, d\beta/d\Omega] / \beta$$

where we used $V_p = \Omega / \beta$. But again $\beta = \Omega / V_p$ and $d\beta/d\Omega = 1 / V_g$., we get

$$dV_p / d\Omega = [1 - V_p / V_g] / (\Omega / V_p)$$

Rearranging the above equation we finally obtain the relation

$$V_g = V_p /[1 - (\Omega / V_p)(dV_p / d\Omega)] \qquad (1.13)$$

This is very important because signal in lightwave communication is carried by group velocity of light. Because of frequency dependency of phase velocity the signal is attenuated and distorted to a certain extent during it's travel in fiber-optic media.

Define the group index N the relation

$$V_g = c / N \qquad (1.14)$$

Clearly by the definition of the index of refraction n;

$$Vp = c / n \qquad (1.15)$$

Where c is speed of light in vacuum. Relating to the wave propagation constant β, we get (1.12) together with (1.11) and (1.15)

$$1 / V_g = d\beta/d\Omega = d[\Omega n/c]/d\Omega = [n + \Omega\, dn/d\Omega] / c \qquad (1.16)$$

and comparing with (1.14) we conclude that

$$N = n + \Omega\, dn/d\Omega \qquad (1.17)$$

Also clear that the information - bearing spectrum of a wave travels 1 meter in a time τ,

$$\tau = 1/ V_g = d\beta/d\Omega$$

Obviously τ might be a function of Ω. Hence different part of the spectrum will be travelling 1 meter in different time. This causes dispersion,

$$d\tau/d\Omega = d[\, 1/V_g \,] /d\Omega = d^2\beta/d\Omega^2 \qquad (1.18)$$

Sometimes instead of the frequency Ω, one uses expressions in terms of the wavelength λ; $\lambda = 2\pi c / \Omega$

By definition $dn /d\Omega = [dn/d\lambda]\, [d\lambda/d\Omega]$, and noticing that

$$d\Omega / d\lambda = - 2\pi c/\lambda^2 \qquad (1.19)$$

we get the following by substituting (1.19) in (1.17)

$$N = n + [2\pi c/\lambda] \times[-\lambda^2/2\pi c] \, dn/d\lambda = n\text{-}\lambda dn/d\lambda \qquad (1.20)$$

Thus, the group velocity is related to refractive index and laser wavelength as given below

$$V_g = c/N = c [n\text{-}\lambda \, dn/d\lambda]^{-1}. \qquad (1.21)$$

Again for 1 meter distance the time τ, for information bearing wave to travel is

$$\tau = 1/V_g = [1/c] [n\text{-}\lambda \, dn/d\lambda] \qquad (1.22)$$

and the dispersion $D(\lambda)$ is given by

$$D(\lambda) = d\tau/d\lambda = [1/c][dn/d\lambda - \lambda dn^2/d\lambda^2 - dn/d\lambda] = - [\lambda/c][dn^2/d\lambda^2] \qquad (1.23)$$

From (1.23) if fiber is of length z and if the spectral width is $\Delta\lambda$ (where $\Delta\lambda$ is defined as the range of wavelengths over which the spectral power exceeds 50% of the peak spectral power), then the total dispersion

$$\Delta t = -[z/c][\Delta\lambda] [\lambda \, d^2n/d\lambda^2] \qquad (1.24)$$

or

$$\Delta t = -[z/c] [\gamma] [\lambda^2 \, d^2n/d\lambda^2] \qquad (1.25)$$

where γ is the relative spectral width

$$\gamma = | \Delta\lambda/\lambda | = |\Delta\Omega/\Omega| \qquad (1.26)$$

This dispersion is referred to as material dispersion in single mode fiber and is due to finite laser source linewidth. Every fiber has an operating wavelength where material dispersion is nearly equal to

zero, and this wavelength is called zero dispersion wavelength, λ_0. Laser sources operating at wavelengths other than λ_0 would suffer more dispersion as they travel through fiberoptic media.

Since we will be using wave propagation constant, β, in our analysis, we go back to expressing absolute transit time, pulse spread and dispersion in terms of β.

If τ is propagation time delay of a wave propagating in one meter of a dispersive medium, then from equation (1.18)

$$d\tau/d\Omega = d^2\beta/d\Omega^2 \qquad (1.27)$$

If the signal has a spectrum extending from ($\Omega_0 - \Delta\Omega$) to ($\Omega_0 + \Delta\Omega$), where Ω_0 is the central frequency of optical source and $\Delta\Omega$ is source frequency spectrum extension, then the difference in propagation time of parts of this signal at the opposite extremes of the spectrum will be,

$$\Delta\tau = 2\Delta\Omega\, d\tau/d\Omega = 2\Delta\Omega \times d^2\beta/d\Omega^2 \qquad (1.28)$$

The dispersion in the time of arrival of the signal is a form of distortion. It limits the rate at which data can be transmitted through the medium. From equation (1.11) and (1.15) the wave propagation constant, is given by

$$\beta = \Omega n/c \qquad (1.29)$$

Also from equation (1.22)

$$d\beta/d\Omega = [n - \lambda dn/d\lambda]/c = \tau \qquad (1.30)$$

where τ is the delay per 1 meter at the particular wavelength. Obviously $1/V_g = d\beta/d\Omega$ has dimensions of delay.

Also from.(1.23), we have

$$D(\lambda) \triangleq d\tau/d\lambda = -[\lambda/c][dn^2/d\lambda^2] \quad (1.31)$$

The dimensions of $D(\lambda)$ are ps/nm-km ; and is a measurable parameter. $D(\lambda)$ is called the first order dispersion. We can relate first order dispersion, $D(\lambda)$ to second derivative of propagation constant, $d^2\beta/d\Omega^2$, as shown below:

$$d\tau/d\lambda = [d\tau/d\Omega][d\Omega/d\lambda] = [-2\pi c/\lambda^2]d^2\beta/d\Omega^2 \quad (1.32)$$

where we used the fact $\Omega = 2\pi c/\lambda$, so that $d\Omega/d\lambda = -2\pi c/\lambda^2$ and $d\tau/d\Omega = d^2\beta/d\Omega^2$. But $d\tau/d\Omega = D(\lambda)$ implies.

$$d^2\beta/d\Omega^2 = -D(\lambda)\,\lambda^2/2\pi c \quad (1.33)$$

Furthermore to find $d^3\beta/d\Omega^3$ we write,

$$d^3\beta/d\Omega^3 = d/d\Omega\,\{\, d^2\beta/d\Omega^2 \,\} = d/d\Omega\,\{\, -D(\lambda)\,\lambda^2/2\pi c \,\}$$

$$= d/d\lambda\,\{\, -D(\lambda)\,\lambda^2/2\pi c \,\}\, d\lambda/d\Omega = [-1/2\pi c]\,[\lambda^2\, d\,D(\lambda)/d\lambda + 2\lambda\, D(\lambda)]\,[-\lambda^2/2\pi c]$$

$$= [\lambda^2/(2\pi c)^2][\lambda^2\, d\,D(\lambda)/d\lambda + 2\lambda\, D(\lambda)] = [\lambda^4/(2\pi c)^2][d\,D(\lambda)/d\lambda + 2\,D(\lambda)/\lambda] \quad (1.34)$$

Receiver

The wave equation at receiver, after signal on laser light has travelled a distance of z Km in fiber is

$$E(z,t) = E_c\,\{\sqrt{\,[\,1+mA\cos(\,\omega_{rf}t + \theta(t)\,)\,]}\,\}\exp(-\alpha z/2)\cos(\,\Omega_l t - \beta z\,)$$

$$= E_c \exp(-\alpha z/2)\,\Sigma\, a_n \cos(\,\Omega_n t - \beta(\,\Omega_n) z\,) \quad (1.35)$$

where a_n and Ω_n are the different spectral line parameters as part of them are specified in (1.6) for m = 0.8, α is a fiber-optic media attenuation in dB/Km.

$$\Omega_n = \Omega_l \pm n\,(\omega_{rf} + \theta(t))$$

and Ω_l equals either $\Omega_{1.3}$ or $\Omega_{1.5}$ with its spread according to its linewidth. Hence (1.35) can be written as

$$e_t(t) = 0.96\, E_c \cos(\Omega_l t - \beta z) + 0.216\, E_c [\cos(\Omega_l t - \beta z + \omega_{rf} t + \theta(t)) + \cos(\Omega_l t - \beta z - \omega_{rf} t - \theta(t))]$$

$$- 0.02\, E_c [\cos(\Omega_l t - \beta z + 2\omega_{rf} t + 2\theta(t)) + \cos(\Omega_l t - \beta z - 2\omega_{rf} t - 2\theta(t))] + \ldots\ldots\ldots\ldots$$

β as a function of Ω can be expanded using Taylor series around Ω_0, the central frequency of the optical source, as shown below [3, 26 ,27]:

$$\beta(\Omega) = \beta_0 + \{d\beta_0/d\Omega\}[\Omega-\Omega_0] + \{d^2\beta_0/d\Omega^2\}[\Omega-\Omega_0]^2/2 + \{d^3\beta_0/d\Omega^3\}[\Omega-\Omega_0]^3/6 + \text{Higher terms} \quad (1.36)$$

where β_0 is the wave propagation constant at Ω_0. Related to the derivatives of wave propagation constant β at Ω_0 will have the following effects:

Constant Delay due to $\{d\beta_0/d\Omega\}[\Omega-\Omega_0]$ (1.37)

First order dispersion due to $\{d^2\beta_0/d\Omega^2\}[\Omega-\Omega_0]^2/2$ (1.38)

Second order dispersion due to $\{d^3\beta_0/d\Omega^3\}[\Omega-\Omega_0]^3/6$ (1.39)

All these terms as a function of the dispersion $D(\lambda)$ and λ are given in (1.30), (1.33) and (1.34). The last two terms cause dispersion. Substituting Eq(1.36) with Ω taken as Ω_n into Eq.(1.35) for each laser the lightwave at receiver will be given by the following equation:

$$E(z,t) = E_c \exp(-\alpha z/2) \Sigma\, a_n \cos(\Omega_n t - [\beta_0 + \{d\beta_0/d\Omega\}[\Omega_n-\Omega_0] + \{d^2\beta_0/d\Omega^2\}[\Omega_n-\Omega_0]^2/2 + \{d^3\beta_0/d\Omega^3\}[\Omega_n-\Omega_0]^3/6 + \ldots\ldots\}z + \Phi_{nl}]\} \quad (1.40)$$

where Ω_0 are to be taken as the center frequency of the laser $\Omega_{1.3}$ or $\Omega_{1.5}$.

Subcarrier with data will be transmitted on a laser with minimum dispersion wavelength. We could transmit a pilot on a laser close to zero dispersion wavelength, but this will require more expensive optical WDM components.

In order to use relatively small length of fiber we propose to use laser operating close to zero dispersion wavelength for transmitting data on subcarrier and laser in dispersive optical window for transmitting pilot. This will cause high dispersion on our pilot.

1.3 Problem Formulation

To summarize some of previous discussions:

There are various sources of noise that one has to consider in a wavelength division multiplexed system (WDM) such as ours [21]. Each laser will have intensity noise, chirp, phase noise, attenuation, different sensitivity to reflected optical power, laser linewidth and hence different dispersion in fiberoptic media. Because of different optical frequency each laser will generate it's own laser phase noise to intensity noise [24]. If optical power is very high there may be signal degradation due to stimulated Raman scattering in WDM approach [19,28,29] !

We expect that the different lasers carrying pilot and subcarrier with information may or may not be synchronous at the receiver because of different noise phenomenons presented above To quantify the availability of a synchronous pilot for coherent detection of subcarrier and recovery of synchronous timing clock at the receiver is the subject of investigation of this Thesis using our concept presented in introduction and shown in figure I.4.

We ask the following questions and answer them at the end of Thesis:

Q1. If we transmit synchronous microwave subcarrier $\omega_{rf1.3} = \omega_{rf1.5}$ of identical frequency and phase, i.e. the same RF signal on two different lasers, will the two RF detected subcarrier; the pilot and the subcarrier carrying information be sufficiently Coherent. ? *If no, then our concept does not work.*

Because any extra incoherency on 51.840 MHz which may occur, due to frequency multiplication of the 51.840 MHz pilot will cause further degradation.

If yes, then

Q2. We will like to examine, where possible, the effect of all different noise phenomenons caused by the fiber optic media.

Q3. Furthermore using low frequency pilot (51.84 MHz) will the extra jitter due to multiplication be large enough to cause reduction in performance and how much if possible to quantify these effects. Customary step recovery diode, similar to that used at the transmitter, will be used in the receiver for multiplying the pilot frequency. If there is a problem in performance degradation then Phase Lock Loop may be used in pilot frequency multiplication process. **If no, then we demonstrate our concept in total.**

Chapter 2

System Components Characteristics

For our experimental analysis we propose to use the schematic shown in figure I.4, given in introduction. In order to theoretically predict experimental outcome it necessary to know individual component characteristics. At the transmitter we have laser for E/O conversion of subcarrier and pilot, then signal propagates through fiberoptic media with discontinuities due to connections and finally the photo detectors convert incoming optical signal to electrical. Since we are interested in finding the phase and frequency error between pilot and subcarrier we will need a phase detector, and hence it's characteristics are to be measured. We will try to measure the characteristics of the most of the components of the system in this chapter and use them in next chapter.

2.1 Laser Characteristics

Two distributed feedback lasers (DFB) lasers made by Fujitsu were available. DFB lasers are very sensitive to reflections and care should be taken in operating them, because their facets can get damaged and wavelength could drift due to near end reflections. Usually an optical isolator is used between the laser output and fiber pigtail. More details on near end and far end reflections can be found in [19].

The current versus optical output power was measured using an HP 8152 optical power meter. Experiment set up is shown in figure 2.1. Current was increased in a step of 1 milliampere (mA). The measured current versus optical power characteristics are shown in graphs 2.1. To find intensity fluctuations we need the derivative of current VS light output. This is depicted in graph 2.1.

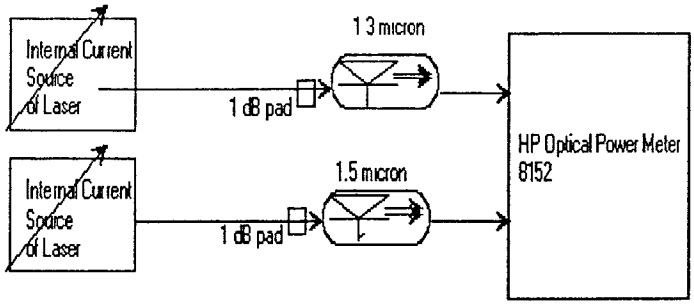

Figure 2.1 Experimental setup to measure laser optical output power and its fluctuations

Laser operating conditions

	Laser λ = 1306 nm	Laser λ = 1533 nm
Temp (^{0}R)	16.2	- 5.37
Threshold Current (mA)	14	14
Bias Current (mA)	[I_{bias} = 1.85 I_{th}]= 26	[I_{bias} = 1.85 I_{th}]= 26
Optical Power at Bias current	0.881 mW	0.259 mW

From the graph shown below, we note that at the bias current optical output of 1.3 micron laser is -0.55 dBm (0.881 mW) and the optical output of 1.5 micron laser is -5.875 dBm (0.259 mW). The laser optical power fluctuations in the absence of any external modulation causes Intensity noise. As discussed in chapter 1, this is an inherent to any laser and minimum fluctuations is clearly preferred. It is also important to note from graph 2.1, note that 1533 nm laser that we are using has more intensity noise than that of 1306 nm laser. The fact that the 1533 nm laser has high intensity noise is not a problem in our concept, since only a single frequency and not a modulated subcarrier is conveyed with this laser. We may look at this fact as an advantage of our concept as we can use less expensive laser for transmitting the pilot.

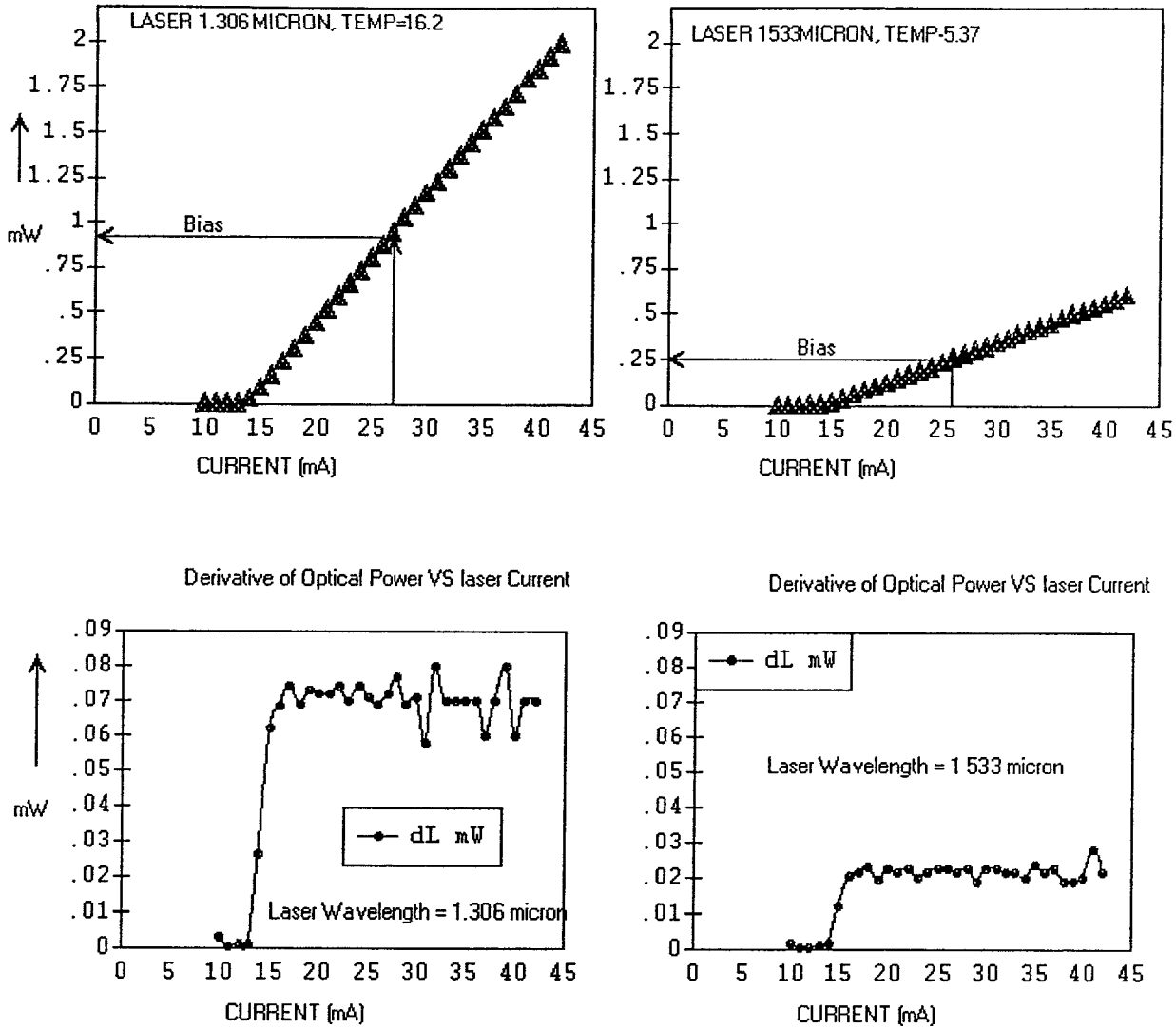

Graph 2.1 Laser optical output power and its fluctuations

Laser Modulation Bandwidth and Intensity Noise

The shape and amplitude of a laser's intensity-noise spectrum provides very useful information about the laser. Spurious, random emissions cause intensity fluctuations in the laser's light output. These fluctuations form the noise floor which varies with frequency, peaking at the relaxation resonance of the laser. The location of the relaxation resonance, or intensity noise peak, is related to the maximum modulation rate of a given laser. This resonance appears as a peaking in the frequency response, or as a rise in the noise floor of the unmodulated laser. The interaction between the optical field in the laser

and the injected-electron density due to the bias current causes the peaking in both responses. Oscillations of both the output light and the electron density result. The position of the relaxation oscillation is most readily affected by the bias current level. Thus, monitoring the noise peak and adjusting the bias can give valuable information regarding the operation and frequency response of lasers. We have the optimum operating conditions for both lasers and are given above.

As per the above argument we determine the maximum modulation bandwidth of lasers that we have, with an HP Lightwave Signal Analyzer (LSA), 7140. Plot 1 shows the location of intensity peak of 1306 nm laser at 5 GHz. We conclude from plot 1 that these lasers might be modulated up to 5 GHz. Nevertheless some experiments we performed show that extreme degradation of performance occur when modulating the laser at or above 2 GHz. Thus we choose 1 GHz for our subcarrier and pilot.

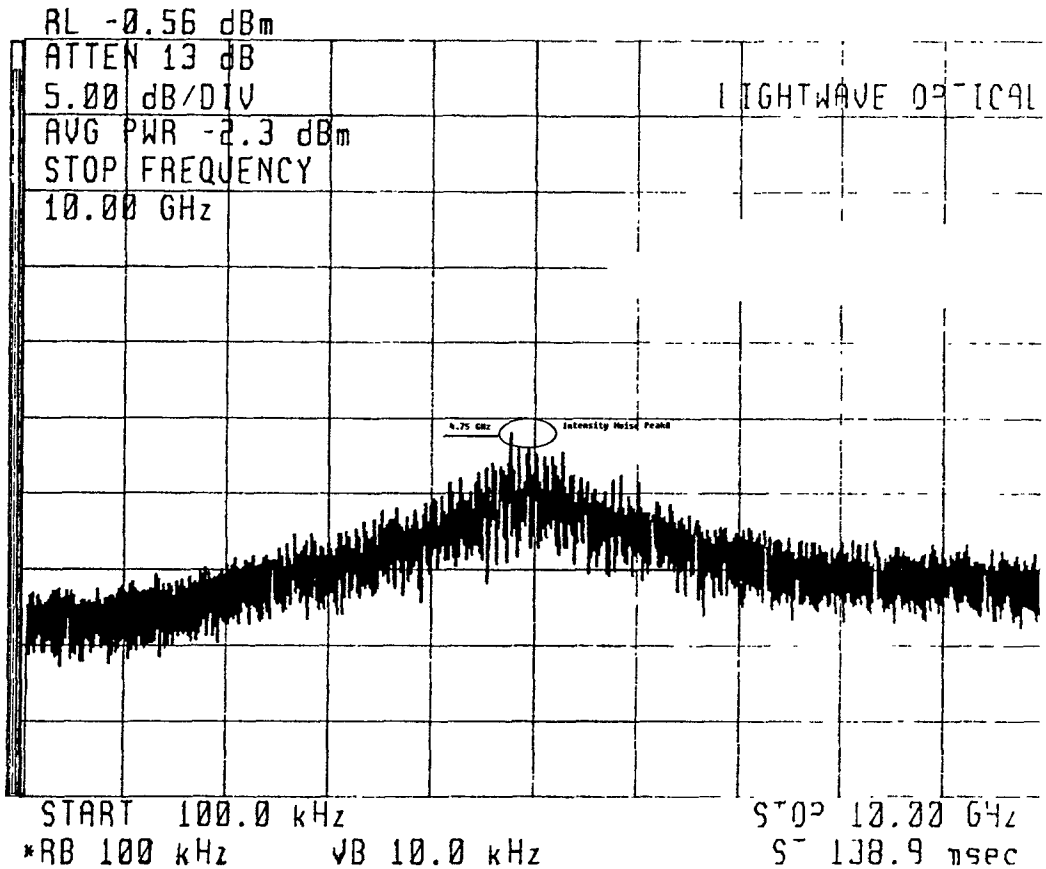

Plot 1 Resonance appears as a rise in the noise floor of the unmodulated 1306 nm laser

Optical Spectrum of Lasers

We have used an Anritsu Optical Spectrum Analyzer, model number MS9001B1, to measure laser linewidth and it's variation for different DC current. We also measure the laser output spectrum when it is modulated with a carrier frequency of 1 GHz and power level of 0 dBm and +5 dBm. The RF modulated experiment is shown in figure 2.2, where the RF source is obtained from HP 8753 Network Analyzer.

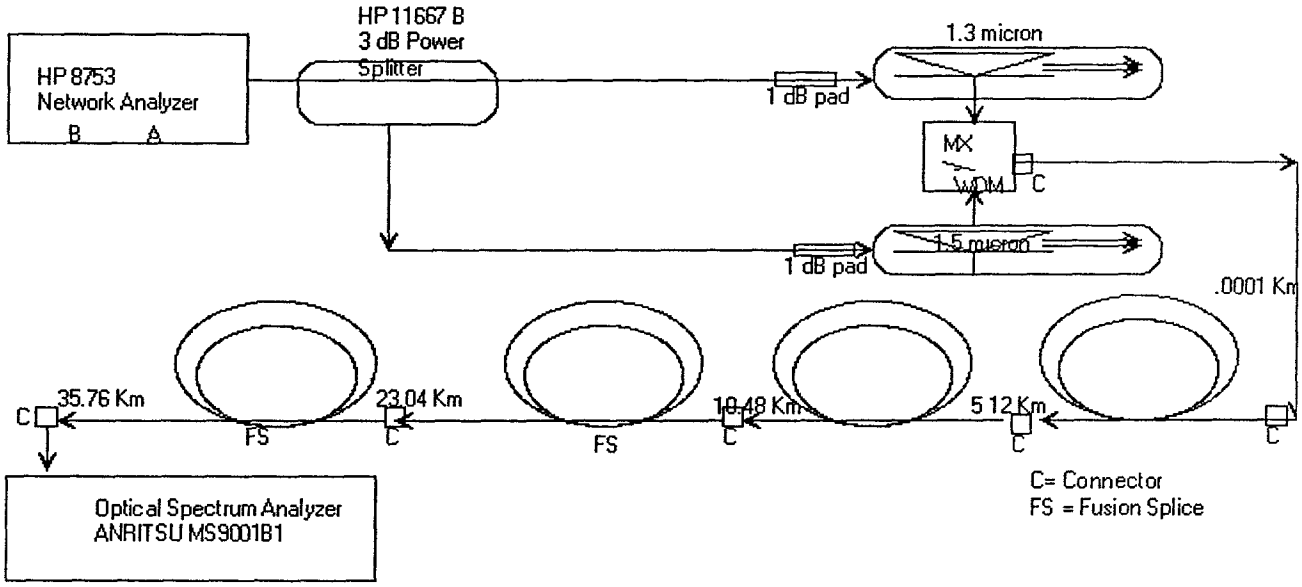

Figure 2.2 Experimental setup to measure RF modulated spectrum of a laser

The RF modulated spectrum is also observed for two different drive conditions of RF power levels, 0 dBm and +5 dBm.

From this we found that the nominal linewidth ($\Delta\lambda$) of both lasers at bias current of 26 mA is 0.12 nm for each laser. The linewidth variations when changing the Dc current as well as RF modulating power were only of the order of 0.04 nm.

2.2 Fiber Characteristics

Because of their importance in sensitivity analysis of fiberoptic system the following three parameters will be measured:

1. Fiber Loss

2. Fiber Reflections

3. Chromatic Dispersion

1. Fiber Loss

With the aid of Anritsu optical time domain reflectometer (OTDR), model number MW910C, we have measured the length of fiber and reflection at each discontinuity. Experiment set up used is shown in figure 2.3.

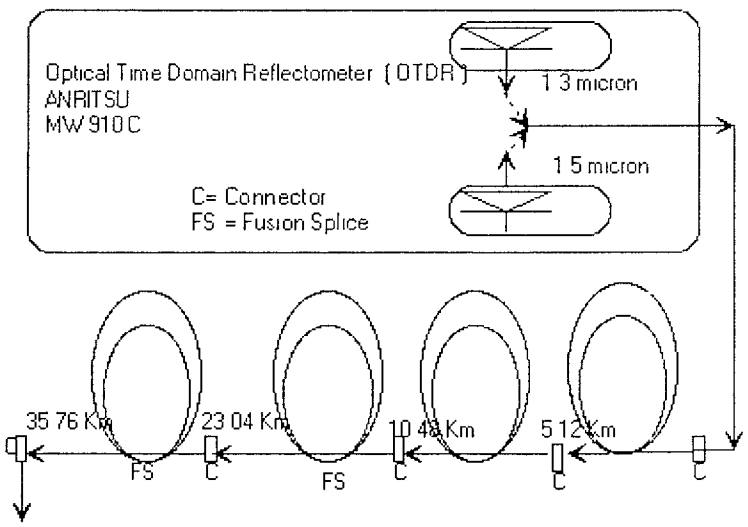

Figure 2.3 Experimental setup to measure fiberoptic attenuation and reflected optical power

Total attenuation of fiber with 6 biconic connectors, 2 fusion splice and 2 WDM device is measured Using manufacturer's data sheet we calculate total loss of our link at 1306 nm and 1533 nm wavelength

At 1306 nm

(nominal fiber loss is 0.45 dB / km, assume a loss of 1 dB for each biconic connector and neglect loss due to fusion splice (0.2 dB/ splice).

Total loss = 35.6 Km × 0.45 dB / Km + 6 × 1 dB = 22.02 dB (2.1)

Similarly, the total loss at 1533 nm wavelength is, (fiber loss = 0.20 dB / Km)

Total loss = 35.6 Km × 0.2 dB / Km + 6 × 1 dB = 13.12 dB (2.2)

The link loss measured by the OTDR and optical spectrum analyzer is more than the calculated loss by less than 3 dB at both wavelengths, which due to different calibrations and insertion loss of two WDM.

It is important to notice that optical power output from 1533 nm laser is less by 5.3 dB as compared to optical power output from 1306 nm laser. Nevertheless after 35.6 Km the low attenuation on the 1533 nm laser will compensate this fact. For further distance the condition will be in favour of 1533 nm lightwave carrying the pilot. Therefore even for larger haul sufficient power of pilot will be available even though the initial power at this wavelength is limited. Clearly because of higher attenuation at 1300 nm will be quite difficult to obtain the required subcarrier for coherent detection and/or timing clock from the modulated signal directly. Since a clean local oscillator for coherent detection and/or satisfactory timing clock is crucial, the approach of this concept seems advantageous particularly for long haul. In short haul systems there will be no problem on pilot carrier power and it's attenuation. This advantage is at the cost of high dispersion at 1500 nm window, but for our purpose it will not be the limiting factor.

With many digital information transmission techniques [30] in order to guarantee a digital clock recovery, particularly for low BER, optical power loss will have to be low to assure certain jitter tolerance for certain BER. With our concept we expect more system margin for same BER and jitter as a single tone sinewave of low frequency will provide better synchronized subcarrier for coherent detection along with a timing clock.

2. Fiber Reflections

Reflections from connectors of each laser pigtail to the WDM are high and hence unmeasurable due to limitation of OTDR resolution. Nevertheless, reflection about -30 dB was measured because of two biconic connectors and a WDM, all within a distance of 2 meters from the laser.

We did not take any special care to minimize refection by introducing index matching gel into connectors. This is to emulate practical field system and may be looked upon as worst case situation.

Calculation of return loss due to reflection

From the measured values of the reflected pulse height the optical return loss can be calculated using the following formula

$$R \text{ (return loss dB)} = B + 10 \log_{10} [\, 10^{0.2 \times H} - 1 \,] \times D \qquad (2.3)$$

for all H, where H is the height of reflected pulse from OTDR in dB, above the backscatter level, D is the duration of optical pulse in nanoseconds, B equals -80 dB for 1.3 window and - 82 dB for 1.5 window.

Reflections due to 6 biconic connectors between the pieces of fiber were also measured. All measured losses and reflections are summarized in the table given below.

For λ = 1306 nm

Connector or fusion splice at Distance (Km) from laser	Total Loss (dB) due to fiber attenuation	R(return loss) dB
.0001 Connector		-30 dB
.0002 Connector		- 30 dB

5.12 Connector	1.61	-37 dB
10.48 Connector	4.34	-35 dB
16.885 Fusion		-65 dB
23.04 Connector	10.38	-35 dB
35.76 Fusion	15.38	-65 dB

Reflections in our system are quite similar to those faced with any standard fiberoptic system. In some systems special care is used to maintain reflectance of -40 dB or better. Such a measure for minimizing the reflection was not persued in order to simulate normal circumstances and examine its effect. To emphasis, it is a well known fact that reflections limit transmission of analog video particularly for longer distances [12, 33] and when subcarrier scheme is implemented. Therefore it is important to not to correct for reflection but rather to include its effect when examining the performance of our concept.

Chromatic Dispersion Measurement

Fibers from different manufactures have been connected together for the experiment, we do not know the mean dispersion and other important characteristics and the values are not guaranteed. Hence for most accurate information we measure dispersion. The instrument used to measure dispersion is made by EG&G, model number CD-3, single mode fiber Chromatic Dispersion Measurement System. This instrument complies with the Electronic Industries Association Standard, FOTP-169, which sets the guidelines for chromatic dispersion measurement of optical fibers by the Phase-Shift Method. The particular issue number is EIA-455-169, August, 1988 [34].

A brief introduction to the dispersion parameters will make the results clear and emphasize importance.

The Sellmeier dispersion equation is very well known to all fiberoptic engineers. This has been the backbone for understanding fiber dispersion and almost all books have discussion of this. Sellmeier equation of 5th order is known but for fiberoptic it's 3rd order is sufficient. It shows the dependence of the index of refraction n on wavelength;

$$n^2-1 = \{[0.6961663\,\lambda^2] / [\lambda^2 -(0.0684043)^2]\} + \{[0..4079426\,\lambda^2] / [\lambda^2 -(0..1162414)^2]\} + \{[0..8974794\,\lambda^2] / [\lambda^2 -(9.896161)^2]\} \quad (2.4)$$

In chapter1, we have derive the dependence of the delay τ (delay per 1 meter propagation in fiber) on the wavelength λ, on the index refraction n and its derivative. Eliminating the dependence of τ on n in (1.22) by using equation (2.4) we can approximate $\tau(\lambda)$ by,

$$\tau(\lambda) = A + B\lambda^2 + C\lambda^{-2} \quad (2.5)$$

where A, B, C are called fit parameters. Using equation (2.5) one can find the dispersion $D(\lambda)$

$$D(\lambda) = d\tau/d\lambda = 2[B\lambda - C\lambda^{-3}] \quad (2.6)$$

Equating (2.6) to zero we find the wavelength λ_o of minimum dispersion

$$\lambda_o = [C/B]^{1/4} \quad (2.7)$$

Substituting this value in eqn. (2.5) we find

$$\tau(\lambda_o) = A + B\lambda_o^2 + C\lambda_o^{-2} = A + 2[BC]^{1/2} = \tau_0 \quad (2.8)$$

That is τ_0 is the delay per 1 meter at the minimum dispersion wavelength λ_o. Now we define the dispersion slope

$$S(\lambda) = dD(\lambda)/d\lambda = 2B + 6C\lambda^{-4} \quad (2.9)$$

The slope at λ_0 is given by

$$S(\lambda_0) = S_0 = 2B + 6C[C/B]^{-1}$$

$$= 8B. \qquad (2.10)$$

Using eqn. (2.6) and (2.9) in eqn. (1.34) we get

$$d^3\beta/d\Omega^3 = [\lambda^2/(2\pi c)^2]\,[\lambda^2(2B+6C\lambda^{-4})+4\lambda(B\lambda-C\lambda^{-3})]$$

$$= [\lambda^2/(2\pi c)^2]\,[\lambda^2 6B+2C\lambda^{-2}]$$

$$= [1/2(\pi c)^2]\,[\lambda^4 3B+C] \qquad (2.11)$$

Using eqn. (2.8) and (2.9) we may write (2.5) and (2.6) in terms of τ_0 and S_0

$$\tau(\lambda) = \tau_0 + [S_0/8]\,[\lambda-\lambda_o^2/\lambda]^2 \qquad (2.12)$$

$$D(\lambda) = [S_0\lambda/4]\,[1-\lambda_0^4/\lambda^4] \qquad (2.13)$$

These equations can be checked to be correct by simple substitution of the values of τ_0 , S_0 and λ_0. The important of these representation lays in the fact that these parameters, rather than the fit parameters A, B and C are directly measurable.

The following table summarize important and necessary data about fiber obtained by chromatic dispersion measurement. Chromatic dispersion measurement were repeated for three times. Dispersion, delay, zero dispersion wavelength of fiber (λ_0), B, C and slope S_0 are all measured and displayed. We have taken mean of three measurements and tabulated the results for 1305 nm and 1550 nm wavelengths.

Fiber Table

Mean **Zero Dispersion** wave length λ = 1309.804		
	λ = 1305 nm	λ = 1550 nm
Mean Dispersion **ps/nm-Km**	- 0.695	14.677
Mean, Delay **ps/Km**	-65.191	1860.378
Mean B **ps/nm^2-Km**	1.27E -02	
Mean C **ps-nm^2/Km**	3.7397733E +10	
Mean Slope(S_0) **ps/nm^2-Km**	0.10166	

In eqn.(2.8) only unknown is A, which can be calculated as shown below:

for 1305 nm

$$-65.191 \text{ (ps/Km)} = A + 1.27E\text{-}2\ (1305)^2\{\text{nm}^2\ \text{ps/nm}^2\ \text{Km}\} + 3.74E+10/(1305)^2\ \{\text{ps nm}^2/\text{nm}^2\ \text{Km}\}$$

$\Rightarrow A_{1305}$ = 43,654.52 ps/Km and similarly

A_{1550} = 44,218.48 ps/Km.

The above values can be varified by calculating them from eqn. (2.6) for dispersion, (2.10) for S_0 and (2.7) for λ_0. For example

$S_0 = 8B = 8 \times 1.27E\text{-}02 = 0.1016$ and

$\lambda_0 = [C/B]^{1/4} = [\,3.7397733\ E+10/1.27\ E\text{-}02\,]^{1/4} = 1309.9869$ nm

These are in good agreement with the measured mean value of S_0 and λ_0.

By now, we have measured all values of data for most of system components. It gives us a better understanding of our system.

The coefficients of β are necessary and important for theoretical prediction from equation (1.40). All coefficients will be calculated in next chapter.

2.3 Photodetectors

The photodetectors and their parameters are detailed below:

Photodetector Number ->	QDEUHS-035-001, 8018238	QDEUHS, 7048335
Responsivity (A/ W)	0.79	0.75
Electrical Bandwidth (GHz)	14	12
Spectral Sensitivity	1000 to 1650 nm	1000 to 1650 nm
Capacitance pF at -25 Volts	< 0.3	<.35
Detector Leakage Current	6.0 nA at -20 V bias	

The two photo detectors are made by Lasertron. Their specifications are more than adequate for our purpose.

2.4 Broadband Double-Balanced Mixer

Instead of a special phase detector, we used mixer as a phase detector. Our calibrations support that this mixer is no different than a phase detector. It's 1 dB compression point is very close to local oscillator drive level. It's Intermediate frequency (IF) response is from DC to 1500 MHz. Our results confirm that it met published specifications. It is made by Anzac, model number is MD-MDC-149.

Chapter 3

Experimental Analysis and Results

In Chapter 1, we formulated the problem of our investigation. A through investigation which would have answered all questions from the point view of readers and the author were developed. The expected experiment schematic was given in figure I.4. In Chapter 2, we collected the available components and measured characteristics of each one of the them in order to predict the experimental outcome.

Equation (1.5) and (1.40) separately for the different source are given below:

$$e_t(t) = E_c \Sigma a_n \cos(\Omega_l t \pm n \omega_{rf} t + n \theta(t)) \qquad (3.1)$$

$$E_{1.3}(z,t) = E_c \exp(-\alpha_{1.3} z/2) \Sigma a_n \cos(\Omega_{1.3} t \pm n \omega_{rf1} t \pm n \theta(t) - [\beta_{01.3} + \{d\beta_{01.3}/d\Omega\}[\Delta\Omega_{1.3} + n \omega_{rf1} t + n \theta(t)] + \{d^2\beta_{01.3}/d\Omega^2\}[\Delta\Omega_{1.3} + n \omega_{rf1} t + n \theta(t)]^2/2 + \{d^3\beta_{01.3}/d\Omega^3\}[\Delta\Omega_{1.3} + n \omega_{rf1} t + n \theta(t)]^3/6 + ... \} z + \Phi_{1.3} \} \qquad (3.2)$$

$$E_{1.5}(z,t) = E_c \exp(-\alpha_{1.5} z/2) \Sigma a_n \cos(\Omega_{1.5} t \pm n \omega_{rf2} t - [\beta_{01.5} + \{d\beta_{01.5}/d\Omega\}[\Delta\Omega_{1.5} + n \omega_{rf2} t] + \{d^2\beta_{01.5}/d\Omega^2\}[\Delta\Omega_{1.5} + n \omega_{rf2} t]^2/2 + \{d^3\beta_{01.5}/d\Omega^3\}[\Delta\Omega_{1.5} + n \omega_{rf2} t]^3/6 + ... \} z + \Phi_{1.5}]\} \qquad (3.3)$$

where Σ is over $n \in [0, \infty)$ and we also used

$$\Omega_n - \Omega_0 = \Omega_l \pm n \omega_{rf} - \Omega_0$$

$$= \Omega_0 \pm \Delta\Omega \pm n \omega_{rf} - \Omega_0$$

$$= \pm \Delta\Omega \pm n \omega_{rf}$$

$\Delta\Omega = \Delta\Omega_{1.3}$ or $\Delta\Omega_{1.5}$ is the spectral spreading of the two lasers respectively. $\beta_{01.3}$, $\beta_{01.5}$ and their derivatives are taken at the center frequencies of the corresponding lasers $\Omega_{1.3}$ and $\Omega_{1.5}$. We also took $\theta(t)=0$ as the modulation of the subcarrier ω_{rf2} used with the 1.5 micron laser for pilot transmission.

Laser modulation depth

A Laser diode generates an optical average power proportional to its average bias current above the lasing threshold. In chapter 2, measured threshold current for both lasers is 14 mA. Optimum operating bias current is 26 mA. Hence we can at the most have an modulating current of 12 mA peak before the signal is clipped at the laser threshold. For higher modulating current laser non-linearity will increase as shown in graph 2.1, displaying derivative of laser optical power VS DC current.

A current of 12 mA in to a 50 ohm front end of laser correspond to 8.57332 dBm (7.2 mW). For most of our experiment RF modulation power was about 7.5 dBm (5.6223 mW), which corresponds to a modulation index, m,

m = 5.6223 mW ÷ 7.2 mW = 0.780875

For the case when m=0.8 equation (3.1) becomes; (see also (1.6))

$$e_t(t) = 0.96\,E_c \cos(\Omega_l t) + 0.216\,E_c [\cos(\Omega_l t - \omega_{rf} t - \theta(t)) + \cos(\Omega_l t + \omega_{rf} t + \theta(t))]$$

$$- 0.02\,E_c [\cos(\Omega_l t - 2\omega_{rf} t - 2\theta(t)) + \cos(\Omega_l t + 2\omega_{rf} t + 2\theta(t))] + \ldots\ldots\ldots\ldots$$

Second RF harmonic has 20 dB less optical power as compared to fundamental. It was measured to be 18 dB instead of 20 dB due to contributions from higher terms. If we have a square wave instead of sinusoid, harmonics upto sixth order will have sufficient power to propagate along with the fundamental frequency. By sufficient power we mean that if fundamental is not above the other harmonics at least by 12 dB then inter-product noise dominates and degrades the system sensitivity. When detected at receiver they will have different arrival time and hence will generate very high

amount of dispersion because of electrical harmonics. Any filtering of these harmonic will generate distortion of data at the receiver. Hence, a sinusoid pilot will have more power in fundamental, will not suffer electrical dispersion as there are no harmonics and will require very small bandwidth at the receiver. Due to small bandwidth requirement for sinusoid SNR will improve and give us more dynamic range. This comparison is between transmitting a square wave and a sinusoid of equal frequency. As the speed of information is increased our concept will have all these advantages further increased.

We can neglect second harmonic terms from equation (3.2) for pilot on 1533 nm laser. For the other laser at 1306 nm we have to keep electrical harmonics from transmitter to receiver.

Optical output of 1533 nm laser is less by 5.3 dB as compared to optical output of 1306 laser. Attenuation for both lasers is measured as a function of fiber length and proved in Chapter 2, that low power from 1533 nm laser will not be a limiting factor of our concept since 1533 nm wavelength will suffer less attenuation.

Therefore, we can drop exp($-\alpha z/2$) term from the received signal equation (3.2) and (3.3). The received subcarrier and pilot are then given by

$$
\begin{aligned}
E_{1.3}(z,t) = E_c \{\, & 0.96 \cos(\Omega_{1.3} t - [\beta_{01.3} + \{d\beta_{01.3}/d\Omega\}[\Delta\Omega_{1.3}] + \{d^2\beta_{01.3}/d\Omega^2\}[\Delta\Omega_{1.3}]^2/2 + \\
& \{d^3\beta_{01.3}/d\Omega^3\}[\Delta\Omega_{1.3}]^3/6 + \ldots\ldots \}z + \Phi_{1.3}]\} + E_c \{\, 0.216 \cos(\Omega_{1.3} t + \omega_{rf1} t \theta(t) \\
& - \beta_{01.3} + \{d\beta_{01.3}/d\Omega\}[\Delta\Omega_{1.3} + \omega_{rf1}] + \{d^2\beta_{01.3}/d\Omega^2\}[\Delta\Omega_{1.3} + \omega_{rf1}]^2/2 + \{d^3\beta_{01.3} \\
& /d\Omega^3\}[\Delta\Omega_{1.3} + \omega_{rf1}]^3/6 + \ldots\ldots \}z + \Phi_{1.3}]\} + E_c \{\, 0.216 \cos(\Omega_{1.3} t - \omega_{rf1} t - \theta(t) - [\\
& \beta_{01.3} + \{d\beta_{01.3}/d\Omega\}[\Delta\Omega_{1.3} + \omega_{rf1}] + \{d^2\beta_{01.3}/d\Omega^2\}[\Delta\Omega_{1.3} + \omega_{rf1}]^2/2 + \{d^3\beta_{01.3} \\
& /d\Omega^3\}[\Delta\Omega_{1.3} + \omega_{rf1}]^3/6 + \ldots\ldots \}z + \Phi_{1.3}]\} + E_c \{\, 0.002 \cos(\Omega_{1.3} t + 2\omega_{rf1} t \\
& + 2\theta(t) - [\beta_{01.3} + \{d\beta_{01.3}/d\Omega\}[\Delta\Omega_{1.3} + 2\omega_{rf1} + 2\theta(t)] + \{d^2\beta_{01.3}/d\Omega^2\}[\Delta\Omega_{1.3} \\
& + 2\omega_{rf1} + 2\theta(t)]^2/2 + \{d^3\beta_{01.3}/d\Omega^3\}[\Delta\Omega_{1.3} + 2\omega_{rf1} + 2\theta(t)]^3/6 + \ldots\ldots \}z + \Phi_{1.3}]\} + \\
& E_c \{\, 0.002 \cos(\Omega_{1.3} t - 2\omega_{rf1} t - 2\theta(t) - [\beta_{01.3} + \{d\beta_{01.3}/d\Omega\}[\Delta\Omega_{1.3} + 2\omega_{rf1} + 2\theta(t) +
\end{aligned}
$$

$$\{d^2\beta_{01.3}/d\Omega^2\}[\Delta\Omega_{1.3} + 2\omega_{rf1} + 2\theta(t)]^2/2 + \{d^3\beta_{01.3}/d\Omega^3\}[\Delta\Omega_{1.3} + 2\omega_{rf1} + 2\theta(t)]^3/6 + \ldots\ldots\}z + \Phi_{1.3}]\} \quad (3.4)$$

$$E_{1.5}(z,t) = E_c\{0.96\cos(\Omega_{1.5}t - [\beta_{01.5} + \{d\beta_{01.5}/d\Omega\}[\Delta\Omega_{1.5}] + \{d^2\beta_{01.5}/d\Omega^2\}[\Delta\Omega_{1.5}]^2/2 + \{d^3\beta_{01.5}/d\Omega^3\}[\Delta\Omega_{1.5}]^3/6 + \ldots\ldots\}z + \Phi_{1.5}]\} + E_c\{0.216\cos(\Omega_{1.5}t + \omega_{rf2}t - [\beta_{01.5} + \{d\beta_{01.5}/d\Omega\}[\Delta\Omega_{1.5} + \omega_{rf2}] + \{d^2\beta_{01.5}/d\Omega^2\}[\Delta\Omega_{1.5} + \omega_{rf2}]^2/2 + \{d^3\beta_{01.5}/d\Omega^3\}[\Delta\Omega_{1.5} + \omega_{rf2}]^3/6 + \ldots\ldots\}z + \Phi_{1.5}]\} + E_c\{0.216\cos(\Omega_{1.5}t - \omega_{rf2}t - [\beta_{01.5} + \{d\beta_{01.5}/d\Omega\}[\Delta\Omega_{1.5} + \omega_{rf2}] + \{d^2\beta_{01.5}/d\Omega^2\}[\Delta\Omega_{1.5} + \omega_{rf2}]^2/2 + \{d^3\beta_{01.5}/d\Omega^3\}[\Delta\Omega_{1.5} + \omega_{rf2}]^3/6 + \ldots\ldots\}z + \Phi_{1.5}]\} \quad (3.5)$$

In equation (3.4 and (3.5) there is fiber related noise due to dispersion. In previous chapter we have measured the linewidth of both lasers, dispersion and fiber length. Therefore in order to facilitate approximation, we calculate β and its derivatives. Even though our lasers wavelengths are 1306 nm and 1533 nm we can use measured values of 1305 and 1550 nm wavelengths for our calculations.

β Table

expression	λ = 1305 nm	λ = 1550 nm
$\beta = 2\pi n / \lambda$ **1/Km**	7.077611E+9	5.958891E+9
CONSTANT DELAY MEASURED $d\beta / d\Omega = \tau(\lambda) = A + B\lambda^2 + C\lambda^{-2}$ **s/Km** (2.5)	-61.97E-12	1860 E-12
$d^2\beta / d\Omega^2 = D(\lambda)\lambda^2 / 2\pi c$ (1.33) $= 2[B\lambda^3 - C\lambda^{-1}] \div 2\pi c$ **s^2/Km** (2.6)	-6.292E-25	+2.4577E-23

$d^3\beta/d\Omega^3 = [\lambda^4/(2\pi c)^2][d\,D(\lambda)/d\lambda + 2\,D(\lambda)/\lambda]$ (1.34) $= +1[3B\lambda^4 + C]/2\pi^2c^2$ **s^3/Km** (2.11)	+8.325E-38	+1.2378E-37
Ω	1.4433 E+15	1.229 E+15
$\Delta\Omega = \Omega - \Omega_0 = \Delta\lambda \times 2\pi c \div \lambda^2$ (Both laser have $\Delta\lambda$ = 0.14 nm)	1.54718 E+11	1.1229 E+11
$d^2\beta/d\Omega^2\ (\Omega - \Omega_0)^2/2$ **Km^{-1}**	-7.53E-03	0.154946
$d^3\beta/d\Omega^3\ (\Omega - \Omega_0)^3/6$ **Km^{-1}**	5.13872E-05	2.9093E-05

In equation (3.4) we can neglect ω_{rf1} and its harmonics in dispersion calculations if $\Delta\Omega_{1.3} / \omega_{rf1} >> 1$. For the given lasers this is true and hence we neglect ω_{rf1} and its harmonics in dispersion calculations.

$$E_{1.3}(z,t) = E_c\{0.96\cos(\Omega_{1.3}t - [\{d^2\beta_{01.3}/d\Omega^2\}[\Delta\Omega_{1.3}]^2/2 = \text{-5.82882E-03}\} + \{\{d^3\beta_{01.3}/d\Omega^3\}[\Delta\Omega_{1.3}]^3/6 = 5.13872\text{E-}05\} + \ldots\ldots\}z + \Phi_{1.3}]\} + E_c\{0.216\cos(\Omega_{1.3}t + \omega_{rf1}t + \theta(t) - [\{d^2\beta_{01.3}/d\Omega^2\}[\Delta\Omega_{1.3}]^2/2 = \text{-5.82882E-03}\} + \{\{d^3\beta_{01.3}/d\Omega^3\}[\Delta\Omega_{1.3}]^3/6 = 5.13872\text{E-}05\}\} + \ldots\ldots\}z + \Phi_{1.3}]\} + E_c\{0.216\cos(\Omega_{1.3}t - \omega_{rf1}t - \theta(t) - [\{d^2\beta_{01.3}/d\Omega^2\}[\Delta\Omega_{1.3}]^2/2 = \text{-5.82882E-03}\} + \{\{d^3\beta_{01.3}/d\Omega^3\}[\Delta\Omega_{1.3}]^3/6 = 5.13872\text{E-}05\} + \ldots\ldots\}z + \Phi_{1.3}]\} + E_c\{0.002\cos(\Omega_{1.3}t + 2\omega_{rf1}t + 2\theta(t) - [\{d^2\beta_{01.3}/d\Omega^2\}[\Delta\Omega_{1.3}]^2/2 = \text{-5.82882E-03}\} + \{\{d^3\beta_{01.3}/d\Omega^3\}[\Delta\Omega_{1.3}]^3/6 = 5.13872\text{E-}05\} + \ldots\ldots\}z + \Phi_{1.3}]\} + E_c\{0.002\cos(\Omega_{1.3}t - 2\omega_{rf1}t - 2\theta(t) - [\{d^2\beta_{01.3}/d\Omega^2\}[\Delta\Omega_{1.3}]^2/2 = \text{-5.82882E-03}\} + \{\{d^3\beta_{01.3}/d\Omega^3\}[\Delta\Omega_{1.3}]^3/6 = 5.13872\text{E-}05\} + \ldots\ldots\}z + \Phi_{1.3}]\} \quad (3.6)$$

After neglecting first two terms of **constant delay** and z = 100 Km fiber, we conclude that total dispersion effect is negligible at 1.3 wavelengths as compared to RF subcarrier(1 GHz) and $\theta(t)$ signal (signal period < subcarrier period). All dispersion effect at 1.3 micron wavelength is negligible, this is also true since it is very close to zero dispersion wavelength. Therefore in Eqn. (3.6) we can drop all

dispersion related terms for 100 Km or less fiber length and the given laser linewidth and RF frequency. Hence (3.6) is reduced to

$$E_{1.3}(z,t) = E_c \{ 0.96 \cos(\Omega_{1.3} t + \Phi_{1.3}\} + E_c \{ 0.216 \cos(\Omega_{1.3} t + \omega_{rf1} t + \theta(t)) + \Phi_{1.3}\} + E_c \{ 0.216 \cos(\Omega_{1.3} t - \omega_{rf1} t - \theta(t)) + \Phi_{1.3}]\} + E_c \{ 0.002 \cos(\Omega_{1.3} t + 2\omega_{rf1} t + 2\theta(t) + \Phi_{1.3}]\} + E_c \{ 0.002 \cos(\Omega_{1.3} t - 2\omega_{rf1} t - 2\theta(t) + \Phi_{1.3}]\}$$

$$= E_c \{ 0.96 \cos(\Omega_{1.3} t + \Phi_{1.3}) + 0.432 \cos(\Omega_{1.3} t + \Phi_{1.3}) \cos(\omega_{rf1} t + \theta(t)) + .0.004 \cos(\Omega_{1.3} t + \Phi_{1.3}) \cos(2\omega_{rf1} t + 2\theta(t) +) \} \quad (3.7)$$

For the 1550 nm laser, we neglect the constant delay terms in equation (3.5) and use the values of β and its derivatives from the β Table:

$$E_{1.5}(z,t) = E_c \{ 0.96 \cos(\Omega_{1.5} t - [\{d^2\beta_{01.5}/d\Omega^2\}[\Delta\Omega_{1.5}]^2/2 = 0.1545\} + \{d^3\beta_{01.5}/d\Omega^3\}[\Delta\Omega_{1.5}]^3/6 = 2.909E\text{-}05\} + \ldots\ldots\ldots \}z + \Phi_{1.5}]\} + E_c \{ 0.216 \cos(\Omega_{1.5} t + \omega_{rf2} t - [\{d^2\beta_{01.5}/d\Omega^2\}[\Delta\Omega_{1.5}]^2/2 = 0.1545\} + \{d^3\beta_{01.5}/d\Omega^3\}[\Delta\Omega_{1.5}]^3/6 = 2.909E\text{-}05\} + \ldots\ldots\ldots \}z + \Phi_{1.5}]\} + E_c \{ 0.216 \cos(\Omega_{1.5} t - \omega_{rf2} t - [\{d^2\beta_{01.5}/d\Omega^2\}[\Delta\Omega_{1.5}]^2/2 = 0.1545\} + \{d^3\beta_{01.5}/d\Omega^3\}[\Delta\Omega_{1.5}]^3/6 = 2.909E\text{-}05\} + \ldots\ldots\ldots \}z + \Phi_{1.5}]\} \quad (3.8)$$

In the above equation we notice that after 100 Km fiber the second order dispersion is of the order of E-03 and is negligible. Therefore (3.8) is reduced to

$$E_{1.5}(z,t) = E_c \{ 0.96 \cos(\Omega_{1.5} t - [\{d^2\beta_{01.5}/d\Omega^2\}[\Delta\Omega_{1.5}]^2/2 = 0.1545/\text{Km}\}100 \text{ Km} + \Phi_{1.5}]\} + E_c \{ 0.216 \cos(\Omega_{1.5} t + \omega_{rf2} t - [\{d^2\beta_{01.5}/d\Omega^2\}[\Delta\Omega_{1.5}]^2/2 = 0.1545 /\text{Km}\}100 \text{ Km} + \Phi_{1.5}]\} + E_c \{ 0.216 \cos(\Omega_{1.5} t - \omega_{rf2} t - [\{d^2\beta_{01.5}/d\Omega^2\}[\Delta\Omega_{1.5}]^2/2 = 0.1545/\text{Km}\}100 \text{ Km} + \Phi_{1.5}]\} \quad (3.9)$$

From equation (3.6) we conclude that as the RF frequency is increased for a given laser linewidth the amount of dispersion in comparison to the RF period increased making coherency with the subcarrier

poorer. Similarly if the linewidth increases then for the same RF coherency with the subcarrier deteriorates. Nevertheless the fact that there is no higher harmonic content at the pilot, extracted at the receiver, help obtain easier coherency. Notice that even with no dispersion phase noise may have some effect on performance. This noise might be further reduced if the laser linewidth is decreased. Further examination of (3.6) and (3.9) shows that due to dispersion there will be a certain penalty due to amplitude reduction after O/E conversion as shown below:

$$I_{1.3}(t) = A_1 \times E_{1.3}(z,t) \times E^*_{1.3}(z,t) \qquad (3.10)$$

$$|e_{1.3}(t)|^2 = \Sigma a_n \cos[\{d^2\beta_{01.3}/d\Omega^2\}[\Delta\Omega_{1.3}]^2/2]\cos(n\,\omega_{rf}t + n\,\theta(t))$$

$$|e_{1.3}(t)|^2 = \Sigma a_n\,\textbf{[Disp Loss 1.3 nm]}\cos(n\,\omega_{rf}t + n\,\theta(t)) \qquad (3.11)$$

The **[Disp Loss 1.3 nm]** is a function of length of fiber and is negligible for 50 Km fiber. No phase noise due to dispersion. Similarly

$$I_{1.5}(t) = A_2 \times E_{1.5}(z,t) \times E^*_{1.5}(z,t) \qquad (3.12)$$

$$|e_{1.5}(t)|^2 = \Sigma\, a_n \cos[\{d^2\beta_{01.5}/d\Omega^2\}[\Delta\Omega_{1.5}]^2/2]\cos(\omega_{rf}t)$$

$$|e_{1.5}(t)|^2 = \Sigma\, a_n\,\textbf{[Disp Loss 1.5 nm]}\cos(\omega_{rf}t) \qquad (3.13)$$

From (3.11) and (3.13) we conclude that the phase noise will be negligible. The amplitude of the recovered signal will be reduced more due to dispersion at 1550 nm wavelength. However, this penalty will depend on the fiberoptic cable length. In above equations we have neglected laser phase noise, laser phase noise to intensity noise conversion in fiber, noise due to reflections, receiver shot noise and amplifier noise and obtained sufficiently synchronized pilot and subcarrier with a fixed amount of delay.

In order to demonstrate our principle and investigate subcarrier synchronization with pilot in the presence of above mentioned noise processes, we rely on experiment.

3.1 Phase and Frequency Distortion Using Phase Detector

A phase detector can be used to quantify the level of coherency between the pilot and the information subcarrier, wavelength domain multiplexed and communicated through a fiber. In our measurements to follow the pilot was taken to be equal to the subcarrier frequency at 1 GHz rather than at sub-harmonic of the subcarrier frequency at 51.84 MHz. This was done for the sake of simplicity, since otherwise a chain of multipliers and dividers would be needed. Normally for a mixer to work as a phase detector its 1 dB compression point has to be close to the local oscillator (LO) power level. 1 dB compression point is defined as the RF input power that causes one dB increase above mixer's small signal (-15 dBm) conversion loss.

Three different experiments were conducted. In the first (fig. 3.1a) no light sources were used and obviously no fiber was needed as communication channel. An RF signal at frequency of 1 GHz from HP 8753 was split by a 3 dB power splitter into two paths, feeding the RF through a variable phase shifter and local oscillator (LO) ports of the mixer respectively. The signal level to LO port was set to about +7.5 dB and RF port was set to about -14.5 dB. The input level to RF port is below the 1 dB compression point of the mixer as required. The phase signal into the RF port was varied from 0 to 520 degrees maximum in steps of 20 degrees or varied from 0 to 180 degrees in steps of 4 degrees for measurement accuracy. The output of the phase detector as measured at the IF port is monitored.

In second experiment (fig. 3.1b) we add electrical to optical conversion (E/O) by modulating two separate lasers at 1306 nm and 1533 nm wavelengths. These two wavelengths are then wavelength division multiplexed (WDM), and attenuated to an adequate level by optical attenuators (OA). The optical signal is then de-multiplexed and using PIN diode at each path, the intensity modulations of these signal are detected. Finally after some bandlimiting through a BPF filter, the two electrical

signals are fed to the RF and LO port of the mixer. The output of the mixer at the IF port is monitored as before.

In the third experiment (fig. 3.1c), further we introduce fiberoptic cable of 36 Km instead of optical attenuators. From the results of the first two experiments we might deduce about the effect of electrical to optical conversion at the laser and back to electrical conversion at the PIN diode detector. Clearly imbedded in this will be the contribution to noise due to different electrical amplifiers added. The effect of the fiber on phase noise or distortion will be obtained by comparing the results of the last two experiments.

In order to do measurements in a controlled manner we monitored the signal levels to the mixer at each experiment and set it according to specifications. Then we used spectrum analyzer (HP 8566B) to plot signal spectra at different points. The spectral bandwidths used were DC to few KHz. The output of the phase detector was monitored using FLUKE 8840A multimeter. DC and AC measurements of the phase detectors were performed. To monitor noise difference between the two phase detectors inputs and which is not within the bandwidths of the FLUKE, we use spectrum analyzer as well.

To prevent overloading the Fluke multimeter a 10 MHz LPF was added in front of its input. The Fluke 8840A itself acts as a LPF with it's true Root Mean Square (RMS) measurement in 100 KHz bandwidth. FLUKE's 3 dB roll off is at 300 KHz and when, **terminated into 50 ohms it has as an AC noise floor of 0.139 mV and DC offset of 0.000 V DC.**

Using spectrum analyzer spectrum plots were are taken at the following point of the experiment setup:-

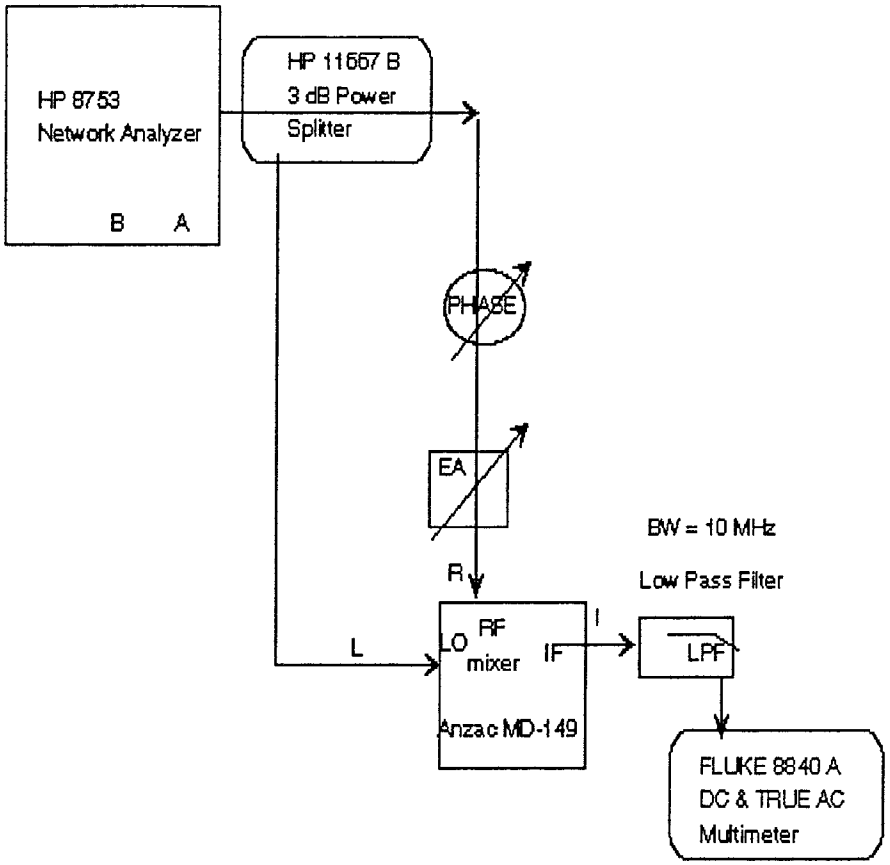

Figure 3.1a Block diagram for direct electrical signal phase noise measurement

input to laser, electrical signals used to modulate the subcarrier or as a pilot, to monitor inputs to the mixer, to monitor detected signals after O/E conversion. The spectral spans of these measurements were set to 100 Hz centered at 1 GHz. Finally spectrum plots were taken at the output of mixer at baseband frequency of 100 Hz, 500 KHz and 10 MHz. Due to the fact that in the first experiment there was no E/O conversion and vice-versa and therefore some of the measurements were omitted as they were redundant. Similarly plots of laser input are not repeated for the second and third experiment.

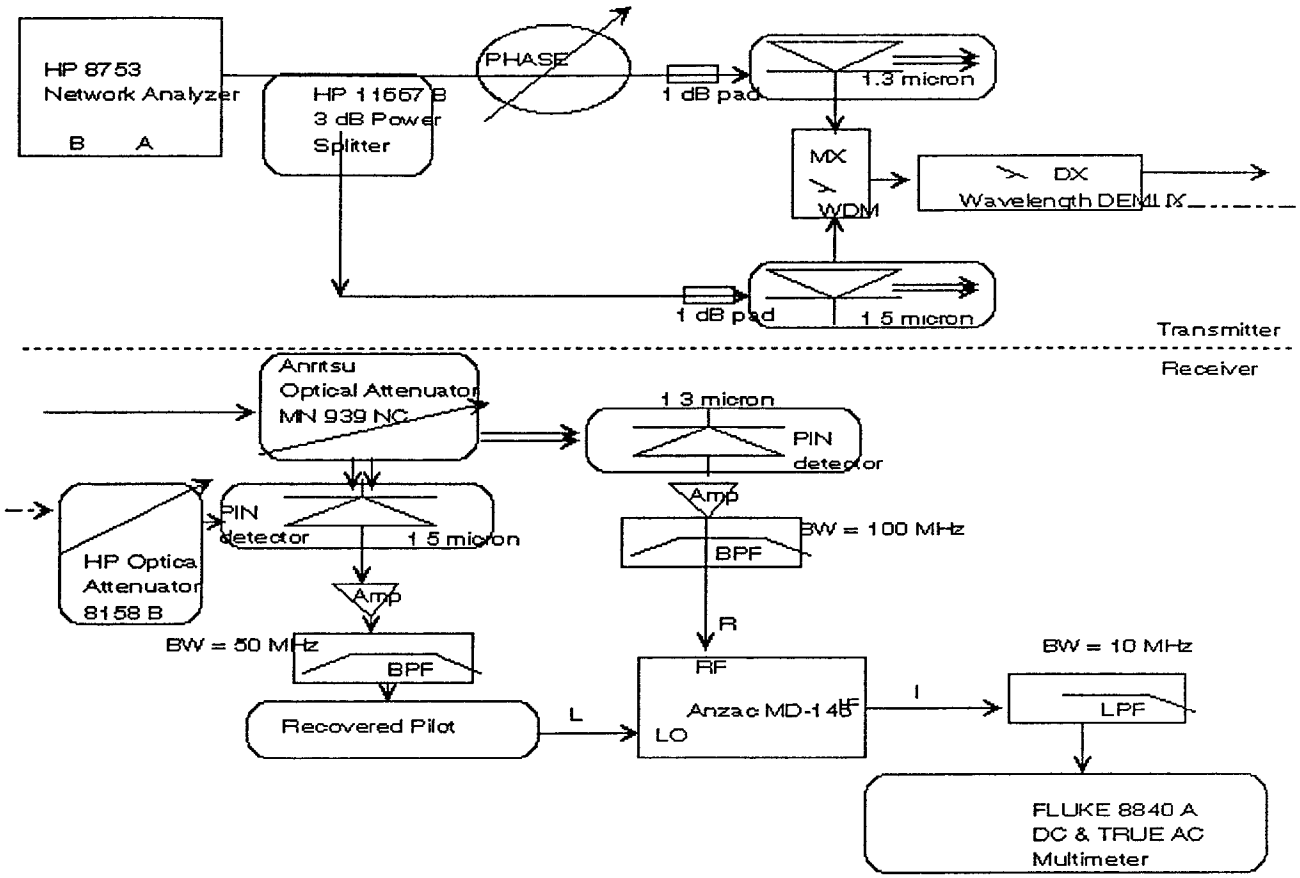

Figure 3.1b Block diagram for phase noise measurement with E/O and O/E conversion included

List of the spectrum plots as mentioned above are listed in the table below where L is for LO port of mixer, R is for RF port of mixer and I is for IF output port of mixer. Different parts of the table depicts the plots for the different experiments. The plots are numbered sequentially. The corresponding wavelengths are also marked where necessary, 1306 nm for subcarrier and 1533 nm for pilot. Spectrum spans are also emphasized in this table.

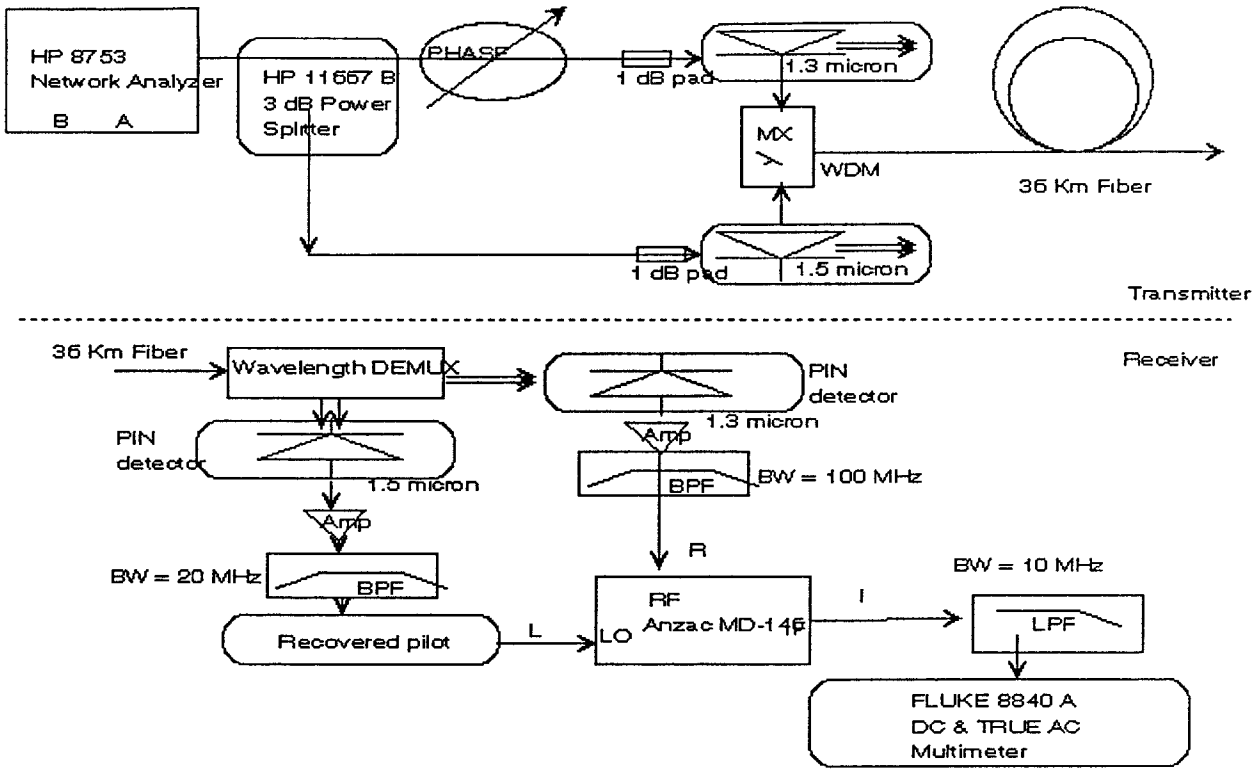

Figure 3.1c Block diagram for phase noise measurement with 36 Km fiber added

Plot	Point	λ nm	
Fig 3.1a			**Direct Electrical Signal Measurements**
3.1	L		LO + **7.4 dBm**, 100 Hz span
3.2	R		RF **-14.8 dBm**, 100 Hz span
Fig 3.1b			**Measurements with E/O and O/E conversion included**
3.3	L	1533	LO + **5.2 dBm**, 100 Hz span
3.4	R	1306	RF **-14.4 dBm**, 100 Hz span

3.5	I		IF noise, 100 Hz
3.6	I		IF noise, 500 KHz
3.7	I		IF noise, 10 MHz
Fig 3.1c			**Measurements with 36 Km fiber added**
3.8	L	1533	LO + **7.4 dBm**, 100 Hz span
3.9	R	1306	RF **-17.0 dBm**, 100 Hz span
3.10	I		IF noise, 100 Hz
3.11	I		IF noise, 500 KHz
3.12	I		IF noise, 10 MHz

Results

Signals Spectra

We compare spectrum plots of recovered pilot from 1533 nm laser (plot 3.3 and 3.8) with and without fiber in the system, respectively and with the original signal, (plot 3.1) used to modulate the light. We notice no noticeable broadening in spectrum due to E/O and O/E conversion or due to propagation through 36 Km fiber. Similar remarks are in effect for the signals recovered from 1306 nm laser (plot 3.4 and 3.9)

Comparison of IF output plots for noise without fiber (plot 3.5, 3.6 and 3.7) and those with 36 Km fiber added (plot 3.10, 3.11 and 3.12) respectively do not show any noticeable increase in noise floor.

Phase Noise

Phase variations of the1 GHz subcarrier used to modulate 1306 nm laser was recovered with coherent detection at receiver with and without 36 Km fiber. Graph 3.1 shows phase variations at the output of the phase detector in a step of 20 degrees.

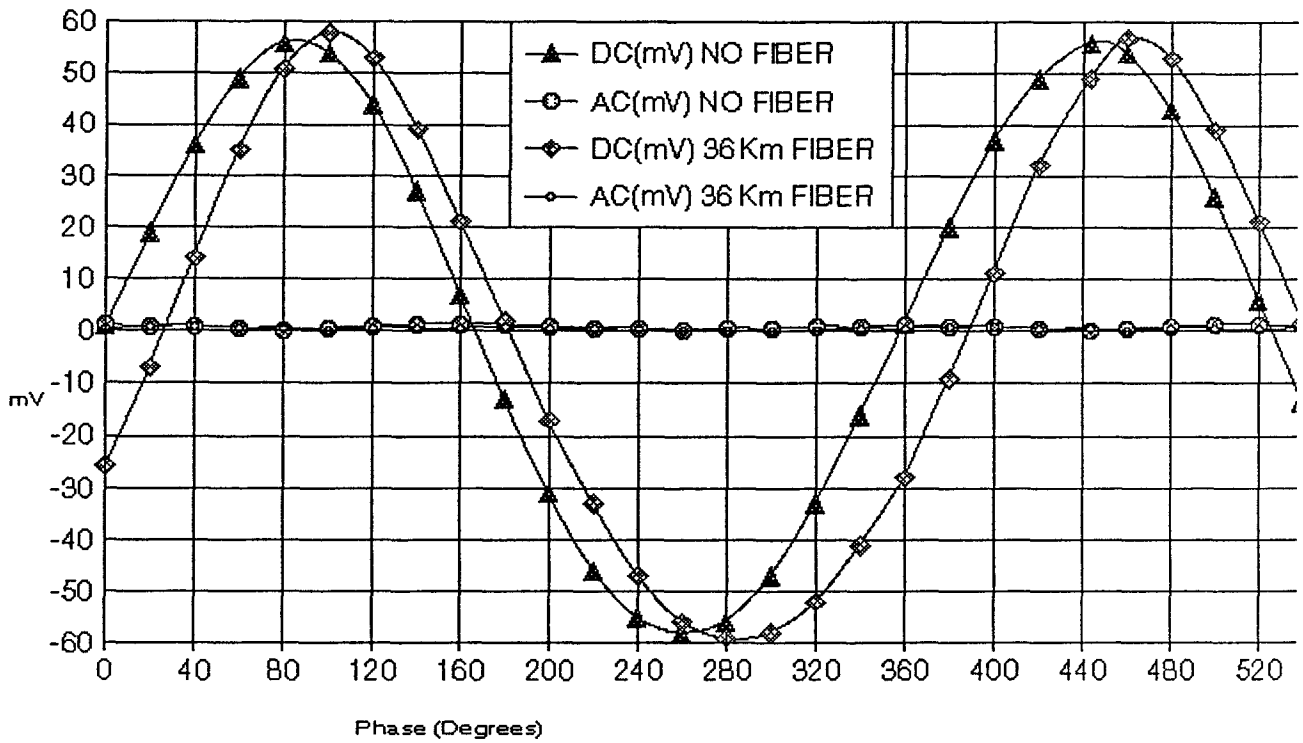

Graph 3.1 Phase variations (AC and DC) at the output of the phase detector in a step of 20 degrees

Graph 3.2a and 3.2b depicts phase output in a step of 4 degrees. The AC phase at phase detector output represent the residual noise. From graph 3.2a and 3.2b, we may calculate phase degradation with and without 36 Km fiber.

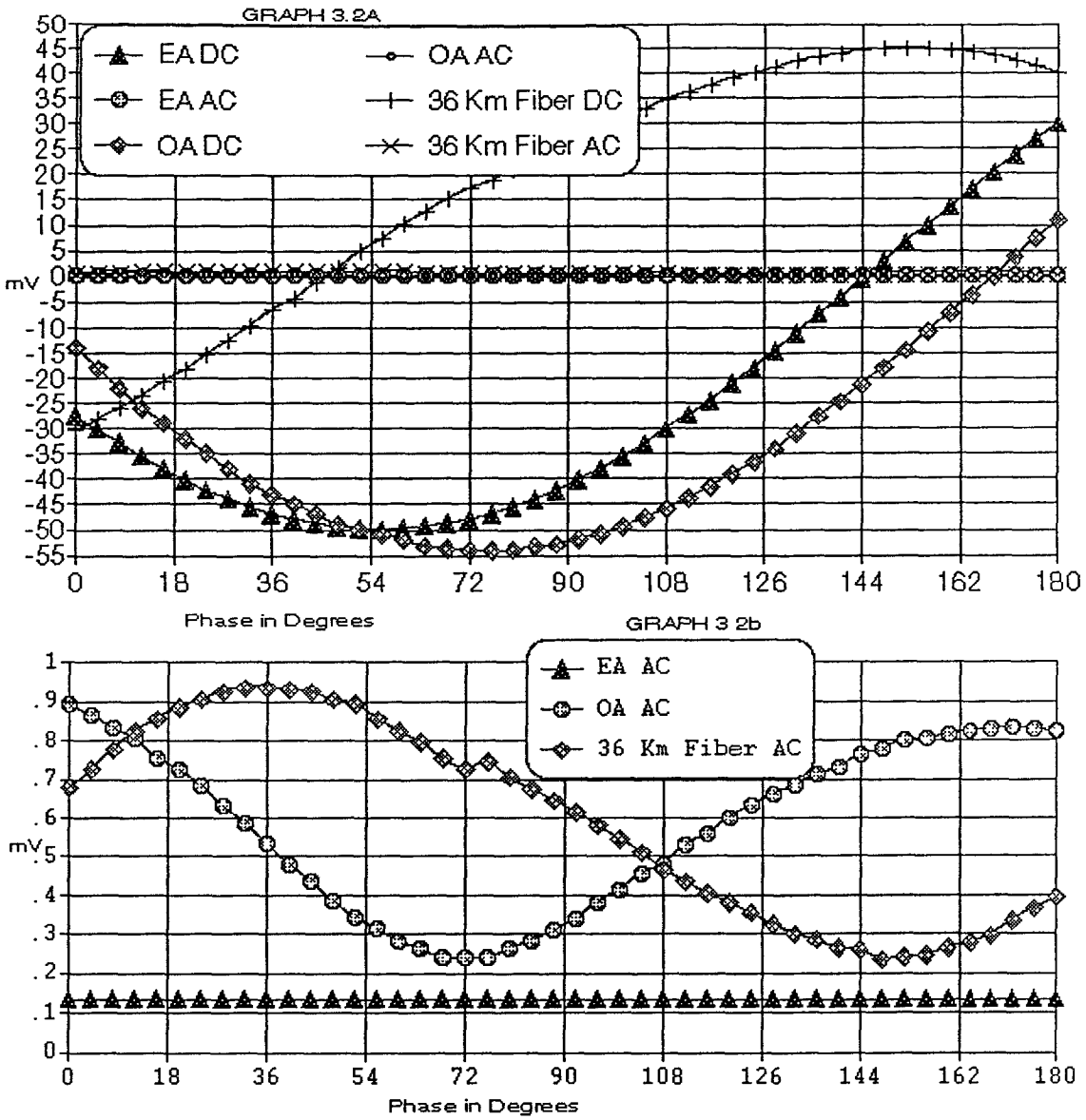

Graph 3.2a Phase variations (DC) at the output of the phase detector in a step of 4 degrees and

Graph 3.2b Phase variations (AC) at the output of the phase detector in a step of 4 degrees

Let the phase noise be defined as the ratio of peak DC output / peak AC output (signal/noise ratio), then for the case without electrical to optical (E/O) conversion and vice-versa;

20 Log_{10} [peak DC output of / peak AC output] = 20 Log_{10} [50.0 / 0.135] = 51.37 dB.

With E/O conversion and without fiber

20 Log_{10} [peak DC output of / peak AC output] = 20 Log_{10} [53.95 / 0.895] = 35.60 dB

With the addition of 36 Km Fiber

20 Log_{10} [peak DC output of / peak AC output] = 20 Log_{10} [45.2 / 0.935] = 33.68 dB

The above results indicate that the phase sensitivity with 36 Km fiber is decreased by a 1.91 dB as compared to without fiber.

Phase and Frequency Distortion Measurement Using HP Network Analyzer

In the next set of experiments we use HP Network Analyzer (NA), model HP 8753 instead of the mixer as a phase detector, and repeat the previous three set of measurements. The microwave signal is taken as before from the NA. The IF bandwidth is taken to be 3000 Hz. Therefore the block diagram of these experiments set up are shown in figure 3.2a for direct electrical signal, 3.2b with E/O and O/E conversion and 3.2c 36 Km fiber added. Notice that except for using the NA as a measurement tool these are the same as in figure 3.1a, 3.1b and 3.1c respectively.

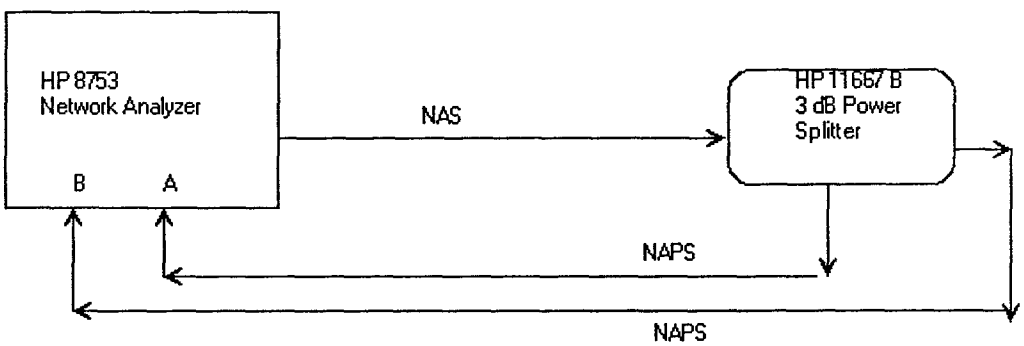

Figure 3.2a Block diagram for relative phase stability of source with its internal reference

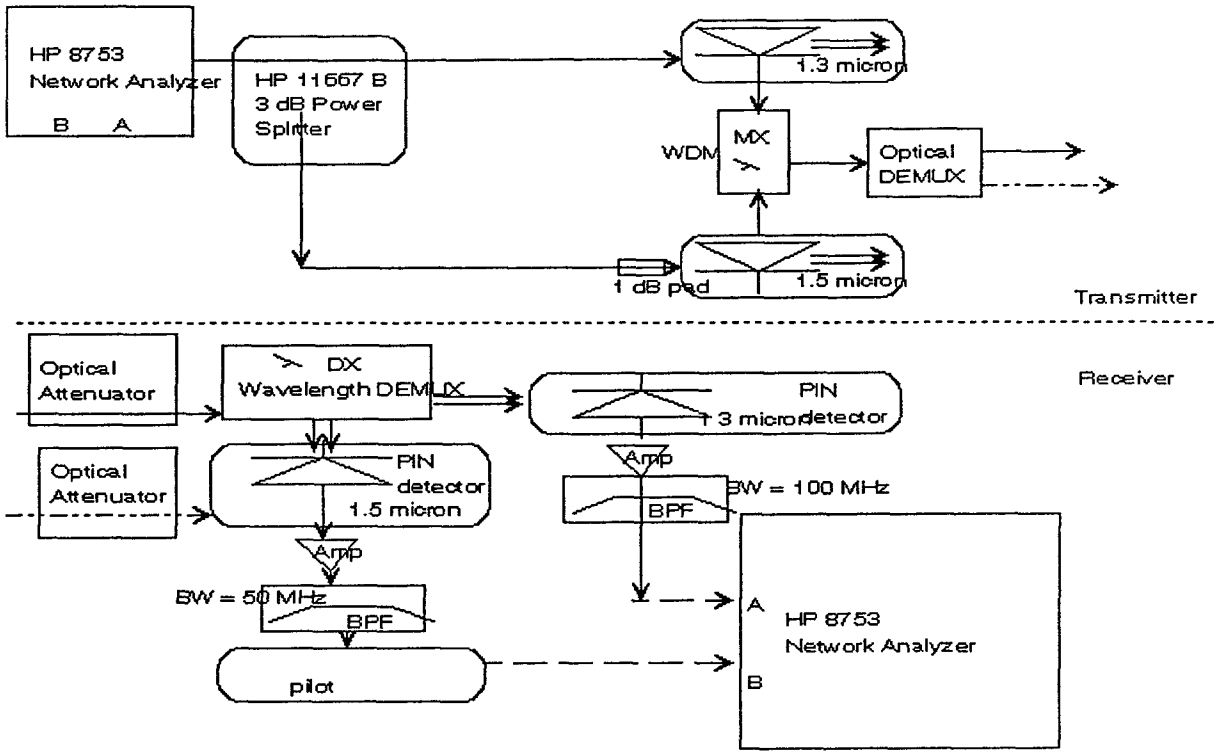

Figure 3.2b Block diagram for relative phase stability measurement without fiber

Channel A of NA is connected to recovered RF from 1306 nm laser and channel B is connected to recovered pilot from 1533 nm laser. The ratio of phase stability of A with respect to the phase stability B is monitored over a long time on a continuous basis.

These measurements were monitored for 5 hours and the long term stability of phase noise is measured. Continuous and long-term monitoring of phase noise was not possible in the experiment with phase detector. Since NA has built in statistic (mean and standard deviation) display, which is advantageous because any random noise will be picked by the NA and the peak to peak deviation would indicate it.

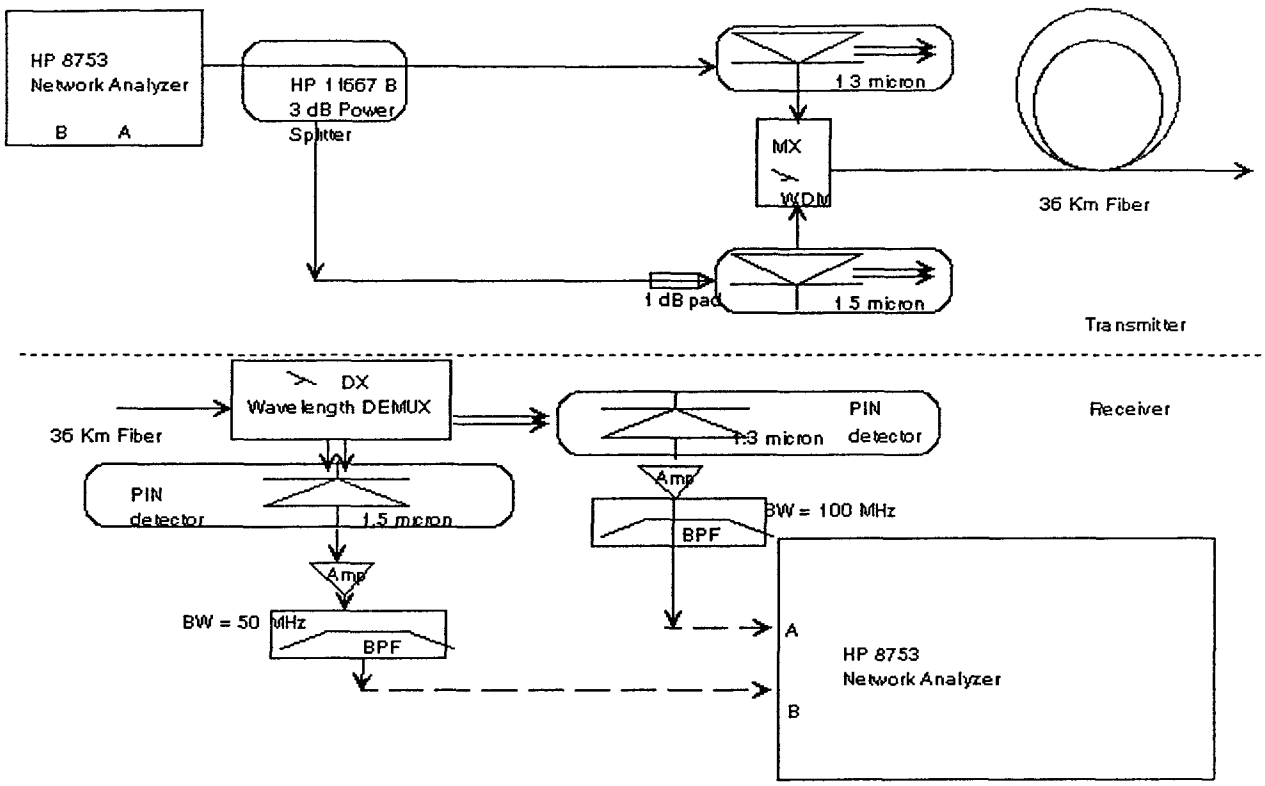

Figure 3.2c Block diagram for relative phase stability measurement with 36 Km fiber

Plot 3.13 shows the magnitude and the phase variations in time of the microwave source- HP 8753 (after a 3 dB power splitter) with respect to its internal reference (R). Plot 3.14 depicts the phase variations without fiber and plot 3.15 depicts phase variations with 36 Km fiber added. A comparison of standard deviation (SD) and peak to peak variation of phase measurement are tabulated below:

Phase Parameter	Direct Electrical Signal Plot 3.13	No Fiber Plot 3.14	36 Km Fiber Plot 3.15
Standard Deviation (SD) $\mathbf{m^0}$	109.04	119.92	114.66
Peak to Peak variation $\mathbf{m^0}$	593.26	675.66	679.78

Results

Comparison of phase statistics from above indicate that insertion of 36 Km of fiber in the system do not result in noticeable change in SD and Peak to Peak variations.

3.2 Transmission of Low Frequency Tone

The subcarrier of 1 GHz that direct modulate 1306 nm laser is now phase modulated by a low frequency tone. The pilot at frequency of 1 GHz (obtained from the same source as the subcarrier) direct modulate the 1533 nm laser as before. Block diagram of this experiment is depicted in figure 3.3.

Fluke 6062A serves as generator for the subcarrier, whose frequency is synthesized from 10 MHz signal originating at HP 8860C. The later instrument serves as a source for the 1 GHz pilot. Therefore the two signals, the subcarrier and the pilot are coherent as they are both synthesized by the same 10 MHz source. The subcarrier generated by the FLUKE is angle modulated to a depth of 1 radian, by low frequency tone (50 Hz to 100 KHz) from HP 3311A signal generator. Spectral plots at various points in the experiment setup of figure 3.3 are tabulated below. The low frequency tone used for modulation was 10 KHz. Nevertheless, with others low frequency tones from 50 Hz to 100 KHz, depicts similar behavior.

Plot #	point	λ nm	**Figure 3.4**
3.16			1 GHz subcarrier phase modulated with 10 KHz, used for intensity modulation of 1306 nm laser, spectral span 25 KHz
3.17	R	1306	Recovered 1 GHz subcarrier phase modulated with 10 KHz tone after 36 Km fiber, 25 KHz span

3.18	L	1533	Recovered pilot to be used as LO for coherent detection, note the presence of 10 KHz tone due to optical cross-talk.
3.19	I		10 KHz tone recovered with coherent detection
3.20	I		Recovered 10 KHz tone, superimposed onto the original 10 KHz signal from source-HP 3311A.

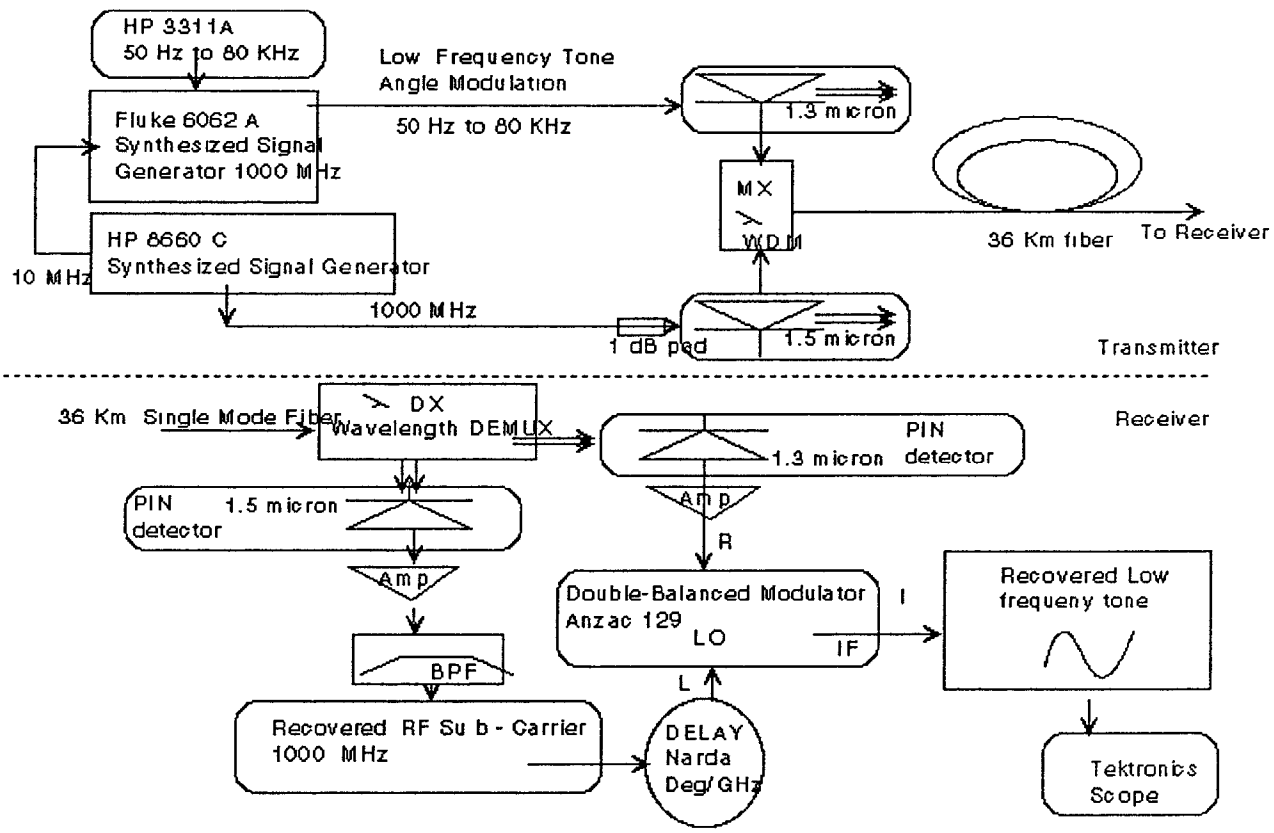

Figure 3.3 Block diagram for low frequency tone transmission over 36 Km fiber

Results

In plot 3.17 we notice the two sidebands 12 dB below the carrier. In plot 3.18, the pilot at 1 GHz is shown 35 dB above sidebands which are believed to result from optical cross-talk.

Plot 3.20, depicting the recovered 10 KHz superimposed onto the original 10 KHz does not show noticeable noise due to 36 Km fiber. Similar results were obtained for different low frequency tone in the range of 50 Hz to 100 KHz. This supports our earlier observations that subcarrier and pilot will maintain synchronization (phase and frequency) even if transmitted on two different wavelength.

3.3 Data Transmission and Recovery

In next experiment we examine transmission of digital data on one laser and reference carrier on the other. Then analyze the recovered data and it's eye diagram.

If the data rate is F_b (non return to zero, NRZ), then for BPSK the baud rate equals bits rate. The maximum bandwidth occurs when the input binary sequence of data is a continuous bit stream of alternating ones and zeroes. That is if we were to transmit a clock of the digital data we would have maximum bandwidth of BPSK. The experimental setup is shown in figure 3.4.

The digital data is provided by ANRITSU BER measurement transmitter, model ME 522A. The subcarrier of 1 GHz is provide by FLUKE 6062A, Synthesized Signal Generator. It's output is +13.5 dBm. The 3 dB power splitter made by KDI, model PSK-210 (BW is from 0.2 to 1500 MHz) is used to obtain pilot of 1 GHz from subcarrier. One output of 3 dB power splitter is used as pilot to direct modulate 1533 nm laser. A 1 dB attenuation pad is inserted between the laser input and power splitter to minimize reflections at the input to the 1533 nm laser. The other output of the power splitter which is to be used as a subcarrier and is connected to the LO port of a mixer, model CLK-7135. The power level of the subcarrier is +8 dBm. The digital data from ANRITSU BER transmitter ME 522A is

connected to the IF port of the mixer. BPSK modulated subcarrier then obtained at the RF port of mixer. This BPSK signal is passed through a BPF filter,

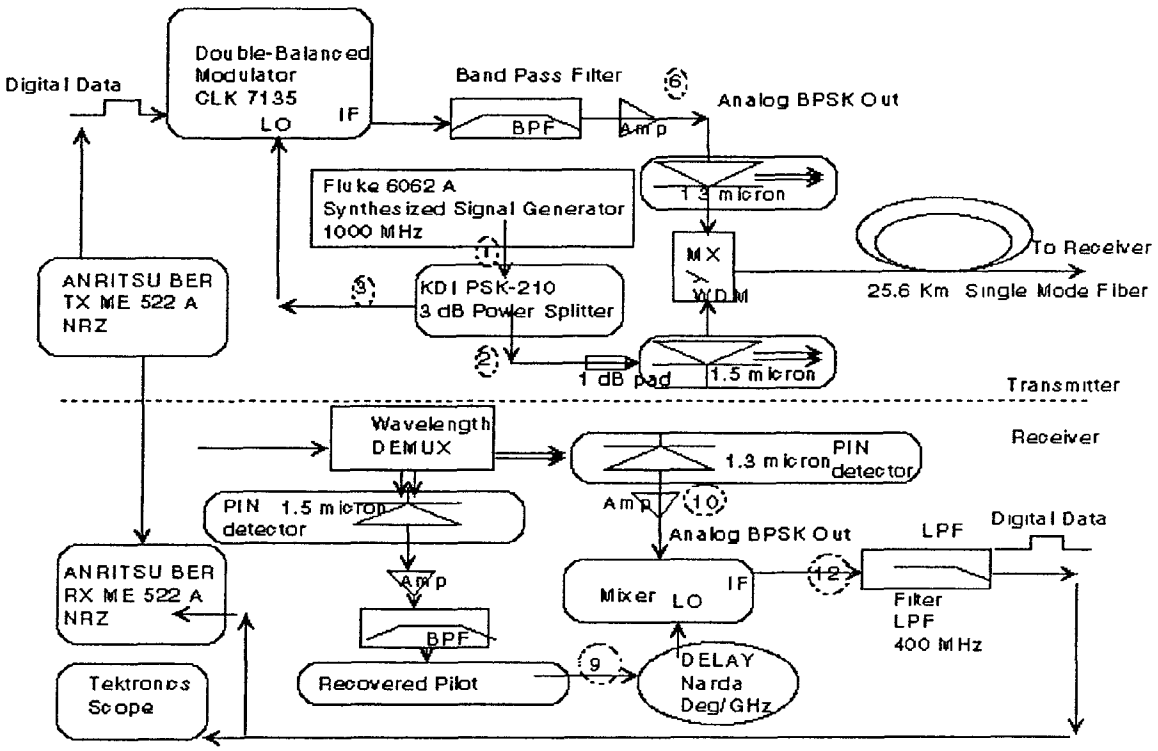

Figure 3.4 Block diagram for BER and eye-pattern generation with 25.6 Km fiber

whose center frequency is 1 GHz and bandwidth less than data rate. The filtered BPSK signal is then amplified to an appropriate level before it is used to intensity modulate the 1306 nm laser. The laser lights carrying the BPSK signal on one hand and pliot on the other are combined with an optical WDM device. We then transmit the two light signals over 25.6 Km of fiber.

At the receiver the two wavelengths are first demultiplexed. The 1533 nm laser signal is intensity demodulated with a PIN diode detector, amplified to the required level and passed through a BPF filter, centered at 1 GHz and with a passband bandwidth of 20 MHz. The BPSK modulated signal is

extracted from 1306 nm laser by again using a PIN diode detector. It is expected that the two laser light will have a fixed amount of delay at the receiver due to dispersion. A coaxial phase shifter, model number 3752, made by NARDA (phase in degrees for 1 GHz) is used for fixed delay compensation.

The two extracted signal; the BPSK modulated subcarrier from 1306 nm laser and pilot from 1533 nm laser are then applied to a mixer for coherent detection of data. The output of the mixer is amplified and low pass filtered with bandwidth of 400 MHz, before it is connected to a 50 ohms impedance, high speed Tektronics oscilloscope.

During this experiment digital data rate was varied from 10 MHz to 600 MHz. The data bit stream used was non-return to zero (NRZ). Bit pattern was fixed as **00101101**.

A few spectral plots are tabulated below. They are taken at different points in the setup as they are marked. The data rate used in this particular case was250 MHz, although other data rate were also used.

plot #	point	λ nm	**Figure 3.4**
3.21	2		1 GHz pilot used to direct modulate 1533 nm laser
3.22	3b		Digital data from BER transmitter, Data rate is 250 MHz.
3.23	6		BPSK amplified to direct modulate 1306 nm laser
3.24	9	1533	Pilot recovered from 1533 nm laser to be used as LO
3.25	10	1306	BPSK as recovered from 1306 nm laser
3.26	12		Data recovered with coherent detection at IF output of mixer

Also examined are the eye diagrams at the transmitter output, and after sub-carrier coherent detection. Photographs of these eye diagrams were also taken. In all photographs, top half depicts the data or eye diagram at the transmitter and lower half of photograph shows the data or eye diagram at the receiver. The photographs of data - transmitted, received and the corresponding eye diagrams are marked and are self explanatory.

Results.

A great deal of system performance information can be deduced from the eye-pattern display. To interpret the eye pattern, consider the simplified drawing shown in figure 3.5. The following information regarding the signal amplitude distortion, timing jitter, and system rise time can be derived:

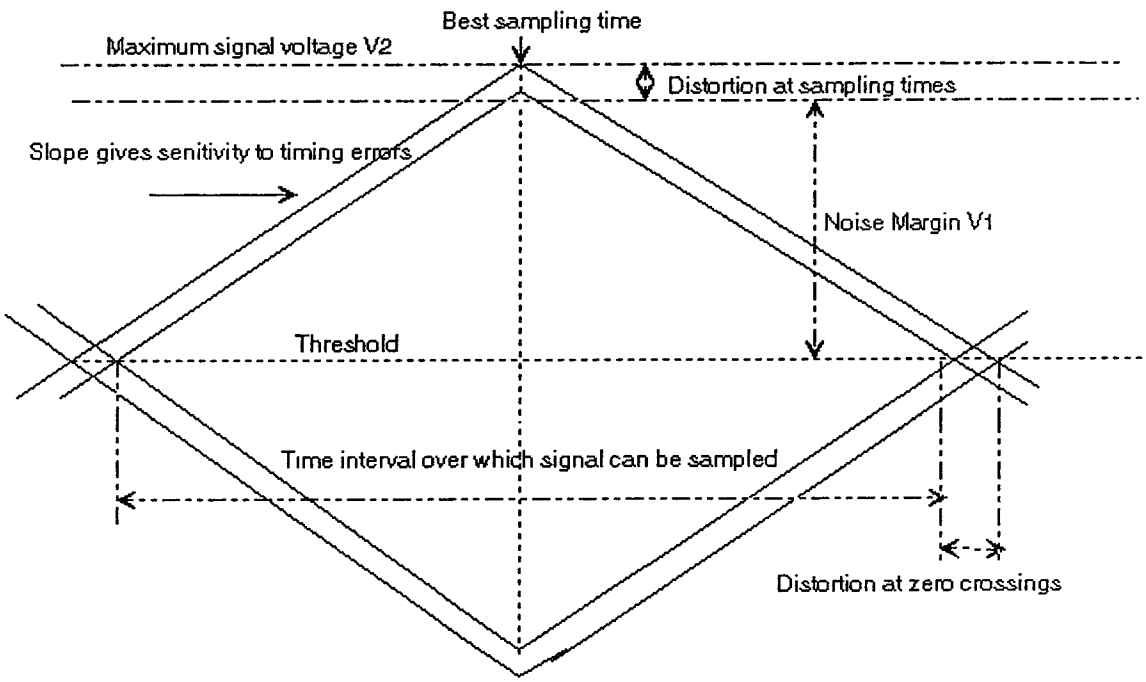

Figure 3.5 Simplified eye-pattern diagram

1. The width of the eye opening defines the time interval over which the received signal can be sampled without error from intersymbol interference. The best time to sample the received waveform is when the height of the eye opening is largest.

2. The height of the eye opening is reduced as a result of amplitude distortion in data signal. The amount of distortion is related to the vertical distance between the top of the eye opening and the maximum signal level. The greater the eye closure becomes the more difficult it is to detect the signal.

3. The height of the eye opening at a specified sampling time shows the noise margin or immunity to noise. Noise margin is defined as the percentage ratio of the peak signal voltage V_1 for an alternating bit sequence (defined by the height of the eye opening) to the maximum signal voltage V_2 as measured from the threshold level, as shown in figure 3.5. that is,

$$\text{Noise Margin (\%)} = V_1 \times 100 / V_2 \qquad (3.14)$$

4. The rate at which the eye closes as the sampling time is varied (that is , the slope of the eye pattern sides) determines the sensitivity of the system to timing errors. The possibility of timing errors increases as the slope is closer to horizontal.

5. Timing jitter (also referred to as edge jitter or phase distortion) in an optical fiber system arises from noise in the receiver and pulse distortion in the optical fiber. If the signal is sampled in the middle of the time interval (that is, midway between the times when the signal crosses the threshold level), then the amount of distortion ΔT at the threshold level indicates the amount of jitter. Timing jitter is thus given by

$$\text{Jitter Margin (\%)} = \Delta T \times 100 / T_b \qquad (3.15)$$

where T_b is one bit interval.

6. Any non linearities of the channel transfer characteristics will create an asymmetry in the eye pattern. If purely random data stream is passed through a truly linear system, all the eye openings will be identical.

From these eye diagram photographs we calculate noise margin and timing jitter for 631 MHz data rate.

Noise Margin (%) = $V_1 \times 100 / V_2 = 85 \times 100 / 125 = 68\%$ and

Jitter Margin (%) = $\Delta T \times 100 / T_b = 0.35$ ns $\times 100 / 1.584$ ns $= 22.09\%$

Above calculations and the eye diagrams shown below indicates that our concept can be used to transmit and recover data with coherent detection.

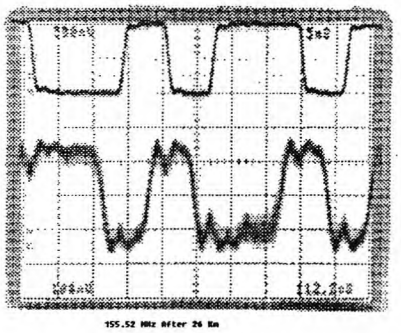

155.52 MHz After 26 Km

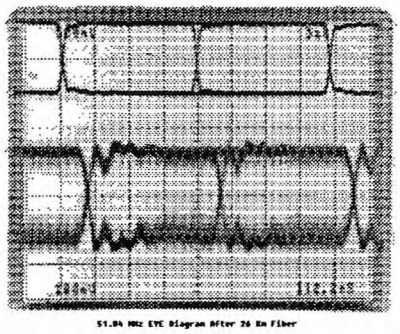

51.84 MHz EYE Diagram After 26 Km Fiber

Data Rate is 155.52 MHz, vertical scale is 100 mV/div and horizontal scale is 2 ns/div for received signal.

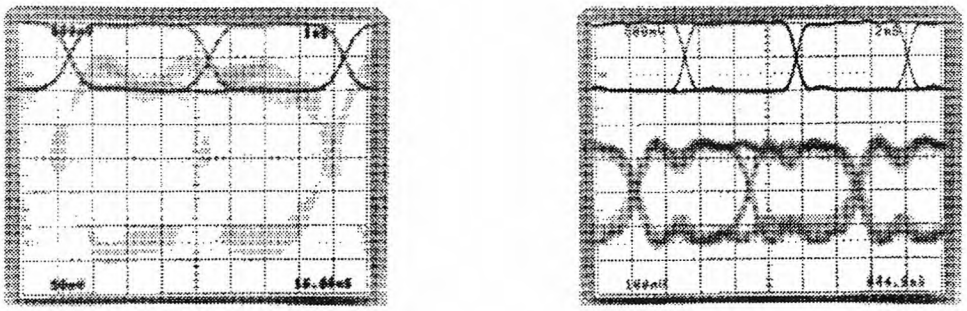

Data Rate is 250 MHz, vertical scale is 50 mV/div and horizontal scale is 1 ns/div for received signal eye diagram alone

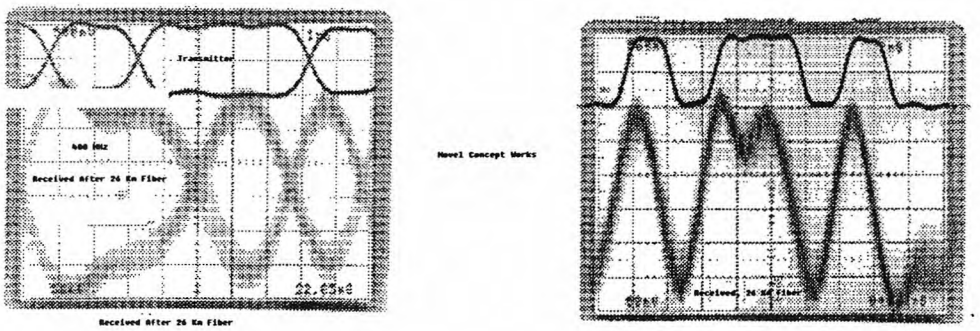

Data Rate is 400 MHz, vertical scale is 50 mV/div and horizontal scale is 1 ns/div for received signal

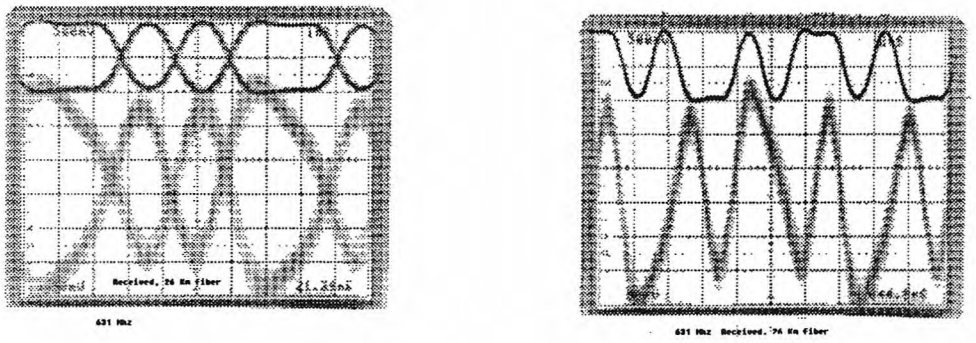

Data Rate is 631 MHz, vertical scale is 50 mV/div and horizontal scale is 1 ns/div for received signal

3.4 Bit Error Rate Measurements

Any digital systems is incomplete without a bit error rate (BER) test. BER test is demonstrated in the next experiment. System set up is same as in figure 3.4, except that now recovered data is fed to the BER receiver. Due to lack of time for design we did not build, as might expect, electronics to generate digital clock from the pilot transmitted on 1533 nm laser and therefore we instead use the clock from the BER transmitter.

The data rate used was 622.08 MHz. PBRS (pseudo random data bit sequence) was 2^{15}-1 and 2^{23}-1. NRZ bit pattern was used. We didn't use appropriate filters (A BPF or LPF) anywhere in data link. Our aim was to see the system stability and BER over a long time. The BER was maintained at 10^{-9} for seven days.

BER Rate and Jitter on Pilot

References [35, 36, 37] give a good insight into the jitter tolerance in fiber-optic systems. In our measurement we introduced a delay in the pilot RF arm different from nominal delay. The optimum delay was found to be 40 degrees for a stable BER of $\times 10^{-10}$.

A delay of 5 degrees from its nominal value of 40 degrees cause BER to degraded from 10^{-10} to $\times 10^{-9}$. An additional delay of 10 degree from the nominal delay of 40 degrees cause BER to become 10^{-8}

CONCLUSION

The aim of the experiment were to examine the validity of theoretical analysis and to prove or contradict our assessment regarding the performance of our system. Despite the fact that we did not take in our theoretical analysis the consideration the effect of laser chirp, laser phase noise, reflection and their combined effect, the experiment almost always agreed with the theoretical conclusion. That is there is no much performance reduction in coherency and the pilot extracted from a different light

wavelength can be satisfactorily used to coherently demodulate the subcarrier carried by the other wavelength. Such good agreement between experimental and theoretical results may be attributed to narrow laser linewidth (0.14 nm), relatively short length of fiber(36 Km) and low RF frequency of 1 GHz (relative to laser linewidth). Therefore both theoretical calculations and experiment results we conclude that fiber dispersion will not be the cause of pilot and subcarrier not remaining coherent . Fiber attenuation will be a limiting factor for longer distance.

At frequencies higher than 5 GHz and 90% modulation depth, laser chirp noise will be present in the bandwidth of the subcarrier and pilot of identical frequencies. Chirp combined with residual dispersion of fiber will generate enough phase noise with 50 to 100 Km of fiber which could be another problem for future investigation.

From the point view of dispersion transmission of a pilot of low frequency will be beneficial. Pilot of 51.840 MHz will not be affected due to laser chirp as chirp frequency will be outside the pilot bandwidth. Low frequency pilot transmission can be used to generate many subcarriers and timing clock. For practical distances of a few 100 Km where fiber attenuation is not the limiting factor in repeater span, pilot will remain coherent with the subcarrier. For relatively short distances laser linewidth can be increased to reduce the system cost as lasers with broad linewidth are cheaper.

We have demonstrated our concept by a complete system demonstration where we recover digital data by coherent detection. The eye diagrams and BER test supports our concept and theoretical calculations. We have also demonstrated long term stability of this concept for over seven days by monitoring BER to be constant.

Our concept could be very useful for a number of applications which one can think of - Full duplex systems, High speed M-ary BPSK or FSK subcarrier coherent detection and clock recovery.

At this point we would like to conclude and answer the three questions that were part of the problem formulation in chapter 1.

Q1. If we transmit synchronous microwave subcarrier $\omega_{rf1.3} = \omega_{rf1.5}$ of identical frequency and phase, i.e. a coherent RF signal on two different lasers, will the detected signal be Coherent. ? *If no, than our concept does not work.*

Answer to this is **YES** from our theoretical and experimental results. Use of different light sources did not generate noticeable noise on pilot.

If yes, than

Q2. What is the penalty that we will have to pay for all different noise phenomenons that we presented above due to fiber alone?

In the experiment with discrete phase variations (fig. 3.1a, 3.1b and 3.1c) the measured penalty due to fiber and other noise phenomenons was 1.91 dB.

Q3. If $\omega_{rf1.3} = [\ 192\ ] \omega_{rf1.5}$ than will the jitter present on multiplication be large enough to cause loss of phase coherency ? If yes than we might look into Phase Lock Loop type solution. *Because any noise present on 51.840 MHz pilot will be multiplied.* **If no, than we demonstrate our concept in total.**

We did not do this experiment. However, since the recovered pilot do not show noticeable noise due to fiber, any noise on multiplication of low frequency to higher frequency will be due to the electrical components which is well understood and can be compensated easily.

We conclude that in order to use Terahertz bandwidth offered by fiber-optic technology we need not wait for development of new digital techniques and their reduced cost, or more expensive optical coherent detection from laboratory optical work benches, but instead one may use our **NOVEL CONCEPT.**

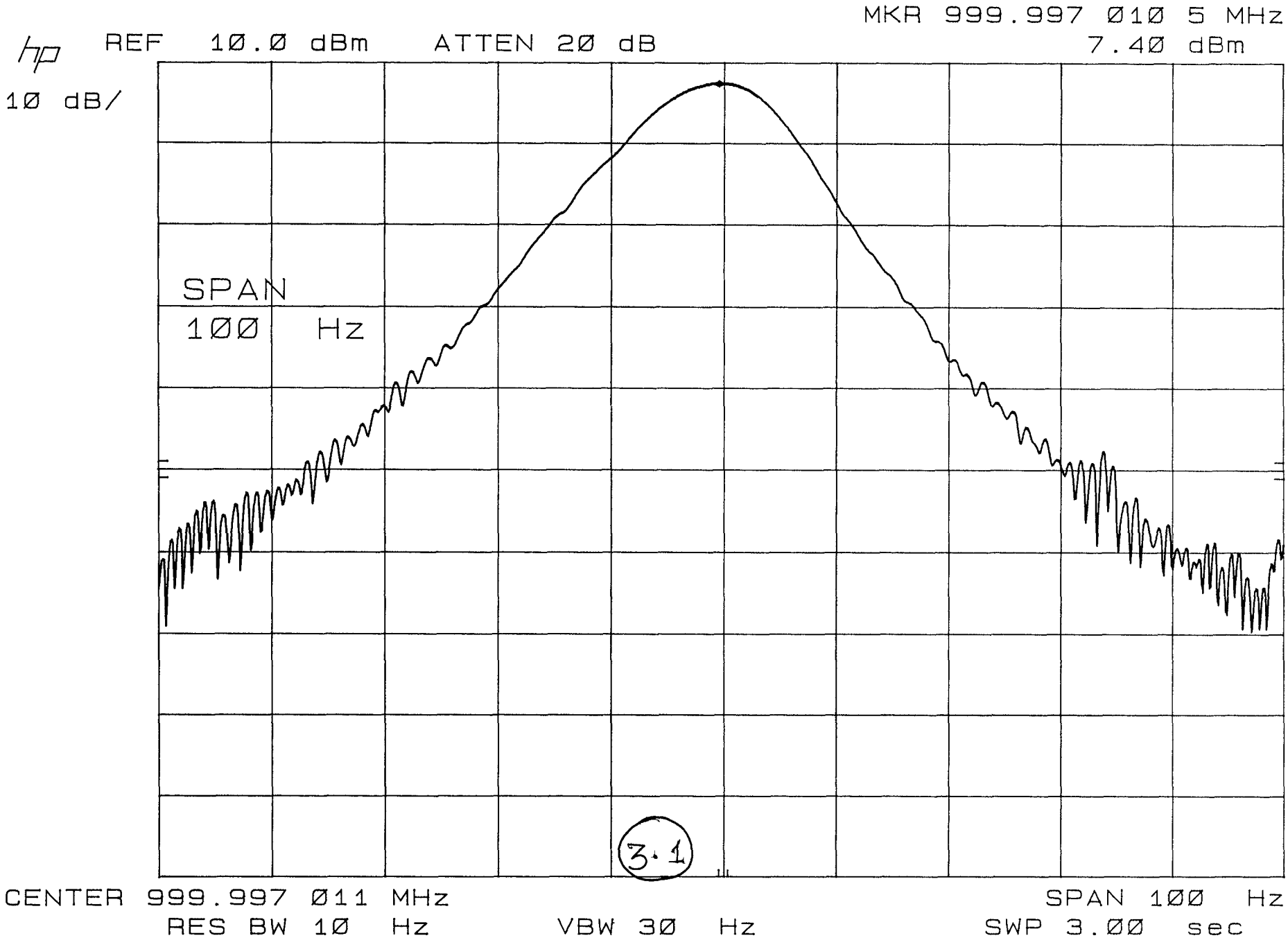
MKR 999.997 Ø1Ø 5 MHz
REF 1Ø.Ø dBm ATTEN 2Ø dB
7.4Ø dBm
1Ø dB/
SPAN
1ØØ Hz
3.1
CENTER 999.997 Ø11 MHz
SPAN 1ØØ Hz
RES BW 1Ø Hz
VBW 3Ø Hz
SWP 3.ØØ sec

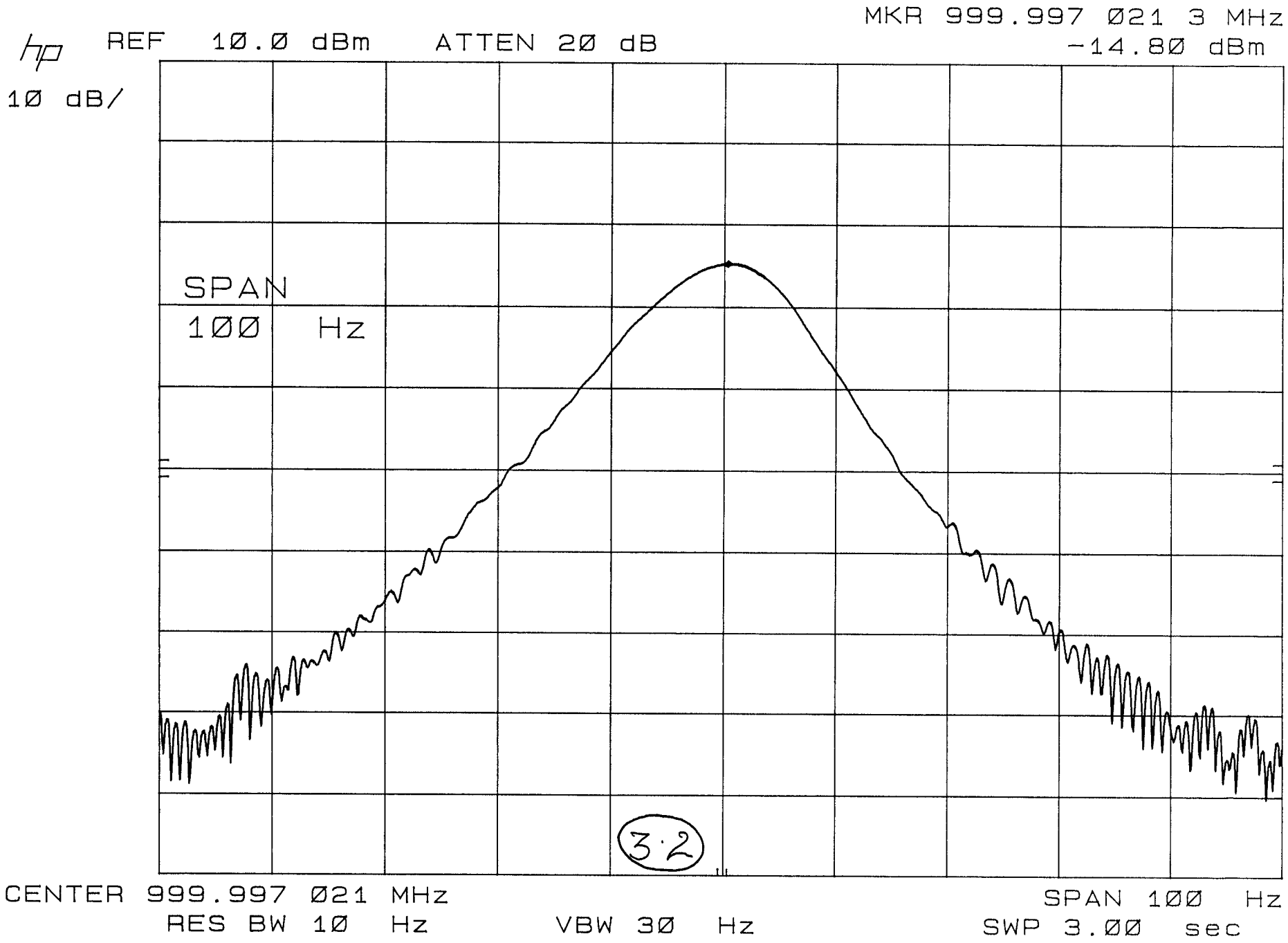
MKR 999.997 Ø21 3 MHz
REF 1Ø.Ø dBm
ATTEN 2Ø dB
-14.8Ø dBm
1Ø dB/
SPAN
1ØØ Hz
3.2
CENTER 999.997 Ø21 MHz
SPAN 1ØØ Hz
RES BW 1Ø Hz
VBW 3Ø Hz
SWP 3.ØØ sec

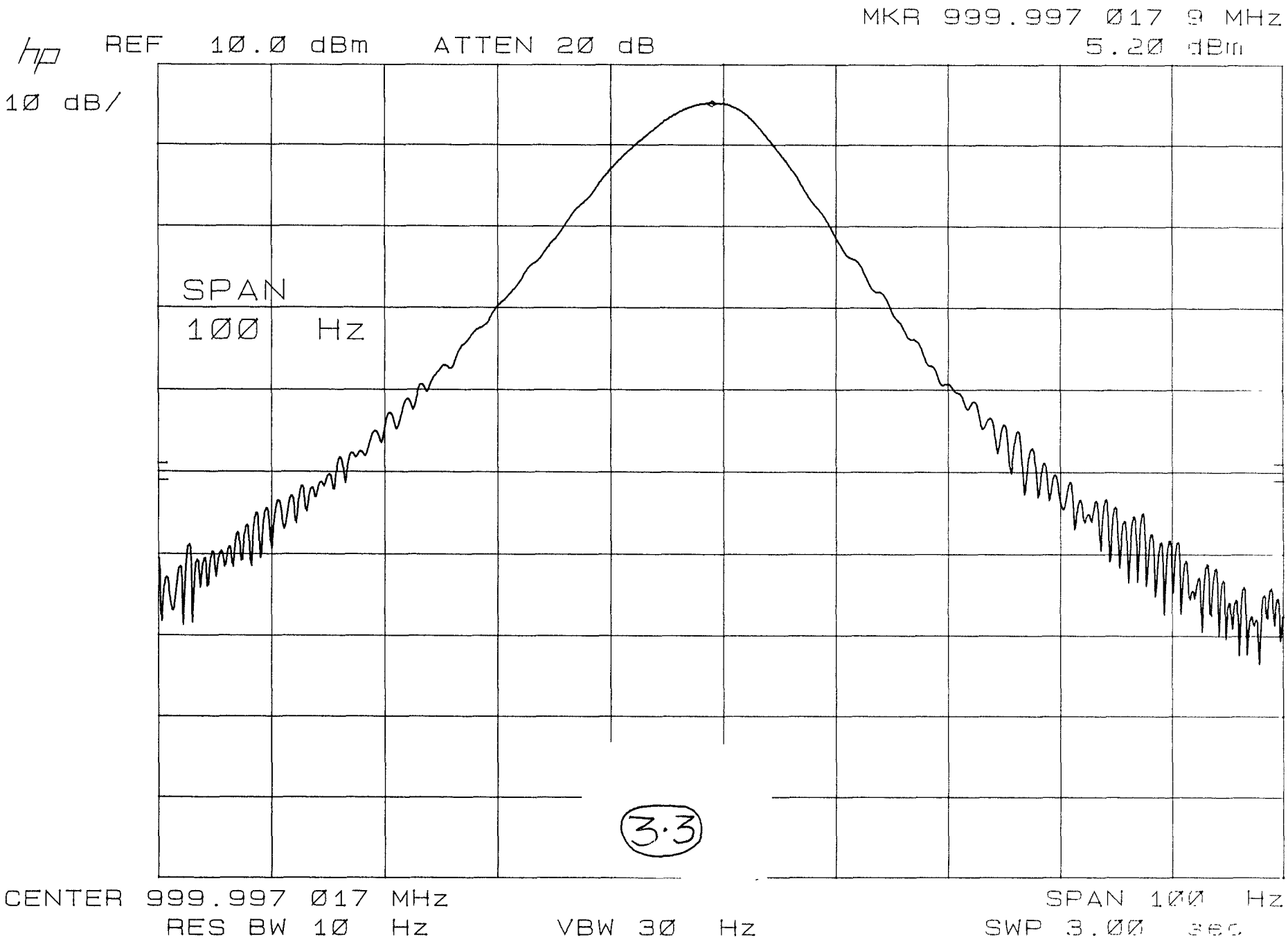
MKR 999.997 Ø17 9 MHz
REF 1Ø.Ø dBm
ATTEN 2Ø dB
5.2Ø dBm
1Ø dB/
SPAN
1ØØ Hz
3.3
CENTER 999.997 Ø17 MHz
SPAN 1ØØ Hz
RES BW 1Ø Hz
VBW 3Ø Hz
SWP 3.ØØ sec

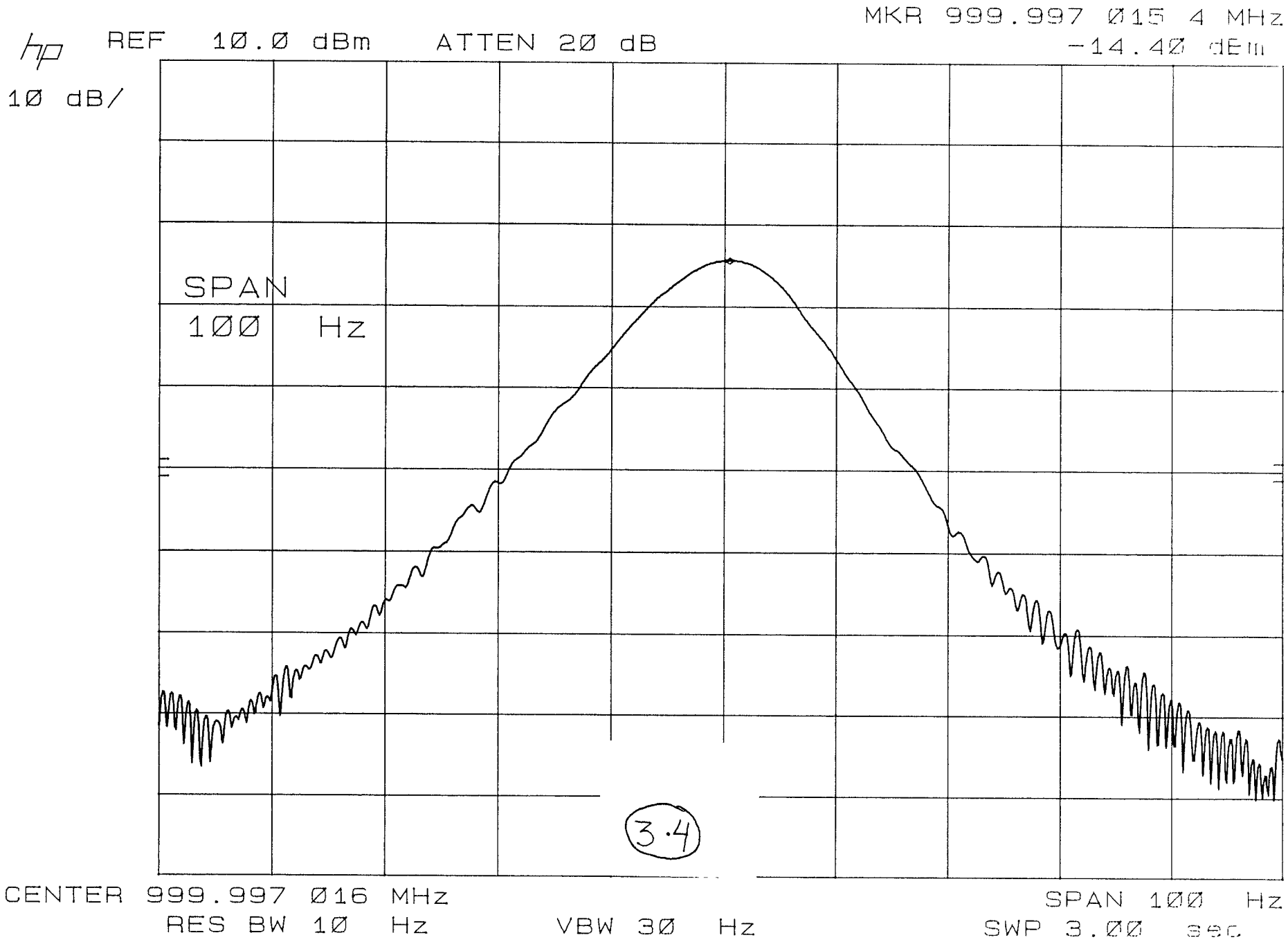
MKR 999.997 Ø15 4 MHz
REF 1Ø.Ø dBm ATTEN 2Ø dB
-14.4Ø dBm
1Ø dB/
SPAN
1ØØ Hz
3.4
CENTER 999.997 Ø16 MHz
SPAN 1ØØ Hz
RES BW 1Ø Hz
VBW 3Ø Hz
SWP 3.ØØ sec


OA-NOISE
REF 10.0 dBm ATTEN 20 dB
10 dB/
STOP
100 Hz
3.5
START 0 Hz
STOP 100 Hz
RES BW 10 Hz
VBW 30 Hz
SWP 3.00 sec

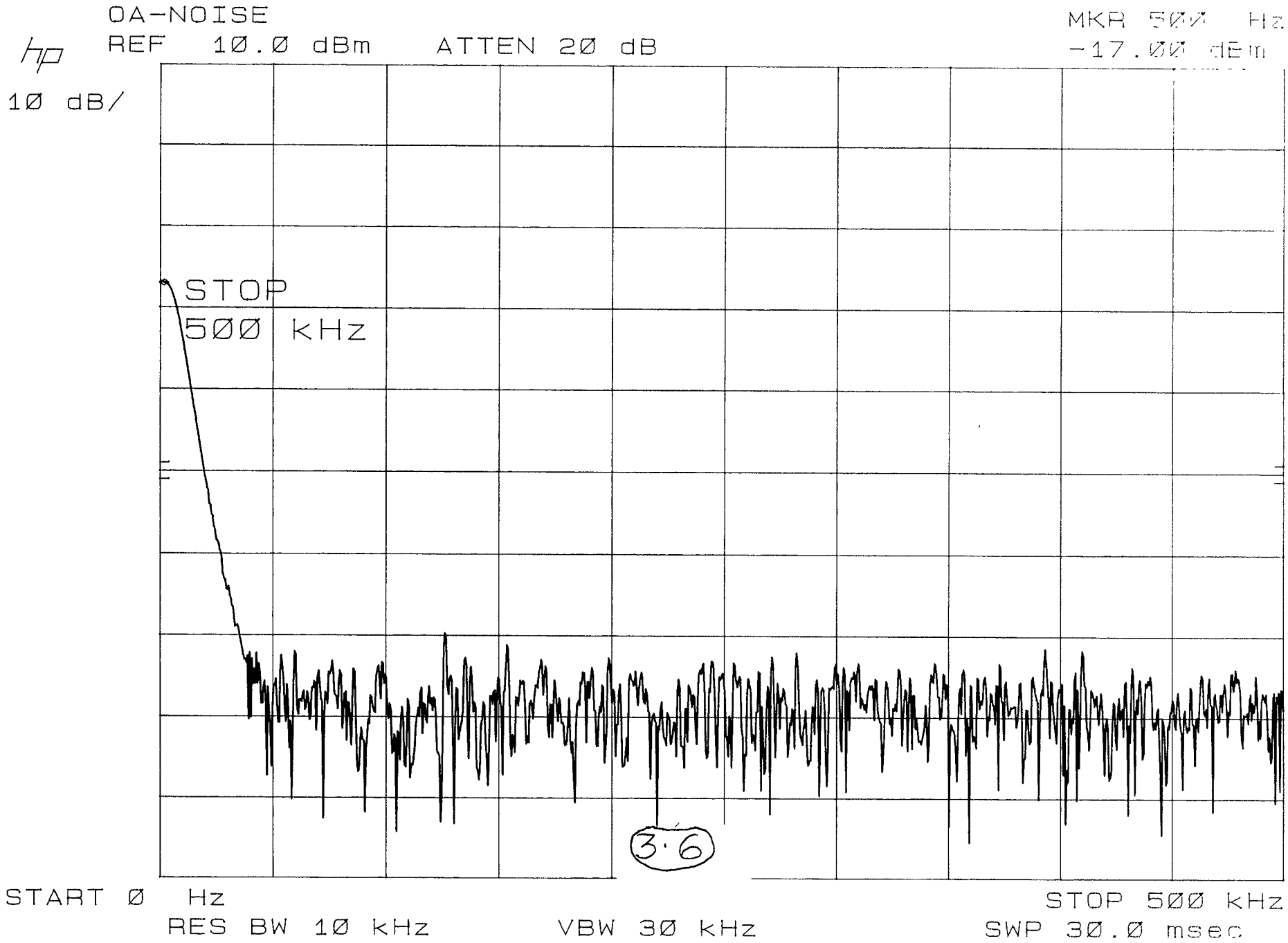
OA-NOISE
REF 10.0 dBm
ATTEN 20 dB
MKR 500 Hz
-17.00 dBm
10 dB/
STOP
500 kHz
3·6
START 0 Hz
STOP 500 kHz
RES BW 10 kHz
VBW 30 kHz
SWP 30.0 msec

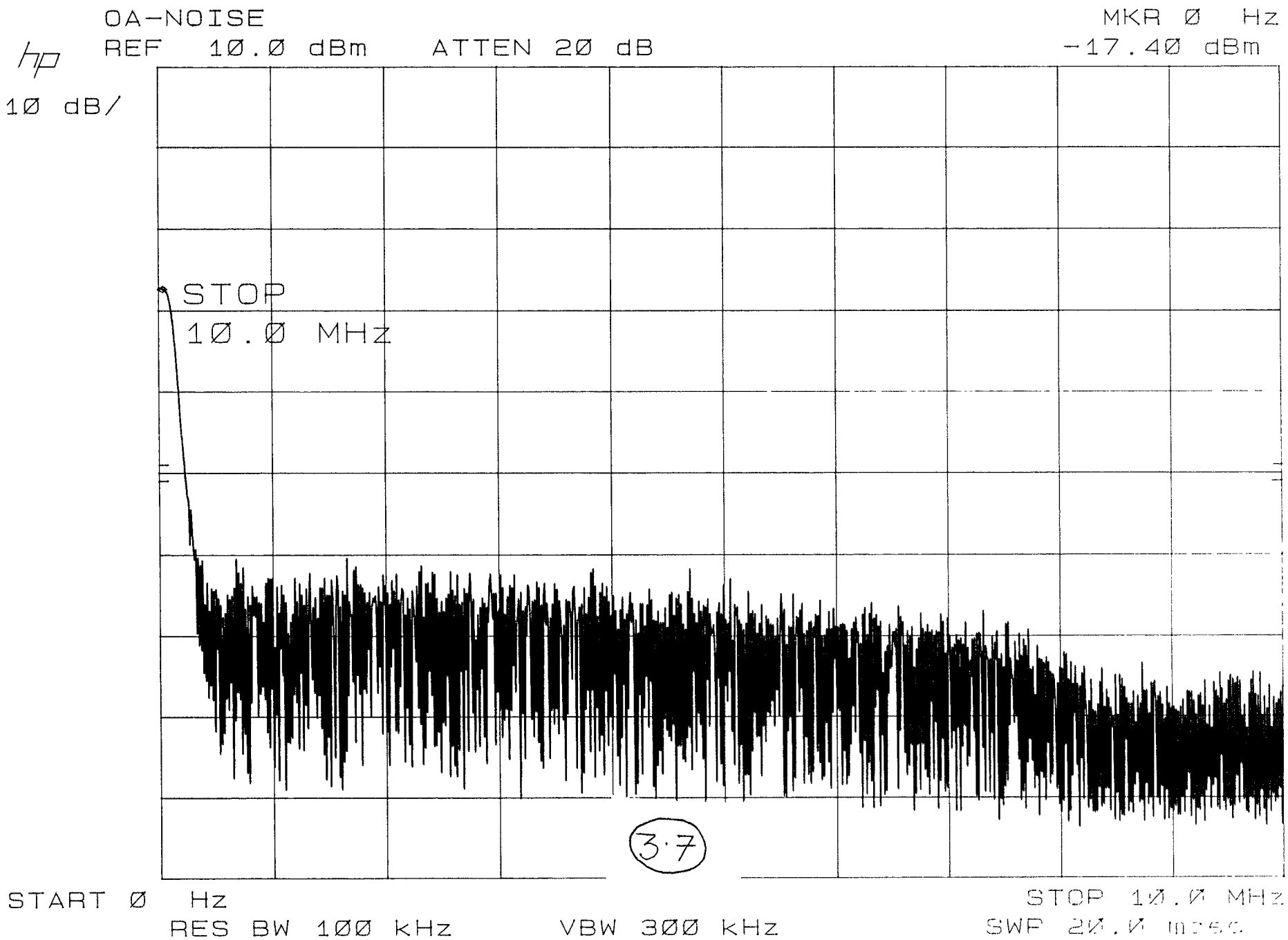
OA-NOISE
REF 10.0 dBm
ATTEN 20 dB
MKR Ø Hz
-17.40 dBm
10 dB/
STOP
10.Ø MHz
3·7
START Ø Hz
RES BW 100 kHz
VBW 300 kHz
STOP 10.Ø MHz
SWP 20.Ø msec

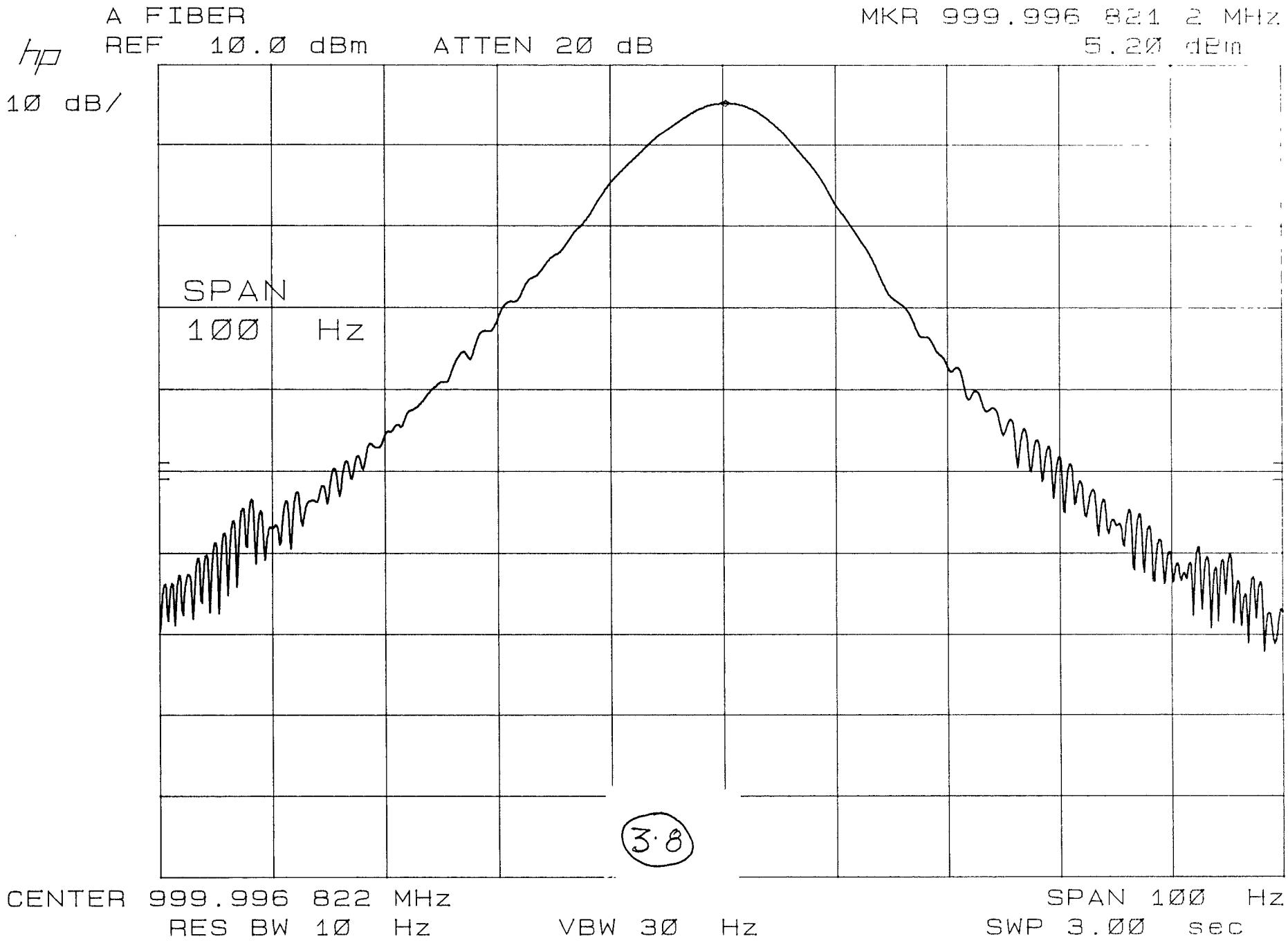
A FIBER
REF 10.0 dBm
ATTEN 20 dB
MKR 999.996 821 2 MHz
5.20 dBm
10 dB/
SPAN
100 Hz
3·8
CENTER 999.996 822 MHz
SPAN 100 Hz
RES BW 10 Hz
VBW 30 Hz
SWP 3.00 sec

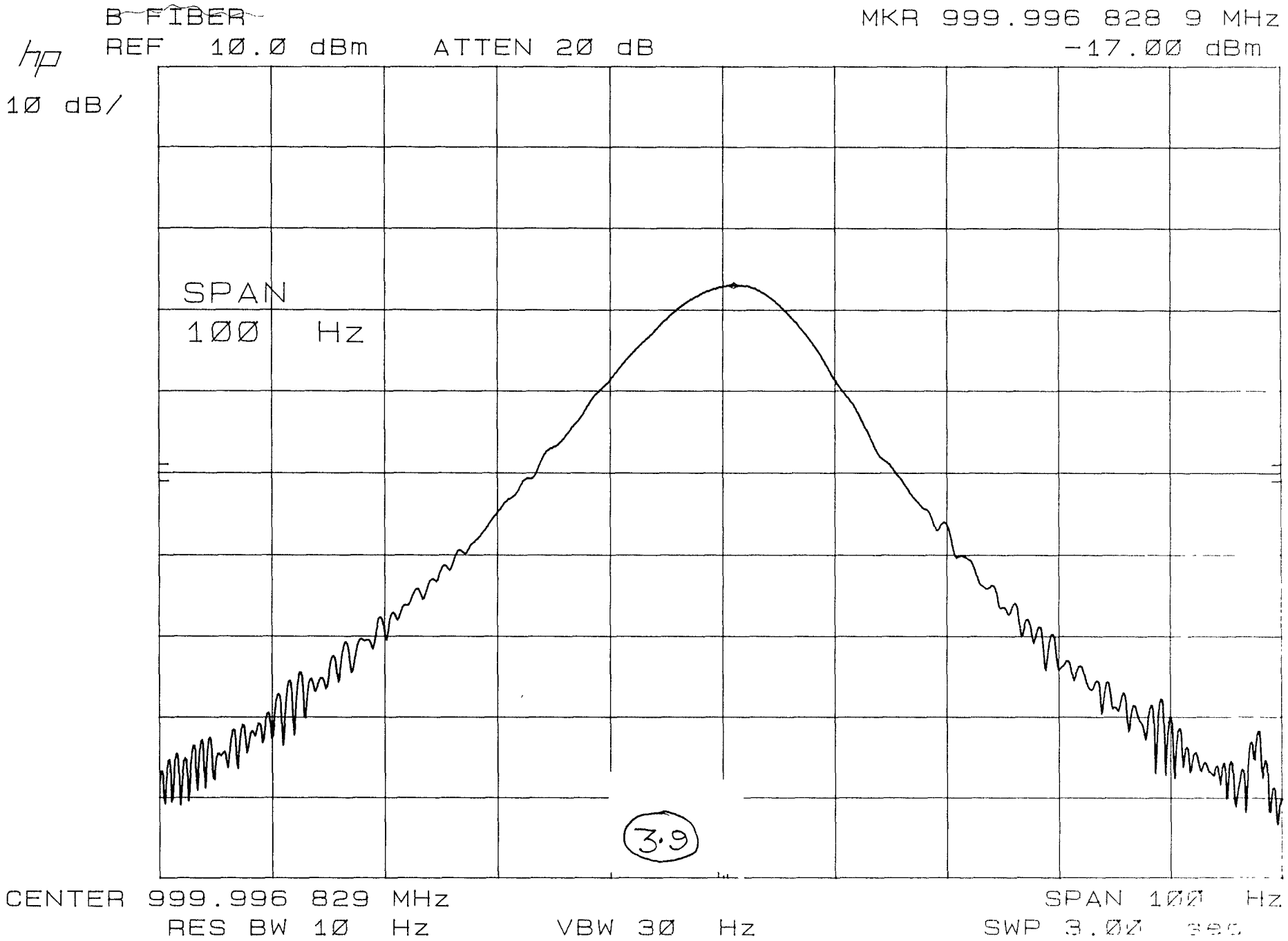
B FIBER
MKR 999.996 828 9 MHz
REF 10.0 dBm
ATTEN 20 dB
-17.00 dBm
10 dB/
SPAN
100 Hz
3.9
CENTER 999.996 829 MHz
SPAN 100 Hz
RES BW 10 Hz
VBW 30 Hz
SWP 3.00


D FIBER NOISE
REF 10.0 dBm ATTEN 20 dB
10 dB/
STOP
100 Hz
3·10
START 0 Hz
STOP 100 Hz
RES BW 10 Hz
VBW 30 Hz
SWP 3.00 sec

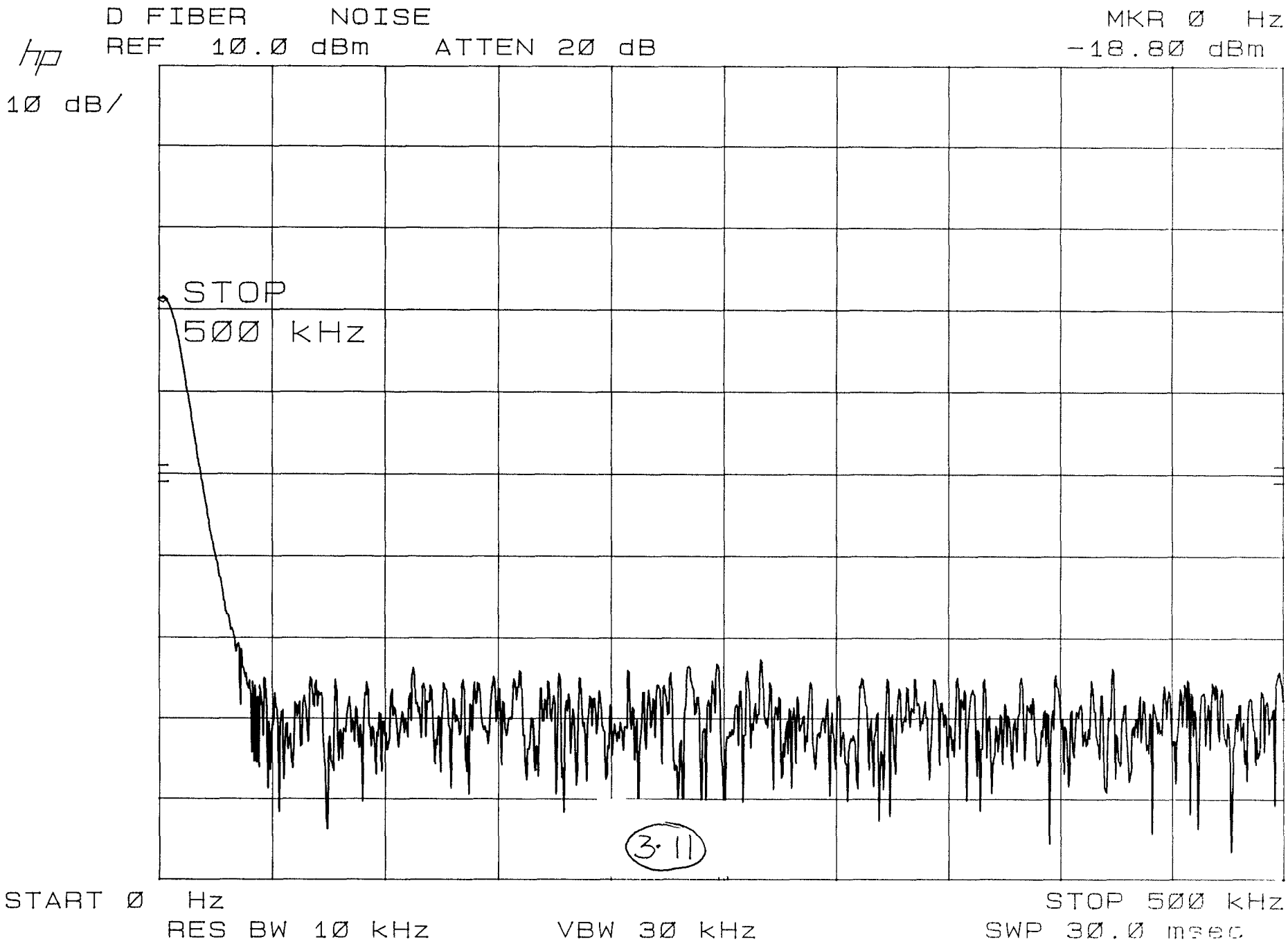
D FIBER NOISE
MKR Ø Hz
REF 1Ø.Ø dBm ATTEN 2Ø dB
-18.8Ø dBm
1Ø dB/
STOP
5ØØ kHz
3.11
START Ø Hz
STOP 5ØØ kHz
RES BW 1Ø kHz
VBW 3Ø kHz
SWP 3Ø.Ø msec

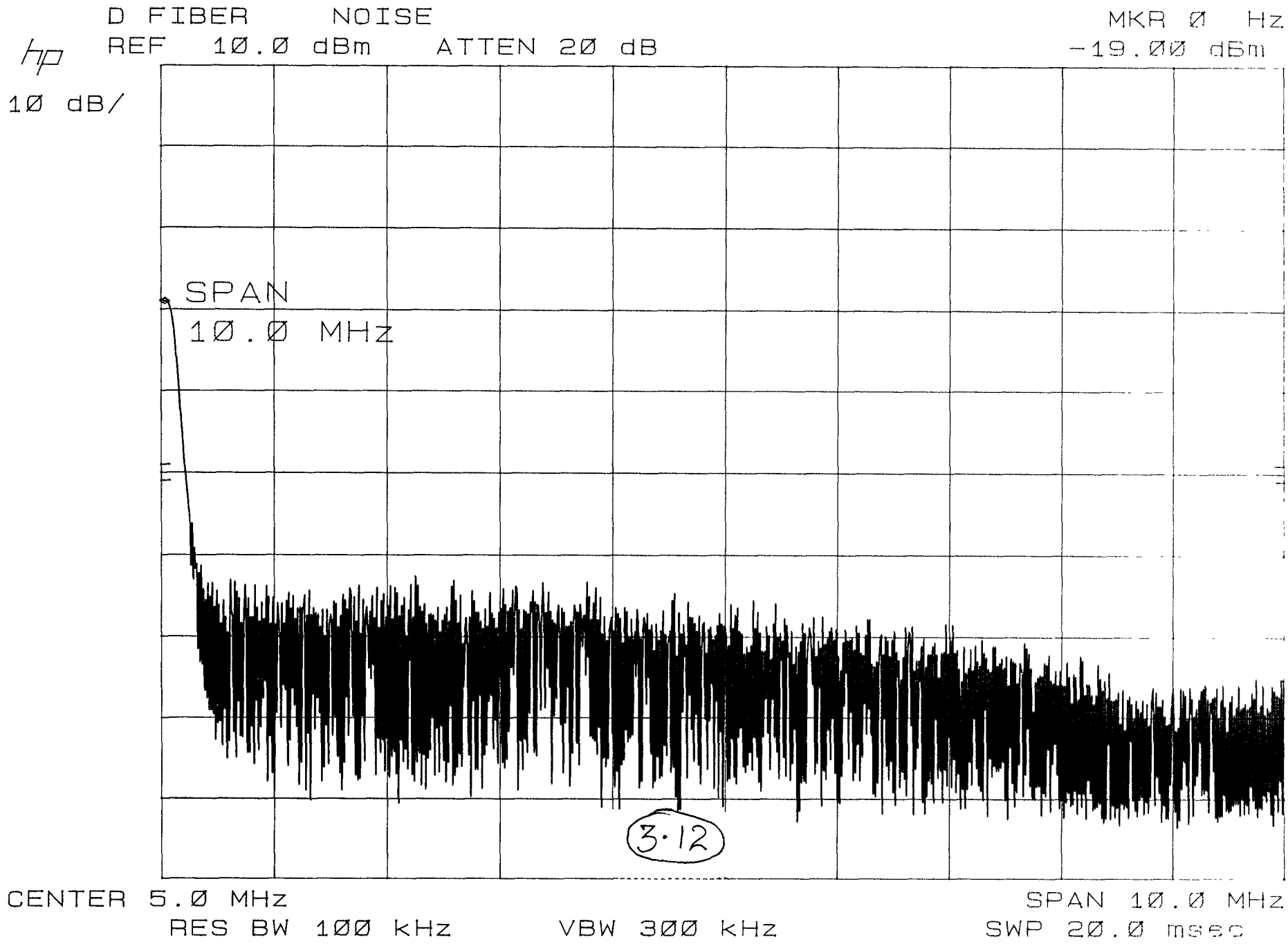
D FIBER NOISE
MKR Ø Hz
REF 10.Ø dBm ATTEN 2Ø dB
−19.ØØ dBm
10 dB/
SPAN
10.Ø MHz
3·12
CENTER 5.Ø MHz
SPAN 10.Ø MHz
RES BW 1ØØ kHz
VBW 3ØØ kHz
SWP 2Ø.Ø msec

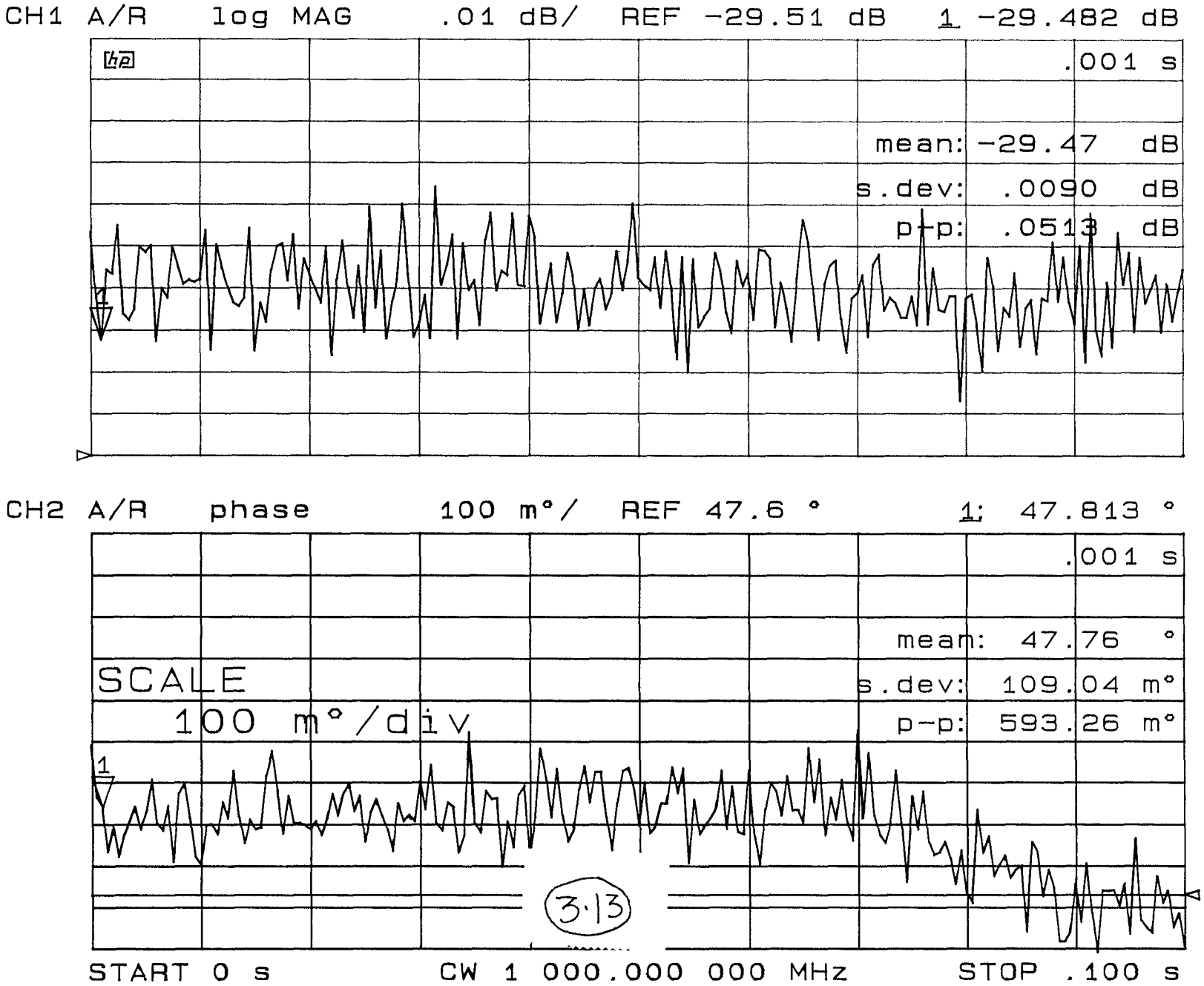
CH1 A/R log MAG .01 dB/ REF −29.51 dB 1 −29.482 dB
.001 s
mean: −29.47 dB
s.dev: .0090 dB
p-p: .0513 dB
CH2 A/R phase 100 m°/ REF 47.6 ° 1: 47.813 °
.001 s
mean: 47.76 °
SCALE
100 m°/div
s.dev: 109.04 m°
p-p: 593.26 m°
3·13
START 0 s
CW 1 000.000 000 MHz
STOP .100 s

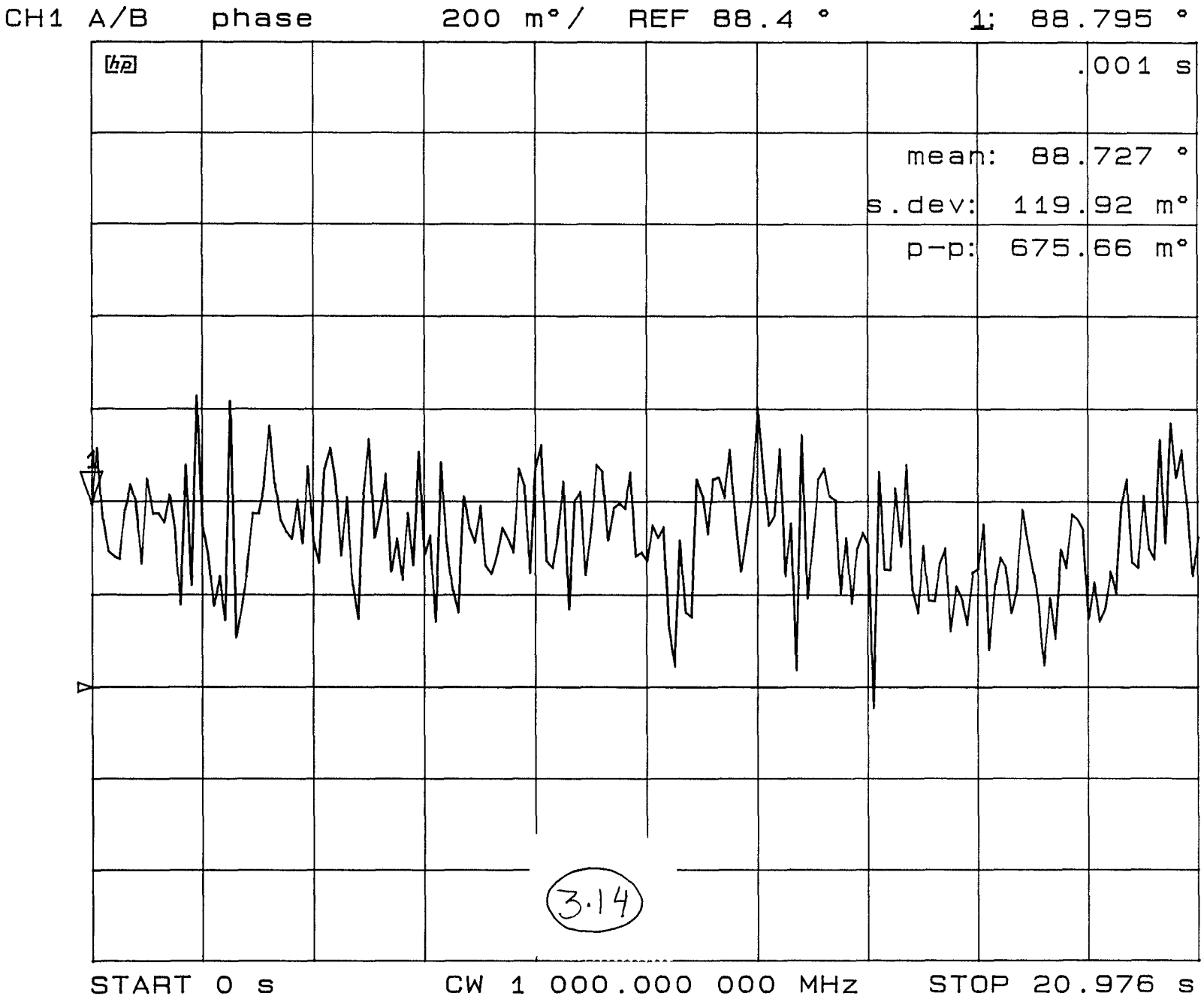
CH1 A/B phase
200 m°/ REF 88.4 °
1: 88.795 °
.001 s
meam: 88.727 °
s.dev: 119.92 m°
p-p: 675.66 m°
3.14
START 0 s
CW 1 000.000 000 MHz
STOP 20.976 s

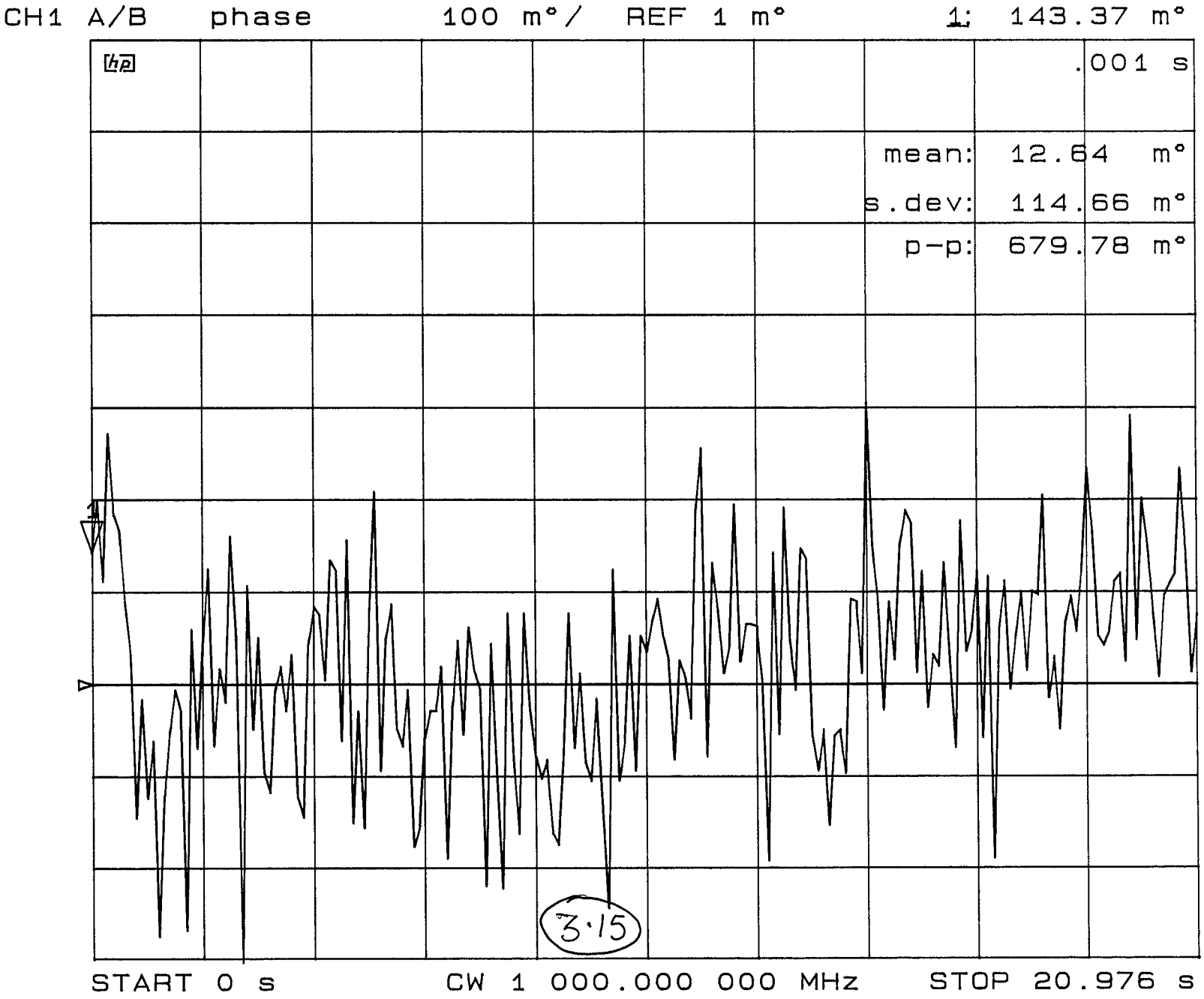
CH1 A/B phase 100 m°/ REF 1 m° 1: 143.37 m°
.001 s
mean: 12.64 m°
s.dev: 114.66 m°
p-p: 679.78 m°
3·15
START 0 s
CW 1 000.000 000 MHz
STOP 20.976 s

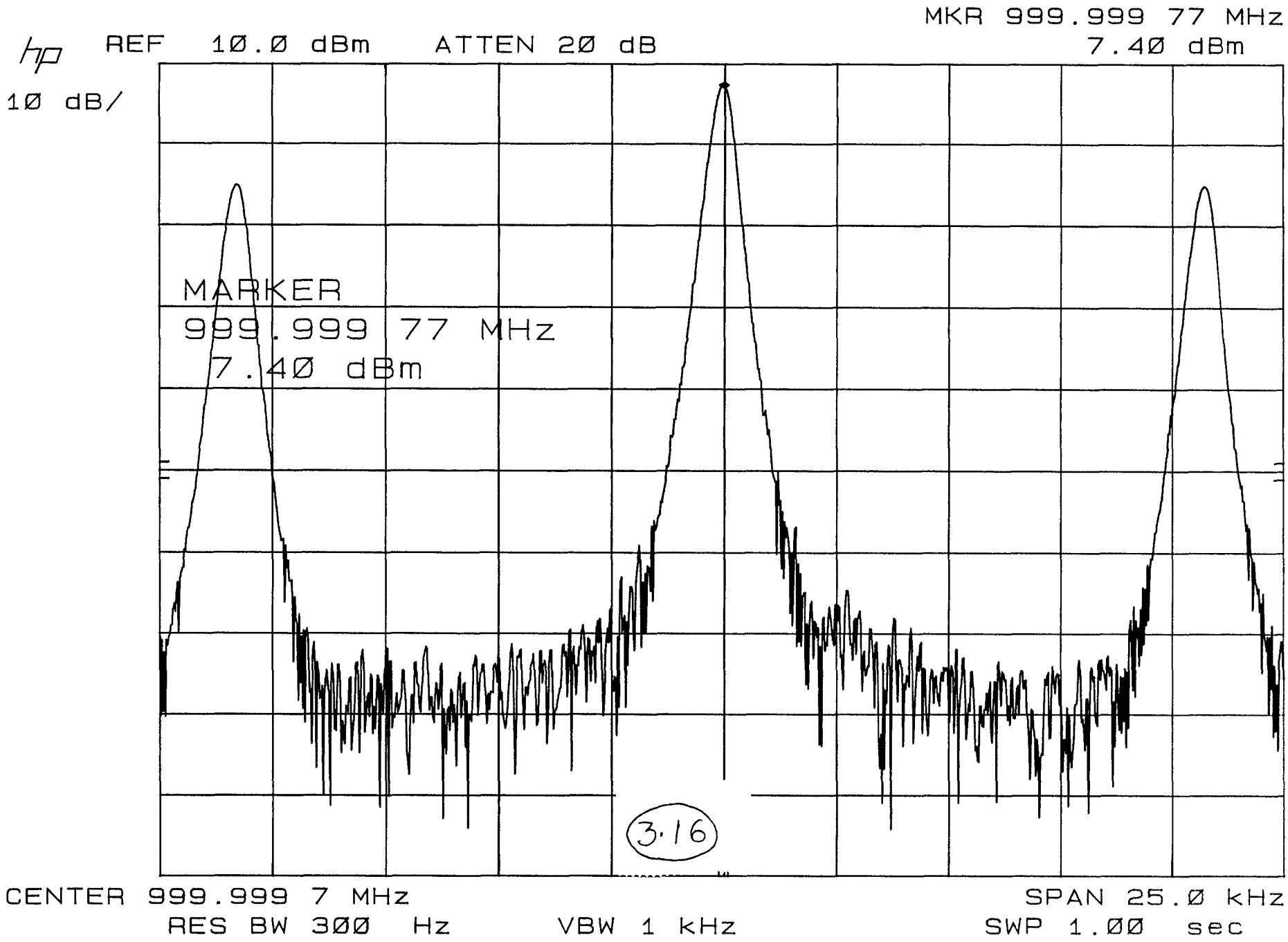
MKR 999.999 77 MHz
7.40 dBm
REF 10.0 dBm
ATTEN 20 dB
10 dB/
MARKER
999.999 77 MHz
7.40 dBm
3.16
CENTER 999.999 7 MHz
SPAN 25.0 kHz
RES BW 300 Hz
VBW 1 kHz
SWP 1.00 sec

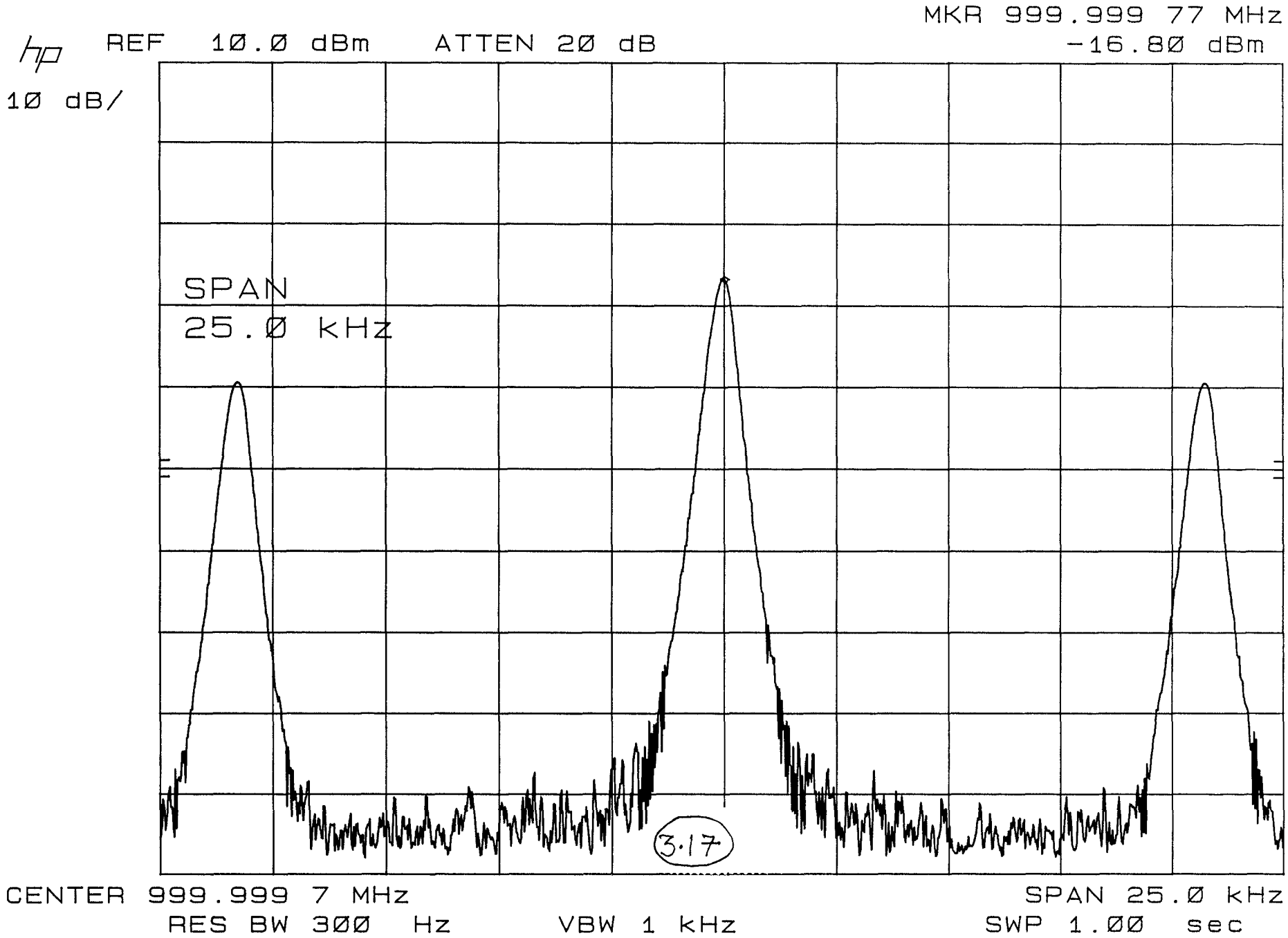
MKR 999.999 77 MHz
REF 10.0 dBm
ATTEN 20 dB
-16.80 dBm
10 dB/
SPAN
25.0 kHz
3.17
CENTER 999.999 7 MHz
SPAN 25.0 kHz
RES BW 300 Hz
VBW 1 kHz
SWP 1.00 sec

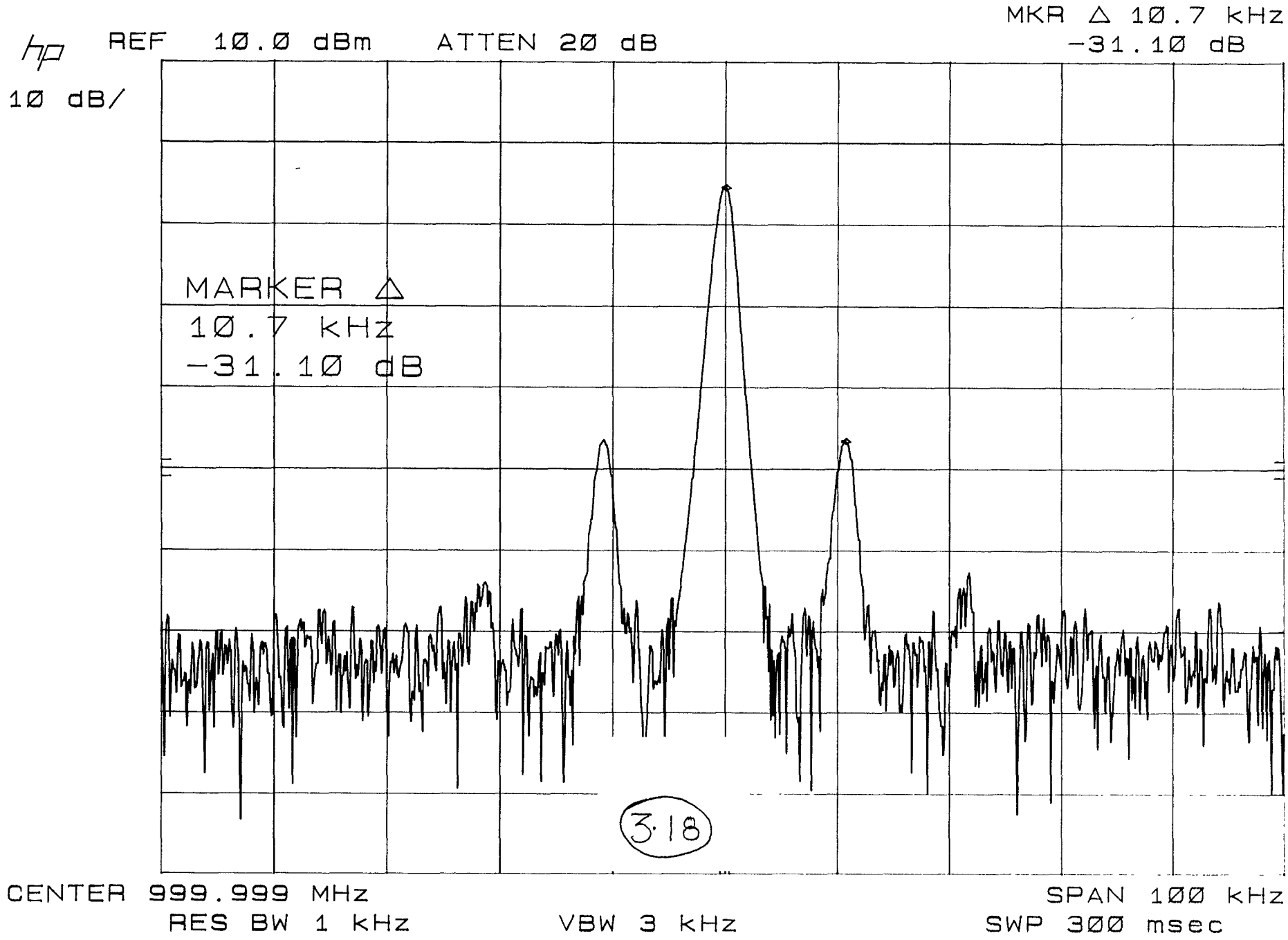
MKR Δ 10.7 kHz
-31.10 dB
REF 10.0 dBm
ATTEN 20 dB
10 dB/
MARKER Δ
10.7 kHz
-31.10 dB
3.18
CENTER 999.999 MHz
SPAN 100 kHz
RES BW 1 kHz
VBW 3 kHz
SWP 300 msec

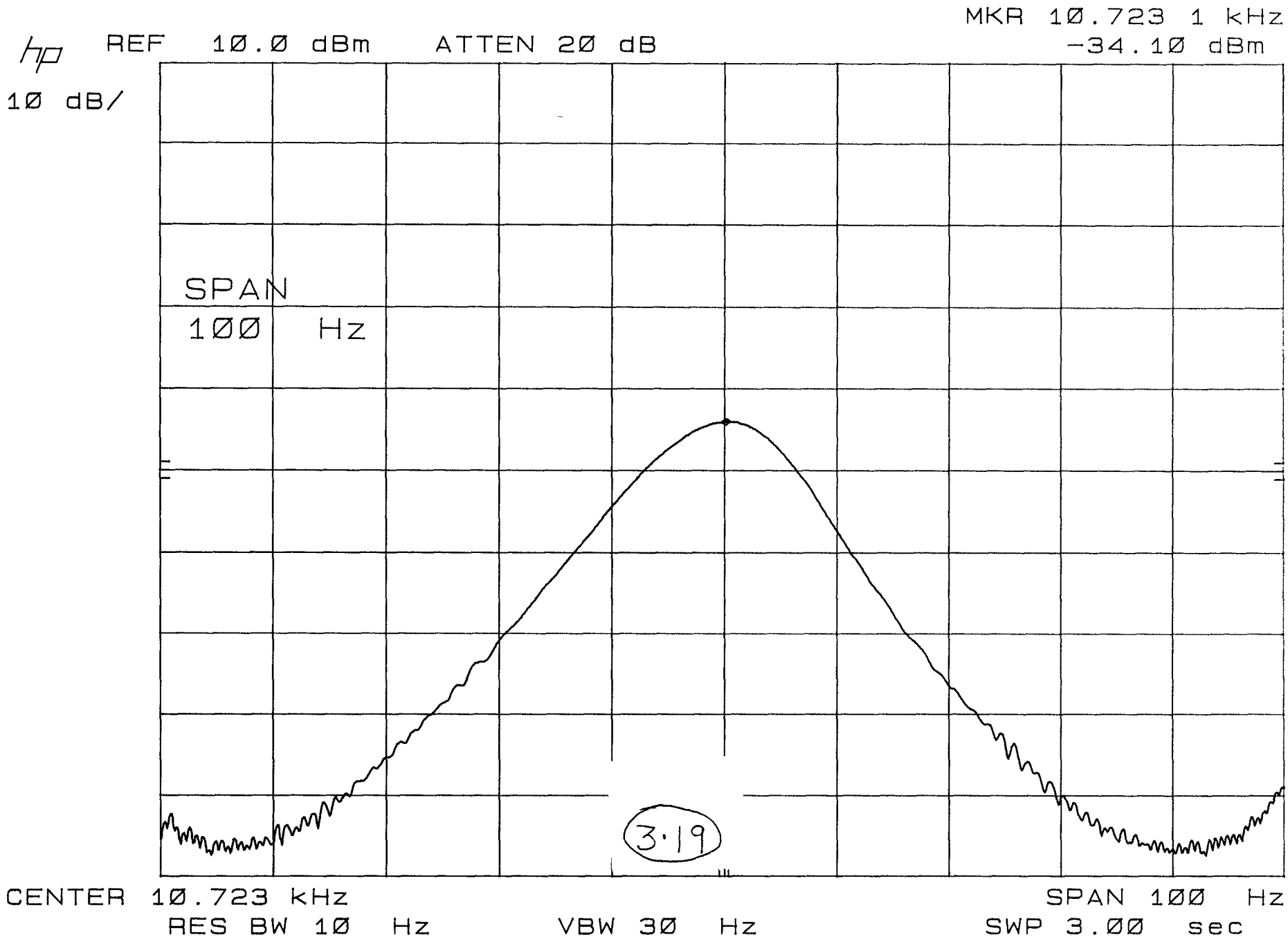
MKR 10.723 1 kHz
-34.10 dBm
REF 10.0 dBm
ATTEN 20 dB
10 dB/
SPAN
100 Hz
3.19
CENTER 10.723 kHz
SPAN 100 Hz
RES BW 10 Hz
VBW 30 Hz
SWP 3.00 sec

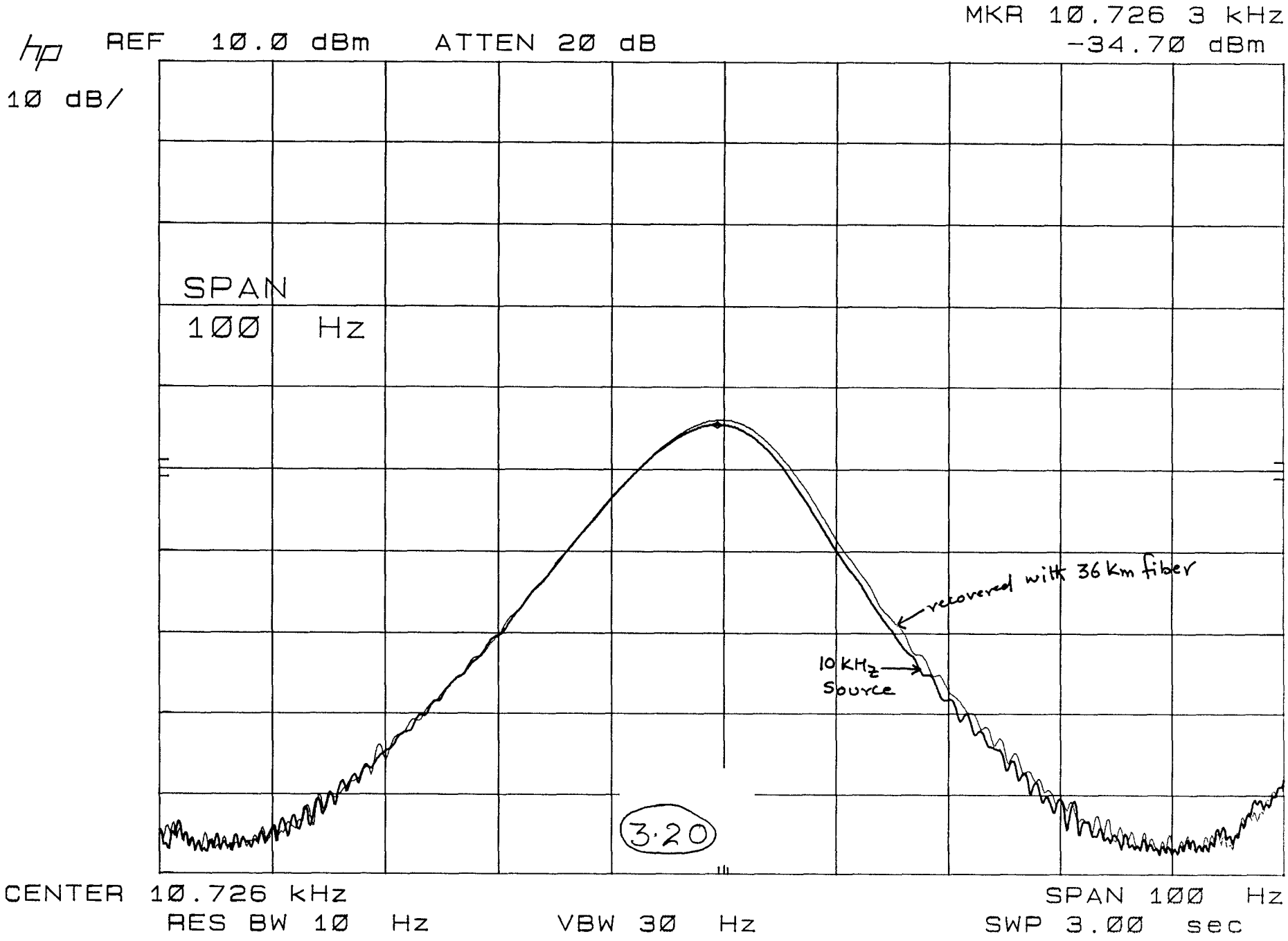
MKR 10.726 3 kHz
-34.70 dBm
REF 10.0 dBm
ATTEN 20 dB
10 dB/
SPAN
100 Hz
recovered with 36 km fiber
10 KHz
Source
3.20
CENTER 10.726 kHz
SPAN 100 Hz
RES BW 10 Hz
VBW 30 Hz
SWP 3.00 sec

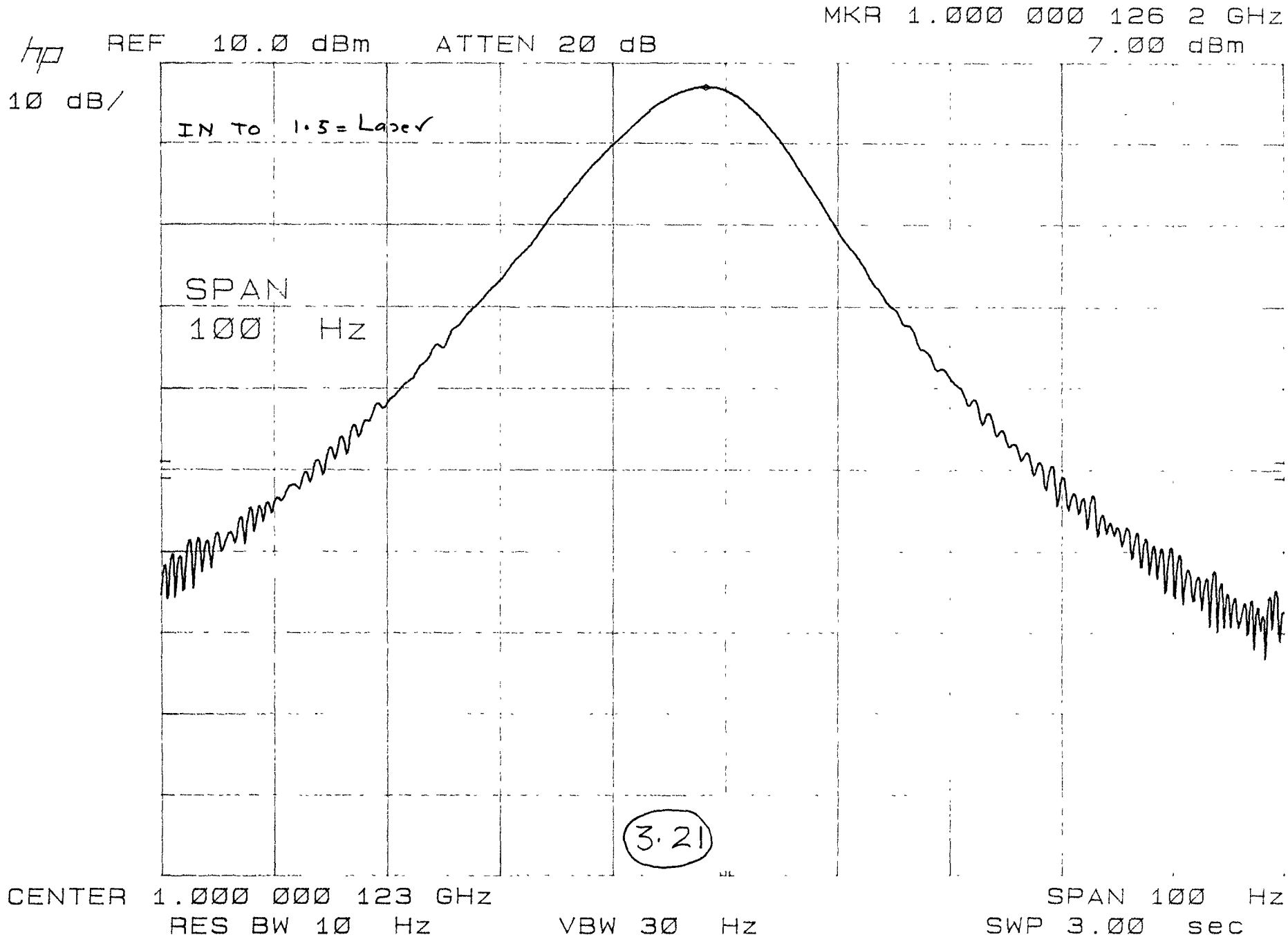
MKR 1.000 000 126 2 GHz
REF 10.0 dBm
ATTEN 20 dB
7.00 dBm
10 dB/
IN To 1·5 = Laser
SPAN
100 Hz
3·21
CENTER 1.000 000 123 GHz
SPAN 100 Hz
RES BW 10 Hz
VBW 30 Hz
SWP 3.00 sec

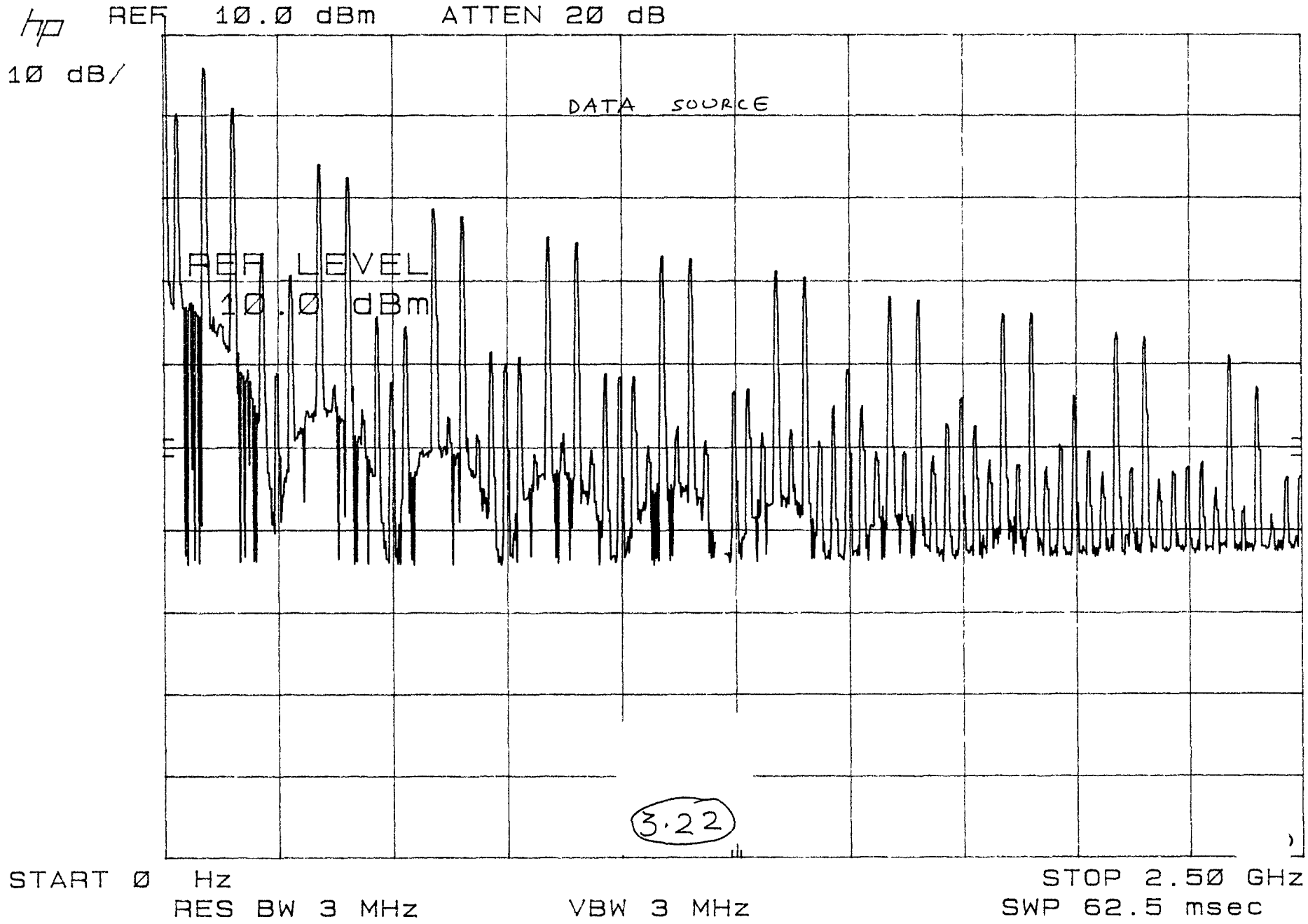
REF 10.0 dBm
ATTEN 20 dB
10 dB/
DATA SOURCE
REF LEVEL
10.0 dBm
3.22
START 0 Hz
STOP 2.50 GHz
RES BW 3 MHz
VBW 3 MHz
SWP 62.5 msec

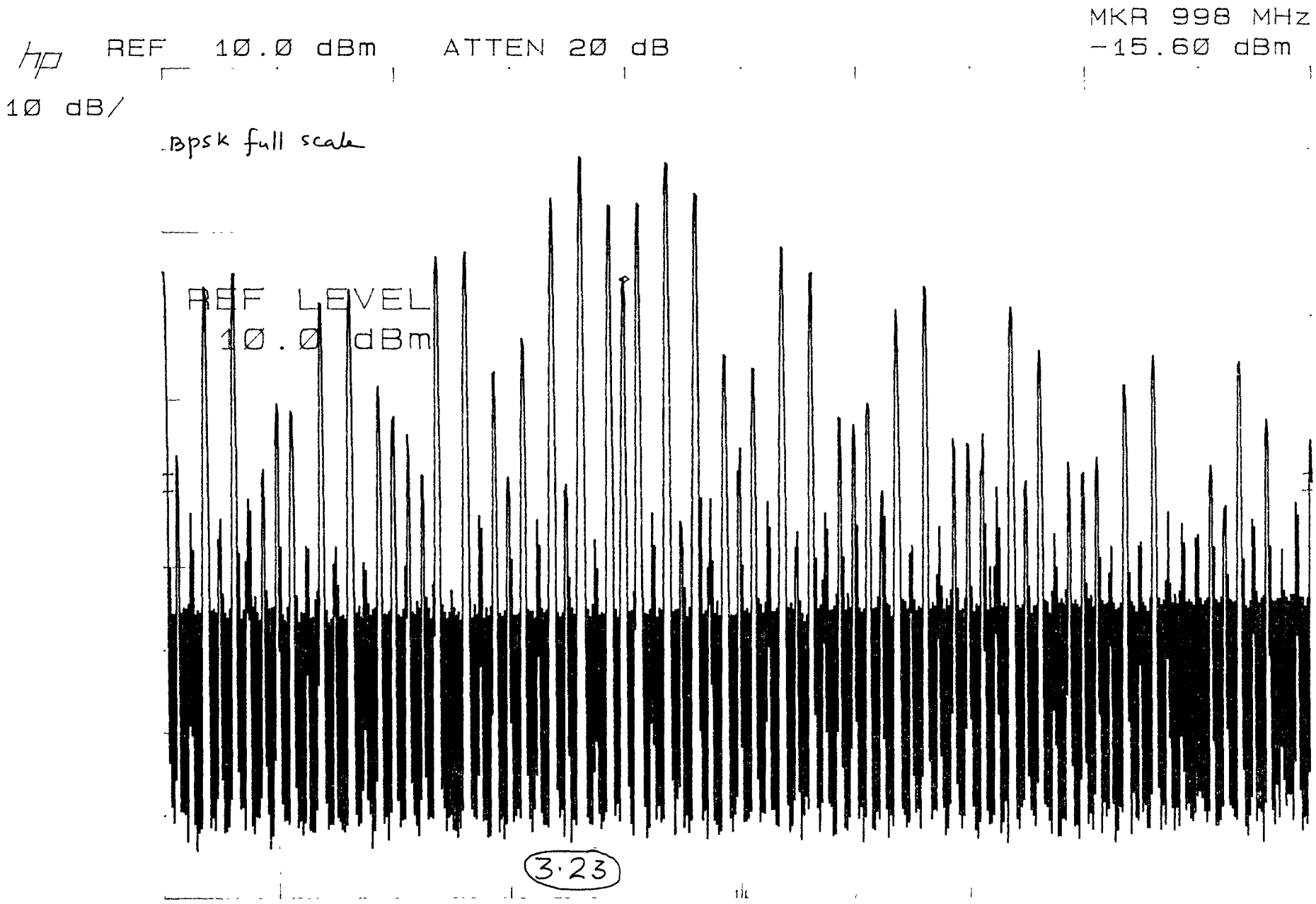
MKR 998 MHz
-15.60 dBm
REF 10.0 dBm
ATTEN 20 dB
10 dB/
bpsk full scale
REF LEVEL
10.0 dBm
3.23
START 0 Hz
STOP 2.50 GHz
RES BW 3 MHz
VBW 3 MHz
SWP 62.5 msec

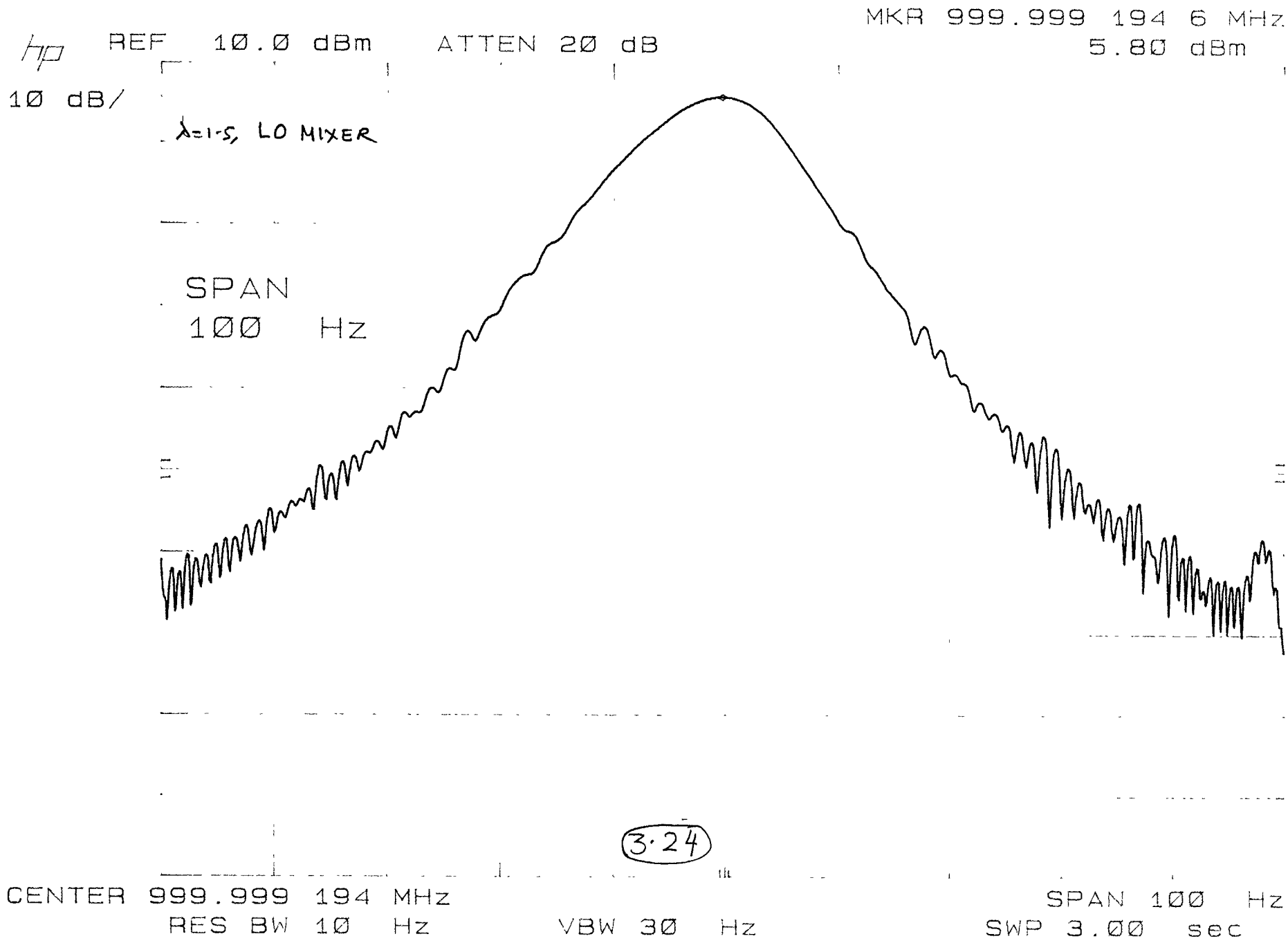
MKR 999.999 194 6 MHz
5.80 dBm
hp REF 10.0 dBm ATTEN 20 dB
10 dB/
λ=1-S, LO MIXER
SPAN
100 Hz
3·24
CENTER 999.999 194 MHz
SPAN 100 Hz
RES BW 10 Hz
VBW 30 Hz
SWP 3.00 sec

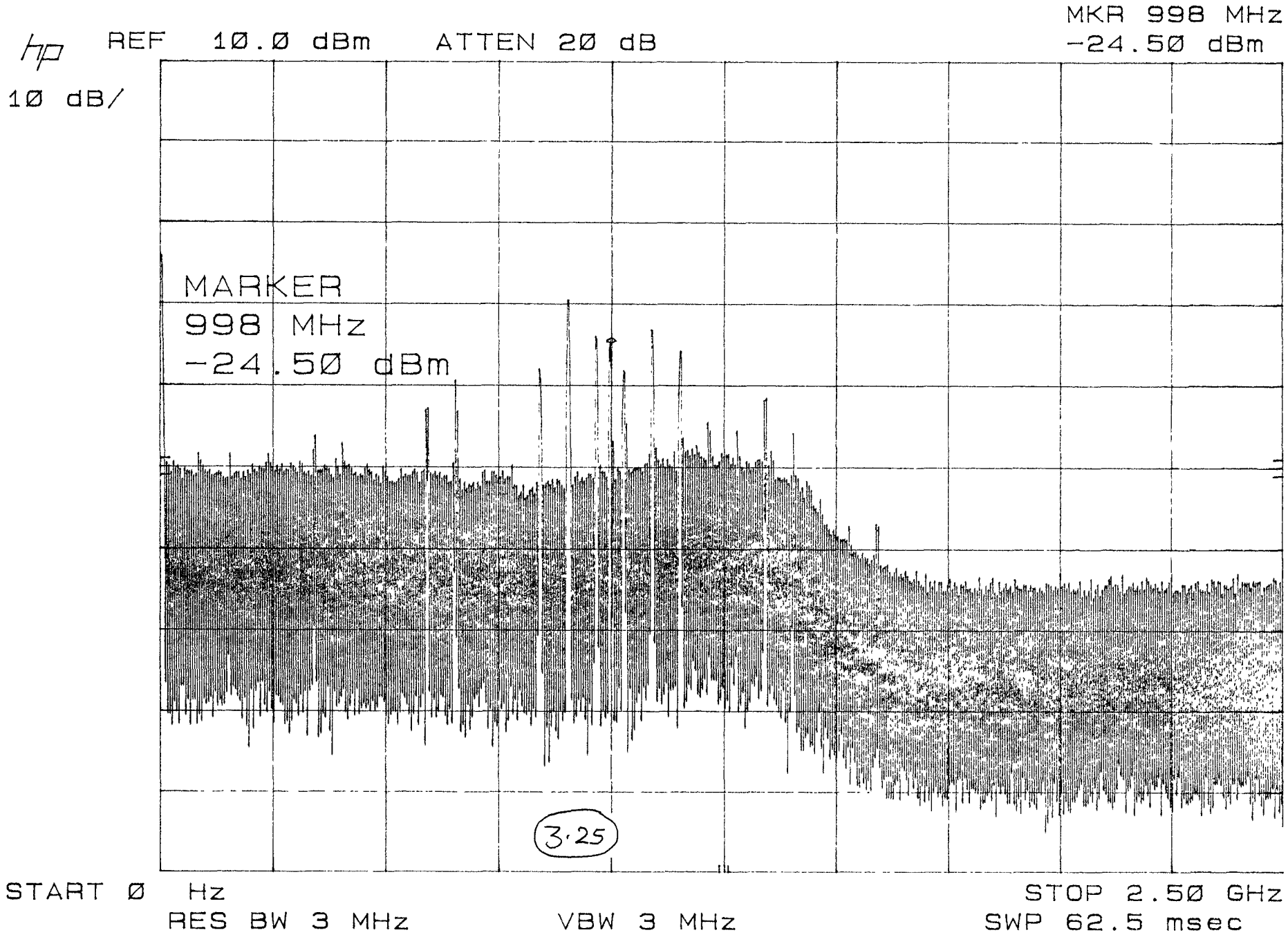
REF 10.0 dBm
ATTEN 20 dB
MKR 998 MHz
-24.50 dBm
10 dB/
MARKER
998 MHz
-24.50 dBm
3.25
START 0 Hz
STOP 2.50 GHz
RES BW 3 MHz
VBW 3 MHz
SWP 62.5 msec

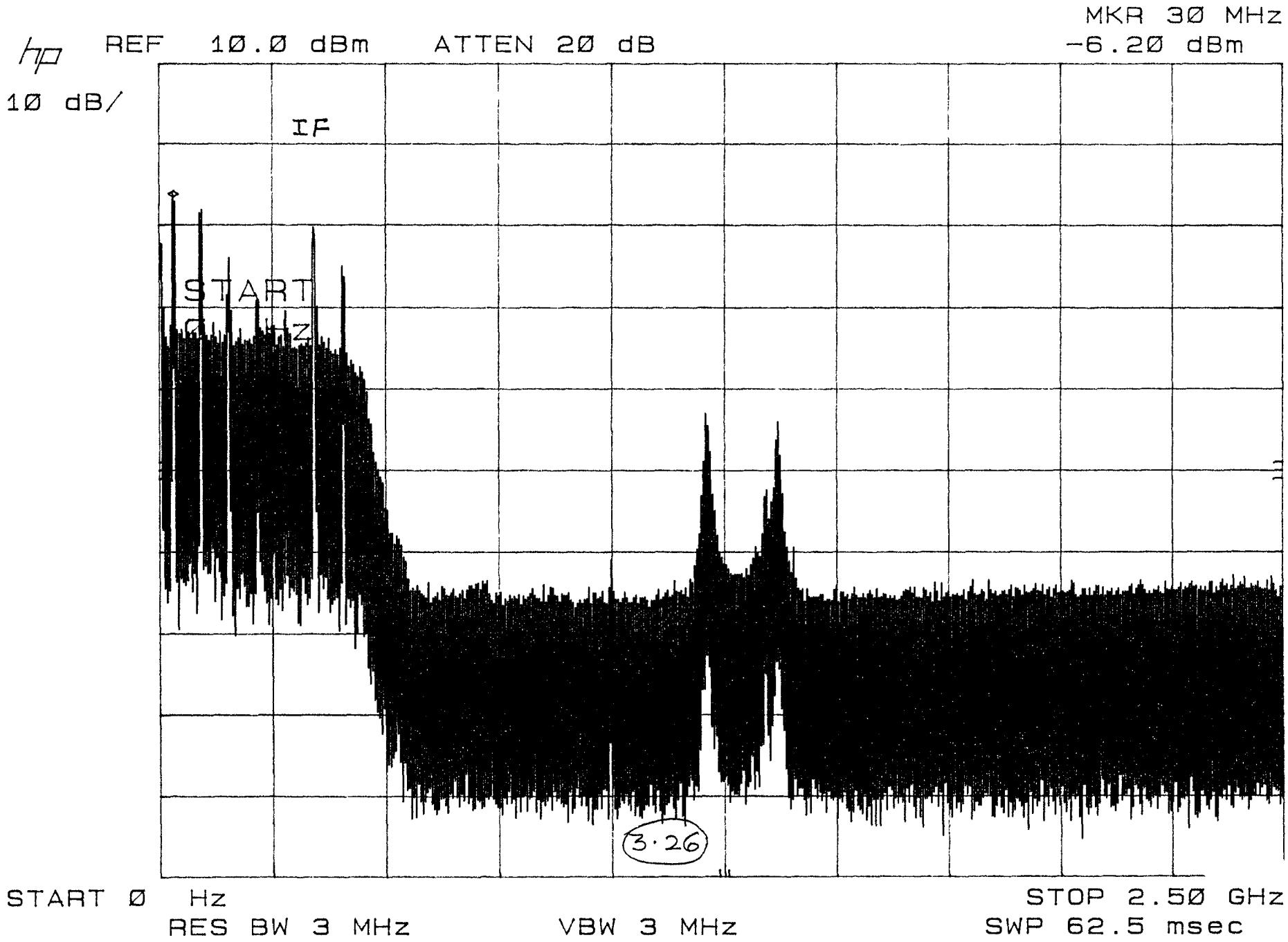
MKR 30 MHz
REF 10.0 dBm
ATTEN 20 dB
-6.20 dBm
10 dB/
IF
START
0 Hz
3·26
START 0 Hz
STOP 2.50 GHz
RES BW 3 MHz
VBW 3 MHz
SWP 62.5 msec

REFERENCES

[1] J.Gowar, Optical Communications Systems. Mc Graw Hill.

[2] W. Jones, "*Introduction to Fiber Communication Systems*", HRW, 1988.

[3] S. Miller and I. Kaminow, "*Optical Fiber Telecommunication Systems II, Academic,*"

[4] W.I. Way, P.S. Natarajan, P.S. Venkatesan, C.W. Lundgren, "Transmission of Ten Channels of Sub-Carrier Multiplexed HDTV Over a Single-Mode Fiber," to be published.

[5] H.Takada et al., "Fiber Optic Data Link for High Speed Local Area Network," Sumitomo Electric Technical review, No. 26, Jan 1987.

[6] T. Okiyama et al., "Evaluation of 4 - G-bit/s Optical Fiber transmission Distance With Direct and External Modulation," J. Lightwave Technol.[JLT], vol. 6, Nov 1988

[7] I.W. Marshal et al., "20 Gbit/s, 100 Km Non-linear Transmission with Semiconductor source," presented at OFC '90, 1990, pap. PD-5

[8] J. Salz, "Modulation & Detection for Coherent Lightwave Communications," IEEE Comm. Magazine, vol 24, June 1986.

[9] S. Betti et al., "Phase Noise and Polarization state Insensitive Optical Coherent Systems," JLT, vol 8, May 1990.

[10] L.Kazovsky et al., "PSK Synchronous heterodyne & Homodyne experiment using Optical Phase Lock Loop," OFC '90, 1990, pap. PD-11.

[11] W.I.Way, "Sub-Carrier Multiplexed Lightwave Systems Design Consideration for Subscriber Loop Application," JLT, vol 7, Nov 1989.

[12] S. Wagner et al., "Technology & System issues for WDM-Based Fiber Loop Architecture," JLT, vol 7, Nov 1989.

[13] T.E. Darcie, "Sub-Carrier Multiplexing for Multiple-Access Lightwave Networks," JLT, vol 5, Aug 1987.

[14] T.E. Darcie et al., "Lightwave System Using Microwave Subcarrier Multiplexing," Electron Lett., 1986, vol 22, pp 774-775.

[15] B.P. Lathi, "*Modern Digital & Analog Communication Systems,*" HRW, 1988.

[16] Lee Edward and David Messerschmitt,'" *Digital Communication,*" John Wiley, 1989.

[17] W. Thomas,"*Electronic Communication System,*" Prentice Hall, 1988.

[18] HP 71400, Application Notes,"Lightwave Signal Analyzer Application Notes," HP Notes 371.

[19] K. Peterman et al.,"Noise and Distortion Characteristics of Semiconductor Lasers In Optical Fibers Communication Systems,"IEEE Journal of Quantum, vol. QE-18, April 1982.

[20] R.S. Tucker,"High-Speed Modulation of Semiconductor Lasers," JLT, vol 3, Dec 1985.

[21] HP Symponisium, "Measurement on Laser for High Capacity Communication Systems ".

[22] C.M. Millerand F.C. Stokes, "Measurement of Laser Diode Intensity Noise Below the Shot Noise Limit," HP Signal Analysis Division Presentation.

[23] Hewelt Packard, "Measurement on Laser for High-Capacity Communicate Systems," Seminar.

[24] S. Yamamoto et al., "Analysis of Laser Phase Noise to Intensity Conversion by Chromatic Dispersion in Intensity Modulation and Direct detection optical Fiber Transmission" JLT, vol 8, Nov 1990.

[25] K.Daikoku, "Direct Modulation Characteristics of Semiconductor laser Diodes." Japanese Journal of Applied Physics, vol 16, Jan 1977

[26] M. Stern et al., "Self-Phase Modulation and Dispersion in High Data Rate Fiber-Optic Transmission Systems," JLT, vol 8, July 1990

[27] F. P. Kapron, "Maximum Information Capacity of Fiber Optic Waveguide," Electron Lett., 1977, vol 13, pp 96-97.

[28] A.R. Chraplylvy et al., "Carrier Induced Phase Noise in Angle Modulated Optical-fiber system," JLT, vol 2, Feb. 1984.

[29] A.R. Chraplyvy, et al., "Performance degradation due to Stimulated Raman Scattering in WDM Optical-Fiber Systems," Electron. Lett., 1983, vol 19, pp 641-642

[30] P. Prucnal et al.,"A Rate Transparent, Self Clocking Line Coding," IEEE Proceedings, vol 75, Aug 1987.

[31] R.B. Childs et al., "50 Channel VSB-AM video Transmission Employing Linearized External Modulation," OFC '90, 1990, pap. PD-23.

[32] W.I. Way, "Large Signal Non-Linear Distortion Prediction for a Single Mode Laser Diode under Microwave Intensity Modulation," JLT, vol 5, March 1987.

[33] R. Pietroiusti, "Analog Transmission of TV Signal on Optical Fiber," Alta frequenza, vol 1, Jan-Feb 1982.

[34] EIA Standards, "Chromatic Dispersion Measurement of Optical Fibers by the Phase Shift Method," FOTP-169, Aug 1988.

[35] P.R.Trischitta et al., "Jitter Tolerance of Fiberoptic Regenerators," IEEE TRANS on Comm, vol. COM-35,1987.

[36] T.M. Shen, "Jitter Penalty Due to Decision Time Jitter in receiver using Avalanche Photodiodes," Electron Lett., 86, VOL 21, pp 1043-1044.

[37] G.P.Agrawal et al., "Power Penalty Due to Decision Time Jitter in Optical Communication System," Electron Lett., 86, vol 22, pp 450-451.

[38] HP Application Notes, "Understanding and Measuring Phase Noise in the Frequency Domain," HP Notes-207, October 1976.